Creation of Functionalized Supramolecular Systems Based on Chiral Recognition of Monoclonal Antibodies

A Doctoral Thesis

by

Takuma Adachi

Submitted to

the Graduate School of Science, Osaka University

February, 2019

Acknowledgement

This research was carried out from 2013 to 2019 under the direction of Professor Dr. Akira Harada and Professor Dr. Hiroyasu Yamaguchi at the Department of Macromolecular Science, Graduate School of Science, Osaka University. The author expresses deep gratitude to Professor Dr. Akira Harada and Professor Dr. Hiroyasu Yamaguchi for their continuing guidance and encouragement throughout the study. Grateful acknowledgements are made to Professor Dr. Akihito Hashidzume and Professor Dr. Yoshinori Takashima for their continuing help, warm encouragement and kind advices. The authors thank Prof. Dr. Michio Murata, Dr. Shinya. Hanashima, and Dr. Hiroshi Tsuchikawa (Department of Chemistry, Graduate School of Science, Osaka University) for their cooperation of the optical rotation measurements. This thesis was reviewed by Professors Hiroyasu Yamaguchi, Akira Harada, Katsumi Imada, Yoshinori Takashima, and Ken Terao. The author appreciates for their careful reviewing and helpful comments on this thesis.

The author would like to express his acknowledgement to Dr. Yuichiro Kobayashi, Dr. Takashi Nakamura, Dr. Takahiro Kakuta, Dr. Masaki Nakahata, Dr. Tokoko Sekine, Dr. Kazuhisa Iwaso, and Dr. Kohei Koyanagi for their help and suggestions, and to all members of Harada laboratory and Yamaguchi laboratory for their cooperation and friendship. Finally, the author would also like to express deep appreciate to his all colleagues, friends and family for their help and encouragements.

February 2019

安達　琢真

Takuma Adachi

Contents

Chapter 1
General Introduction

Supramolecular chemistry

Various biological functions are realized via precise intermolecular interactions of macromolecules such as proteins and DNA. The molecular interactions are achieved by the combination of multiple weak non-covalent interactions such as electrostatic interaction, hydrophobic interaction, hydrogen bonding and metal coordination. The area of science related to non-covalent interactions was defined by one of its pioneers, Jean-Marie Lehn, as supramolecular chemistry. The original definition of supramolecular chemistry is "the chemistry of molecular assemblies and of the intermolecular bond".[1] Accordingly, the earliest history of supramolecular chemistry was opened by molecular recognition based on host-guest interaction employing crown ether, cryptand, and calixarene as host molecules. The importance of the pioneering work is highlighted by the Novel Prize in chemistry in 1987 awarded to Jean-Marie Lehn,[2,3] Donald James Cram,[4,5] and Charles John Pedersen[6,7] "for their development and use of molecules with structure-specific interactions of high selectivity." After that the scope of supramolecular chemistry has been grown rapidly to make it one of the most interdisciplinary areas of chemistry. A large number of natural host molecules such as myoglobin and human serum albumin as well as synthetic ones have been utilized to create functional materials and systems (**Figure 1-1**). Among these molecules, antibodies are thought to be one of the most attractive host molecules because of their superior molecular recognition ability.

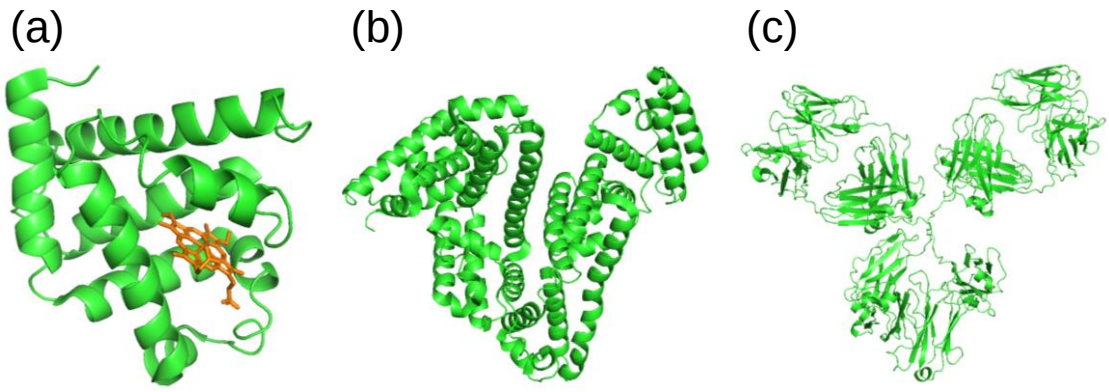

Figure 1-1. Structure of whale myoglobin (a), human serum albumin (b), and murine IgG (c)

Monoclonal antibodies (mAbs)

Antibodies are glycoproteins produced by B cells in response to foreign substances. Antibodies are classified into five classes called immunoglobulin G (IgG), [8–10] IgA,[11,12] IgE[13,14], IgD,[15] and IgM.[16,17] A typical antibody, IgG, has Y-shaped structure consisting of two heavy chains and two light chains connected by disulfide bonds (**Figure 1-2**). Heavy chain and light chain have *ca*. 50 kDa and *ca*. 25 kDa of molecular weight, respectively. Therefore, the molecular weight of IgG molecules is *ca*. 150000 Da. Heavy chain is composed of four domains. The three domains from the C terminus are called constant region where the amino acid sequence is identical for the same subclass. IgG produced in mice is divided into four subclasses (IgG_1, IgG_{2a}, IgG_{2b}, IgG_3) based on the structure of constant region of heavy chains. The N-terminal region of heavy chain is called variable region where the amino acid sequence is different in each antibody produced by different B cells. Light chain has one constant region and one variable region in C terminus and N terminus, respectively. The L chains of murine IgG are divided into two subclasses (κ or λ) based on the structure of constant region. The binding of antigens by antibody is mainly carried out by Fab region (fragment, antigen-binding) consisting of one constant and one variable region of each heavy and light chain. In particular, three loop structures existed on each variable region of heavy chain (V_H) and that of light chain (V_L) play a crucial role in binding. Therefore, the loop structures are called complementarity determining regions (CDRs). The structures of CDRs are classified into several clusters based on the method proposed by Chothia et al.[18] or North et al.[19] The specific recognition of antigens is realized by the structural diversity in variable region of antibodies. The diversification in structure of antibody is enabled by mechanism called class switch,[20,21] V(D)J recombination,[22,23] and somatic hypermutation.[24] The biological functions of antibodies are mainly carried out by Fc region (fragment, crystallizable) where various immune molecules such as Fc receptors interact with.

Monoclonal antibody (mAb) is a chemically homogeneous form of antibody that is produced by a single B cell. In 1975, Cesar Milstein and George Köhler developed a method to culture fused cells of spleen cells and myeloma cells to realize the continuous production of mAbs with predefined specificity[25]. The hybridoma technology has contributed to enlarge the scope the application of mAbs in science and industry. The importance of this work is highlighted by the Novel Prize in Physiology or Medicine in 1984 “for theories concerning the specificity in development and control of the immune system and the discovery of the principle for production of monoclonal antibodies”. In the next year, a major breakthrough in the production of mAbs was achieved.[26] The technique called phage display enabled the expression of a specific protein or peptides on

the surface of bacteriophage. The technology can be used to isolate fragment antibodies such as single-chain variable fragment (scFv), a fusion protein of the V_H and V_L of antibodies, with a desired binding property.[27] In 2002, Adalimumab, a mAb specific for a tumor necrosis factor was approved as a medicine for treatment of rheumatoid arthritis. The development and medical use of phage display achieved by George Pearson Smith and Greg Winter was awarded by Novel Prize in Chemistry in 2018 "for the phage display of peptides and antibodies". The technological development in the production of mAbs[25] has opened the door for the application of mAbs in diagnostic,[28,29] medical,[30–36] and (bio)chemical [36–43] usages including sensing and quantification analytes.

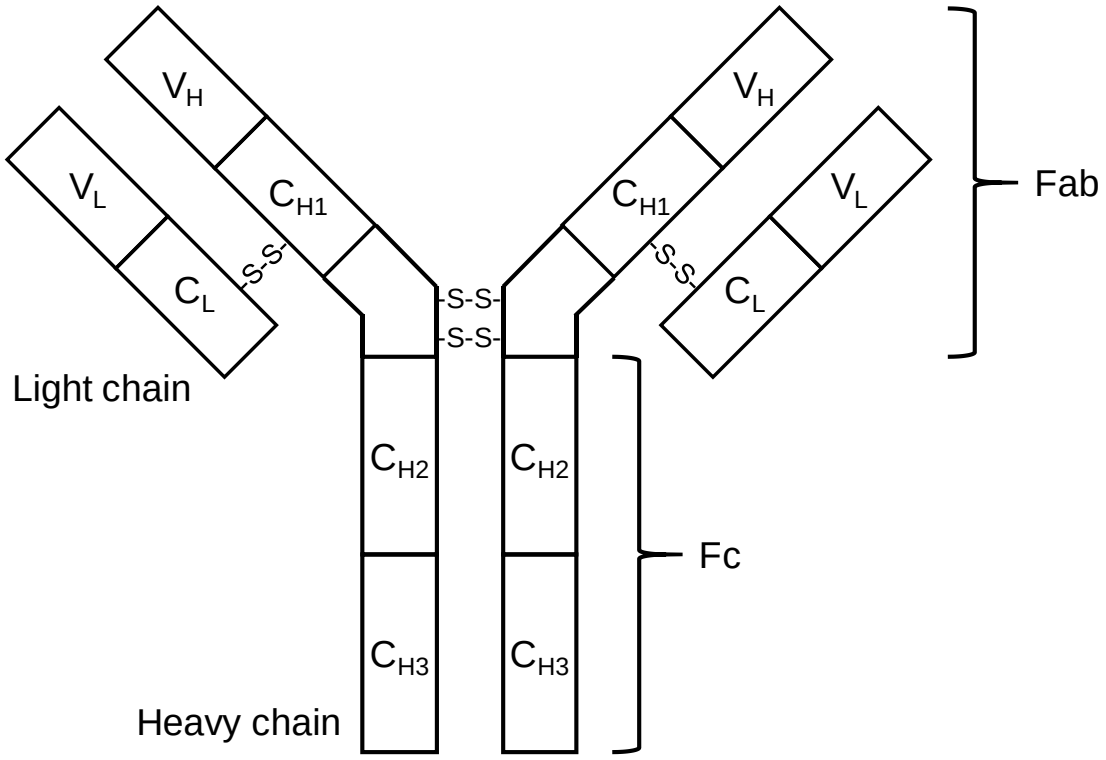

Figure1-2. Chemical structure of IgG.

The use of antibodies in chemistry: Chiral recognition

One of the most attractive targets where antibody exerts their molecular recognition ability is molecular chirality. In 1928, Karl Landsteiner revealed that the antibodies recognize chirality of asymmetric carbon centers.[44] This pioneering work has been followed by the numerous number of generation of antibodies against chiral molecules.[45,46] The dissociation constants for *R*-isomer (K_R) and *S*-isomer (K_S) of each chiral molecule are listed (**Table 1-1)**. The selectivity is calculated by dividing the higher *K* value by the lower one. mAbs were prepared against abscisic acid for the sensing and chiral separation of the plant hormone.[47,48] Abuse drugs with chirality such as nicotine,[49] cotinine, and heroin etc. have also been targets of production of mAbs. mAbs against drug candidates including inhibitors for serotonin receptors,[50,51] aromatase enzymes,[52–57] and β-adrenoreceptors[58] have been prepared and some of them has been used as a chiral selector. [52–57] mAbs against a metabolite were prepared and used in immunohistochemistry.[59] Naproxen and ofloxacin are anti-inflammatory or anti-bacterial drug and mAbs for them were developed and used in hydrolysis[60] or immunoassay[61–63] of them. The chirality of amino acids[64–69] or hydroxy acids[70] can also be recognized by mAbs. Because mAbs can be prepared against virtually any molecules of interest, synthetic chiral molecules can also be antigens. The mAbs prepared by immunization with racemic mixture of a hapten are used in screening of asymmetric catalysts. [71,72] Some of mAbs elicited against achiral haptens showed enantioselectivity for chiral hapten analogs and their enantioselectivity were used in asymmetric catalysis[73–78], chiral sensing,[79,80] and screening of enantioselective catalysts.[81]

Compared with these success, creation of supramolecular functionalized system based on hybridization of mAbs with synthetic chiral compounds is still state-of-art. One example is reported by D. Readan et al. where mAbs were developed against a chiral ethylenediaminetetraacetic acid derivative (EDTA) and their chiral recognition ability was analyzed. The supramolecular complex of mAbs with EDTA chelate of indium altered the biological distribution of radionuclides.[82] After that, the mAbs for chiral hydrophobic compounds including a pyrene modified peptide,[83] a luminescent metal complex,[84] and binaphthyl derivatives[85] were prepared. However, their application in some functionalized system remains future work, even though the new connection of immunology with organic or inorganic chemistry implies new direction.

Table 1-1. Examples of mAbs against chiral compounds and their applications.

Hapten	K_R/M	K_S/M	Selectivity	Application
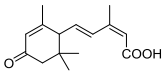 *S*- Abscisic acid	[a]NA	3.69×10^{-9}	-	Sensing[47] Separation[48]
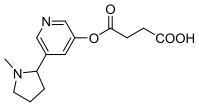 (*rac*)-Nicotine derivative	4.0×10^{-6}	1.5×10^{-7}	26	Sensing[49]
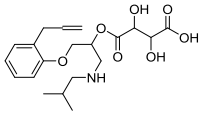 (-)-Alprenolol tartarate	[b]7.0×10^{-9}	[c]3.0×10^{-6}	514	-[50]
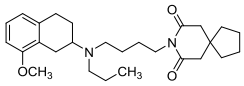 *R* or *S*-agonist for serotonin receptor	2×10^{-9}	3×10^{-11}	70	-[51]
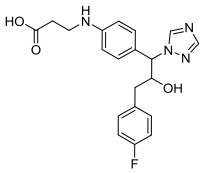 Finrozole	6.3×10^{-8}	5.5×10^{-5}	873	Separation[52–57]
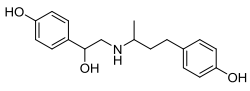 (*rac*)-Ractopamine	[d]1.8×10^{-6}	[e]4.7×10^{-4}	260	-[58]
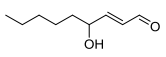 *R or S*-4-hydroxy-2-nonenal	-	-	-	Immunohistochemistry[59]
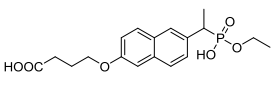 (*rac*)-Naproxen derivative	-	-	[f]-	Catalysis[60]

Continued

Hapten	K_R/M	K_S/M	Selectivity	Application
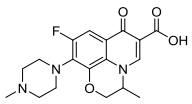 *R or S*-ofloxacin	[g]9.6×10^{-9}	[g]1.8×10^{-9}	5.3	Sensing[61–63]
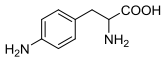 *p*-Amino-*D*-phenylalanine	[g]1.4×10^{-6}	[a]NA	-	Separation[64–66], sensor[67–69]
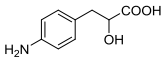 *p*-Amino-*D*-phenyllactic acid	-	-	-	Separation[70]
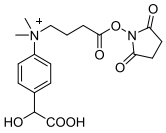 Mandelic acid	[a]NA	5.5×10^{-5}	-	Catalyst screening[71,72]
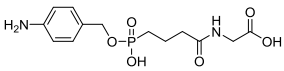 Achiral transition state analog	[i]5.0×10^{-8}	[i]2.6×10^{-9}	[i]19	Catalysis[73–78]
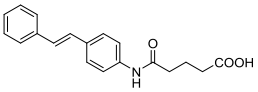 Achiral stilbene derivative	[i]5.2×10^{-5}	[i]4.6×10^{-6}	[i]11	Sensing[79,80] and catalyst screening[81]
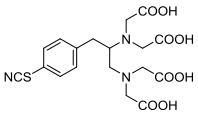 *S*-Benzyl-EDTA	[h]2×10^{-8}	[h]3×10^{-10}	70	Drug delivery[82]
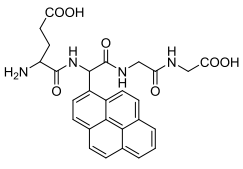 *S*-Tetrapeptide modified with pyrene	[a]NA	1×10^{-7}	-	-[83]

Continued

Hapten	K_R/M	K_S/M	Selectivity	Application
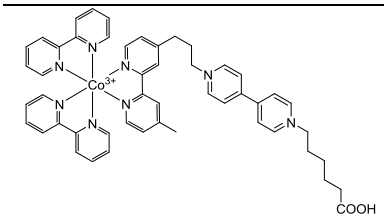 (*rac*)-Co complex	[j]1×10^{-7} (*K* value for racemic hapten)		[k]None	Photochemistry[84]
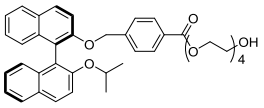 *R or S*-BINOL derivative [l]	[m]-	[m]-	[m]*ca.*10	-[85]

[a]No affinity, [b]Affinity for (−)-alprenolol [c]Affinity for (+)-alprenolol , [d]IC50 for *RR* isomer, [e]IC50 for *SS* isomer, [f]mAbs work as enantioselective catalysts but no binding constants for each enantiomer of substrates are available. [g]IC50, [h]Affinity for metal complex of hapten with indium, [i]mAbs obtained by immunization with achiral hapten showed enantioselectivity for chiral hapten analog. [j]Affinity for (*rac*)-Co complex, [k]Based on spectroscopic measurements, [l]scFVs were isolated using BINOL derivatives as antigens. [m]Relative affinity for immobilized antigens are available.

The use of antibodies in chemistry: Catalytic antibodies

In 1947, Linus Pauling proposed the principle of transition state stabilization to explain enzymatic catalysis.[86] In 1969, William Jencks proposed the idea of catalytic antibodies.[87] A basic idea of catalytic antibodies includes the design of antibodies that stabilize transition states of chemical reaction. This should result in the reduction of the activation energy of chemical reactions to accelerate the chemical reactions. The hybridoma technology that enables the continuous production of mAbs led to the creation of the first catalytic antibodies. In 1986, Richard Lerner et al. and Peter Schultz et al. independently reported the catalytic antibodies based on the hypothesis of Pauling and Jencks (**Figure 1-3**). [88,89] After that, catalytic antibodies have been applied to various chemical reactions.[90–98] Their practical viability is validated from applications in gram scale synthesis,[99] total synthesis of a natural product,[100] and medical usages including activation of prodrug *in vitro*[101,102] and degradation of a prohibited drug.[103] The design strategies of catalytic antibodies other than immunization with transition state analogs have been extensively studied such as bait-and-switch strategy,[104–106] reactive immunization,[107–109] and heterogeneous immunization.[110,111] Technological improvement in the production,[112] screening,[73] and structural analysis[113,114] has supported the rapid development of catalytic antibodies.

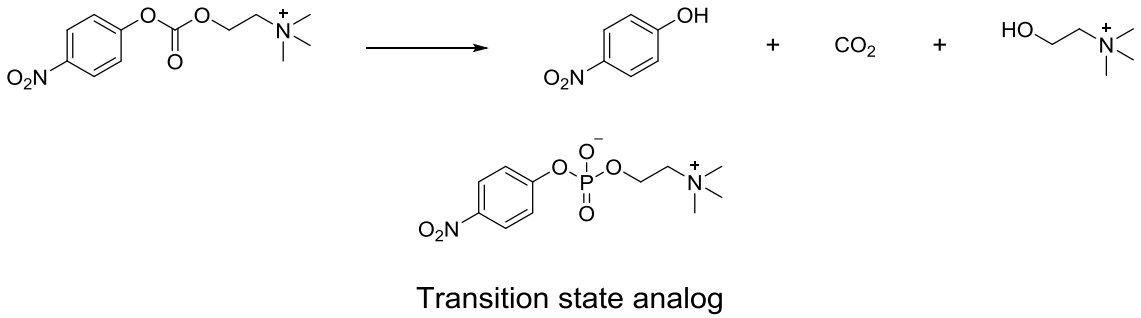

Figure 1-3. An example of hydrolysis reactions catalyzed by mAbs for transition state analogs.[88]

The use of antibodies in chemistry: Creation of artificial metalloproteins

Hybridization of mAbs with metal complexes is a promising way to create supramolecular functionalized systems combining attractive features of both mAbs and metal complexes (**Figure 1-4a**). One of the most extensively studied metal complexes in this context is porphyrins. The mAbs against *meso*-tetra-kis(4-carboxyphenyl)porphyrin (TCPP) are almost simultaneously reported by R. Lerner et al. and A. Harada et al.[115–118] The anti-TCPP mAbs bind porphyrins metalated with various metal ions. A. Harada et al. subsequently reported the peroxidation activity of mAbs-metalloporphyrin complexes.[119,120] Notably, the supramolecular complex of Fe-TCPP and L-chain of an anti-TCPP mAb shows higher thermostability than a natural peroxidase.[119] A. Harada and H. Yamaguchi et al. reported another peroxidases based on the supramolecular complexation of mAbs with cationic porphyrins.[121] The resulting peroxidases show a higher catalytic efficiency than that of anti-TCPP mAbs-based system and the higher H_2O_2 tolerance compared with a natural peroxidase.[121] P. Schultz et al. also reported peroxidases based on the similar strategy using *N*-methylmesoporphyrin IX as a hapten.[122,123] Another possible strategy for the design of anti-porphyrin mAbs-based catalysts is the use of metal porphyrin complexes as a hapten. In this context, E. Keinan et al. prepared mAbs against a Sn porphyrin complex.[124,125] The hybridization of the mAb with Mn porphyrin complex catalyze epoxidation reaction.[125] In 2002, K. Janda et al. reported a strategy to create catalytic antibodies where a metal binding moiety is conjugated to the binding sites of mAbs. The chemically modified-mAbs can hybridize with Cu ion to catalyze hydrolysis.[126] In 2004, J. Mahy et al. reported "Trojan house" strategy to hybridize metal complexes with mAbs. In the strategy mAbs elicited against anchor molecules are hybridized with the conjugates of metal complexes with the anchor.[127] The proof-of-concept of the strategy was validated in sulfoxidation, peroxidation, and epoxidation reaction.[128–130] The scope of application of anti-porphyrin mAbs is not limited in catalysis. A. Harada and H. Yamaguchi et al. created photoinduced electron transfer system inside the antigen binding sites of anti-porphyrin mAbs.[131–133] Furthermore, they developed a hydrogen evolution system based on the complex of a mAb with metalloporphyrin, methylviologen, and colloidal Pt. The supramolecular complex formation of mAbs with metalloporphyrin was successfully applied to sensing system.[134–139] The molecular recognition ability of mAbs can also be used in sensing of explosive substances.[140]

Given the structural diversity in the binding sites of mAbs, the binding partner of mAbs is not limited in naturally occurring cofactors. In 1989, R. Lerner et al. elicited mAbs against a coordinatively inert Co complex. The obtained mAbs bind various metal

complexes as well as the hapten to form supramolecular complexes that catalyze hydrolysis of peptide bonds. In 1995, K. Janda et al. generated catalytic antibodies by using a ferrocene derivative as a hapten to mimic transition state structure of Diels-Alder reaction.[141] In 1996, E. Keinan et al. generated mAbs against a spirosilane derivative. The obtained mAbs also bind a tetra coordinated $Cu(bpy)_2$ complex. The binding of mAbs not only stabilizes the high energy state of the Cu complex but also inhibits the air oxidation reaction of the Cu complex. In the same year, mAbs against Co(bpy)3 derivative were developed. The excited-state life times of a variety of luminescent Ru complexes are enhanced in the existence of the mAbs. In 2006, A. Harada and H. Yamaguchi et al. reported the asymmetric hydrogenases based on the supramolecular complexes of mAbs with an achiral Rh complex.[142] One of the resulting complexes catalyzes hydrogenation with increased yield and complete enantioselectivity. Furthermore, the catalytic antibody shows substrate specificity.[142] Supramolecular complexation and functionalization of mAbs with synthetic metal catalysts have room for further development.[84,85,143–145]

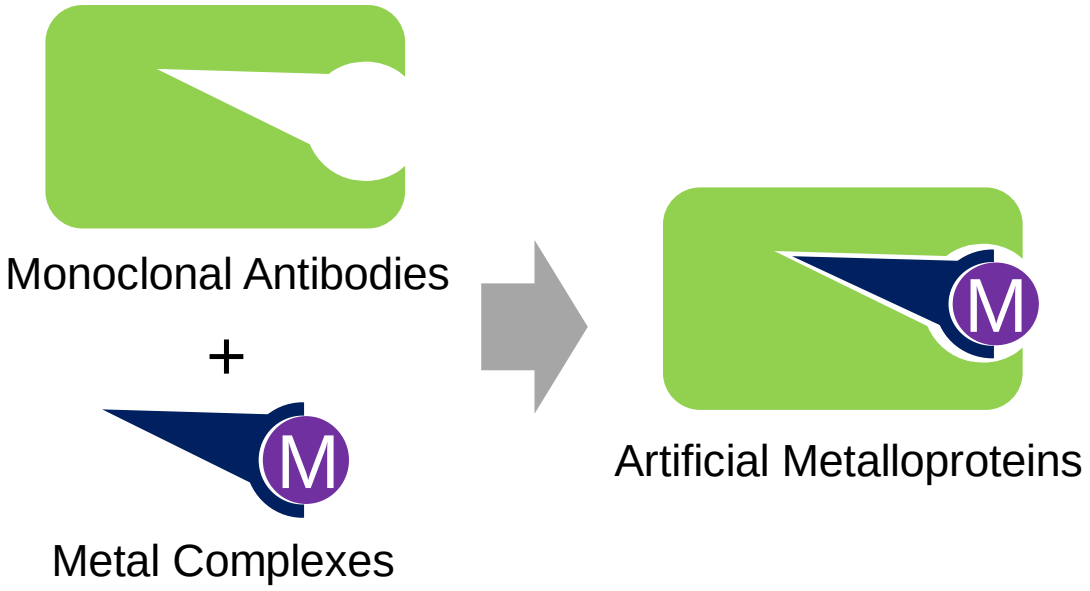

Figure 1-4. Schematic illustration of artificial metalloproteins that provide second-coordination sphere effects to the embedded metal complexes.

Scope and outline of the thesis

In this thesis, the author focuses on the chiral recognition ability of mAbs to develop functionalized supramolecular systems. Axially chirality is chosen as a target because of the unique structure and functions especially in asymmetric catalysis. The mAbs elicited for a binaphthyl derivative recognize axial chirality. Therefore, the author defined the mAbs as *atroposelective antibodies*. Supramolecular functions based on chiral recognition of atroposelective antibodies are explored (**Figure 1-5**).

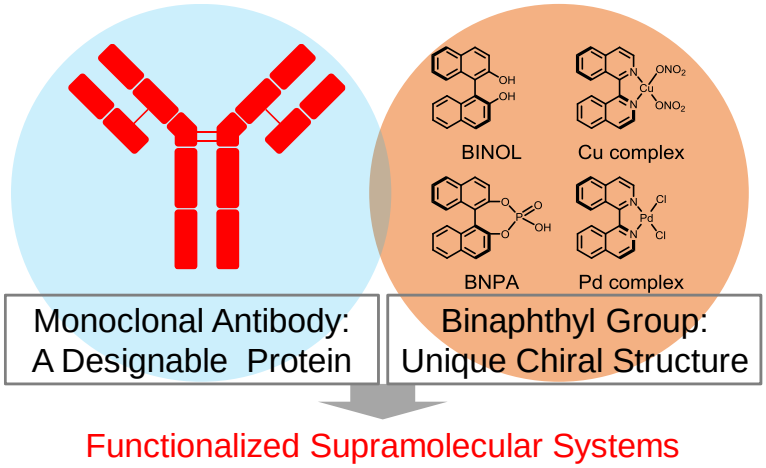

Figure 1-5. Outline of the thesis

In Chapter 2, mAbs against BN are developed and their chiral recognition ability is evaluated (**Figure 1-6**). Immunization with pure enantiomer of BN yields the mAbs with atroposelectivity toward their hapten. Immunization with racemic mixture of BN (BN (*rac*)) can give atroposelective antibodies for both BN (*R*) and BN (*S*) at one time. The mAbs also recognize the chirality of BINOL and BNPA.

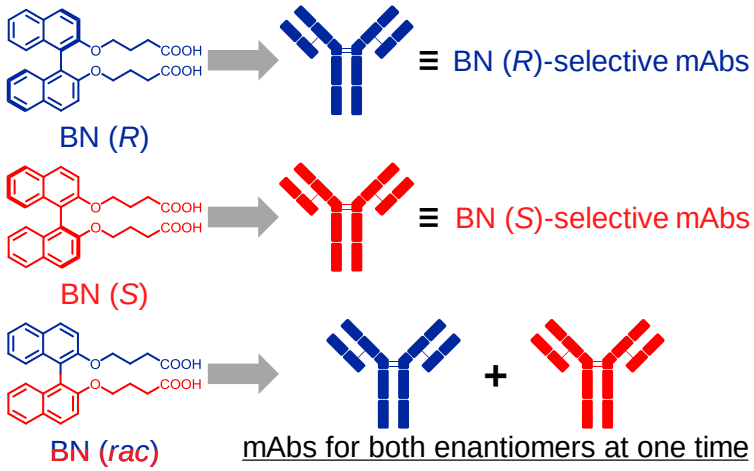

Figure 1-6. Overview of the development of atroposelective antibodies.

In Chapter 3, atroposelective antibodies were used as a chiral selector. A one-step simple procedure for chiral separation that only requires the ultrafiltration of mixture of BN (*rac*) and atroposelective antibodies is developed (**Figure 1-7**). The difference of molecular weight of mAbs and BN enables the direct use of intact antibodies without any pre-processing or immobilization of mAbs on chromatographic supports.

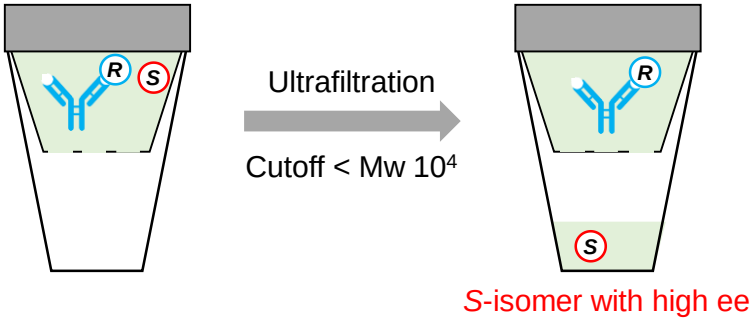

Figure 1-7. Schematic illustration of the procedure for direct chiral separation

In Chapter 4, artificial metalloenzymes consisting of C_2 symmetric metal catalysts and atroposelective antibodies were developed. Anti-BN mAbs bind four kinds of 1,1'-bi-isoquinoline (BIQ)-based metal catalysts to yield artificial metalloenzymes. The resulting artificial metalloenzymes catalyze Friedel-Crafts alkylation reaction with high ee. Notably, asymmetric catalytic reaction is realized by just adding atroposelective antibodies to the mixture of substrates and BIQ-based metal catalysts. Precisely designed second coordination spheres of mAbs control the stereochemistry (**Scheme 1-1**).

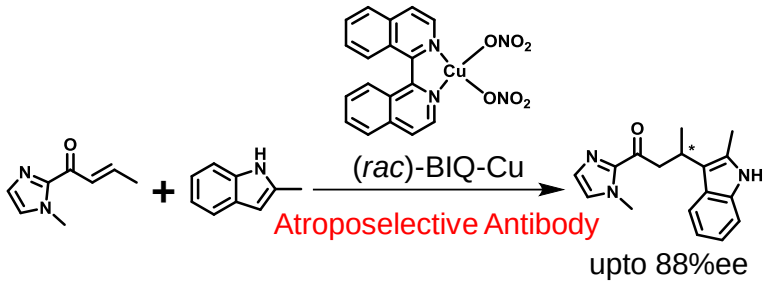

Scheme 1-1. Asymmetric Friedel-Crafts alkylation reaction catalyzed by a complex of mAbs with BIQ-Cu.

In Chapter 5, the author summarizes functionalized supramolecular systems described in Chapters 2, 3, and 4 for chiral recognition and chiral separation by atroposelective antibodies and asymmetric catalysis using atroposelective antibodies.

References

(1) Lehn, J. *Science* **1993**, *260*, 1762–1763.

(2) Lehn, J.-M. *Angew. Chem. Int. Ed. Engl.* **1988**, *27*, 89–112.

(3) Lehn, J.-M. *Angew. Chem. Int. Ed. Engl.* **1990**, *29*, 1304–1319.

(4) Cram, D. J. *Angew. Chem. Int. Ed. Engl.* **1988**, *27*, 1009–1020.

(5) Cram, D. J. *Science* **1983**, *219*, 1177–1183.

(6) Pedersen, C. J. *Angew. Chem. Int. Ed. Engl.* **1988**, *27*, 1021–1027.

(7) Pedersen, C. J. *J. Am. Chem. Soc.* **1967**, *89*, 7017–7036.

(8) Porter, R. R. *Biochem. J.* **1959**, *73*, 119–127.

(9) Edelman, G. M.; Cunningham, B. A.; Gall, W. E.; Gottlieb, P. D.; Rutishauser, U.; Waxdal, M. J. *Proc. Natl. Acad. Sci.* **1969**, *63*, 78–85.

(10) Silverton, E. W.; Navia, M. A.; Davies, D. R. *Proc. Natl. Acad. Sci.* **1977**, *74*, 5140–5144.

(11) Kerr, M. A. *Biochem. J.* **1990**, *271*, 285–296.

(12) Pabst, O. *Nat. Rev. Immunol.* **2012**, *12*, 821–832.

(13) Ishizaka, K.; Ishizaka, T. *J. Immunol.* **1967**, *99*, 1187–1198.

(14) Gould, H. J.; Sutton, B. J. *Nat. Rev. Immunol.* **2008**, *8*, 205–217.

(15) Rowe, D. S.; Fahey, J. L. *J. Exp. Med.* **1965**, *121*, 171–184.

(16) Ehrenstein, M. R.; Notley, C. A. *Nat. Rev. Immunol.* **2010**, *10*, 778–786.

(17) Hiramoto, E.; Tsutsumi, A.; Suzuki, R.; Matsuoka, S.; Arai, S.; Kikkawa, M.; Miyazaki, T. *Sci. Adv.* **2018**, *4*, eaau1199.

(18) Al-Lazikani, B.; Lesk, A. M.; Chothia, C. *J. Mol. Biol.* **1997**, *273*, 927–948.

(19) North, B.; Lehmann, A.; Dunbrack, R. L. *J. Mol. Biol.* **2011**, *406*, 228–256.

(20) Honjo, T.; Kataoka, T. *Proc. Natl. Acad. Sci.* **1978**, *75*, 2140–2144.

(21) Muramatsu, M.; Sankaranand, V. S.; Anant, S.; Sugai, M.; Kinoshita, K.; Davidson, N. O.; Honjo, T. *J. Biol. Chem.* **1999**, *274*, 18470–18476.

(22) Hozumi, N.; Tonegawa, S. *Proc. Natl. Acad. Sci.* **1976**, *73*, 3628–3632.

(23) Tonegawa, S. *Nature* **1983**, *302*, 575–581.

(24) Rajewsky, K.; Forster, I.; Cumano, A. *Science* **1987**, *238*, 1088–1094.

(25) Köhler, G.; Milstein, C. *Nature* **1975**, *256*, 495–497.

(26) Smith, G. *Science* **1985**, *228*, 1315–1317.

(27) McCafferty, J.; Griffiths, A. D.; Winter, G.; Chiswell, D. J. *Nature* **1990**, *348*, 552–554.

(28) Borrebaeck, C. A. . *Immunol. Today* **2000**, *21*, 379–382.

(29) Luppa, P. B.; Sokoll, L. J.; Chan, D. W. *Clin. Chim. Acta* **2001**, *314*, 1–26.

(30) Riechmann, L.; Clark, M.; Waldmann, H.; Winter, G. *Nature* **1988**, *332*, 323–327.

(31) Leach, D. R.; Krummel, M. F.; Allison, J. P. *Science* **1996**, *271*, 1734–1736.
(32) Iwai, Y.; Terawaki, S.; Honjo, T. *Int. Immunol.* **2005**, *17*, 133–144.
(33) Weinblatt, M. E.; Keystone, E. C.; Furst, D. E.; Moreland, L. W.; Weisman, M. H.; Birbara, C. A.; Teoh, L. A.; Fischkoff, S. A.; Chartash, E. K. *Arthritis Rheum.* **2003**, *48*, 35–45.
(34) Carter, P. J. *Nat. Rev. Immunol.* **2006**, *6*, 343–357.
(35) Scott, A. M.; Wolchok, J. D.; Old, L. J. *Nat. Rev. Cancer* **2012**, *12*, 278–287.
(36) Chari, R. V. J.; Miller, M. L.; Widdison, W. C. *Angew. Chem. Int. Ed.* **2014**, *53*, 3796–3827.
(37) Orlandi, R.; Gussow, D. H.; Jones, P. T.; Winter, G. *Proc. Natl. Acad. Sci.* **1989**, *86*, 3833–3837.
(38) Towbin, H.; Staehelin, T.; Gordon, J. *Proc. Natl. Acad. Sci.* **1979**, *76*, 4350–4354.
(39) Liedberg, B.; Nylander, C.; Lunström, I. *Sensors and Actuators* **1983**, *4*, 299–304.
(40) Höök, F.; Rodahl, M.; Brzezinski, P.; Kasemo, B. *Langmuir* **1998**, *14*, 729–734.
(41) Miyata, T.; Asami, N.; Uragami, T. *Macromolecules* **1999**, *32*, 2082–2084.
(42) Abe, R.; Ohashi, H.; Iijima, I.; Ihara, M.; Takagi, H.; Hohsaka, T.; Ueda, H. *J. Am. Chem. Soc.* **2011**, *133*, 17386–17394.
(43) Fukunaga, K.; Watanabe, T.; Novitasari, D.; Ohashi, H.; Abe, R.; Hohsaka, T. *Chem. Commun.* **2018**, *54*, 12734–12737.
(44) Landsteiner, K.; van der Scheer, J. *J. Exp. Med.* **1928**, *48*, 315–320.
(45) Got, P. A.; Scherrmann, J. *Pharm. Res.* **1997**, *14*, 1516–1523.
(46) Hofstetter, H.; Hofstetter, O. *Trends Anal. Chem.* **2005**, *24*, 869–879.
(47) Mertens, R.; Deus-Neumann, B.; Weiler, E. W. *FEBS Lett.* **1983**, *160*, 269–272.
(48) Knox, J. P.; Galfre, G. *Anal. Biochem.* **1986**, *155*, 92–94.
(49) Bjercke, R. J.; Cook, G.; Rychlik, N.; Gjika, H. B.; Van Vunakis, H.; Langone, J. J. *J. Immunol. Methods* **1986**, *90*, 203–213.
(50) Sawutz, D. G.; Sylvestre, D.; Homcy, C. J. *J. Immunol.* **1985**, *135*, 2713–2718.
(51) Got, P.; Raimbaud, E.; Bussey, C.; Caron, G.; Carrupt, P.; Walther, B.; Bensussan, A.; Scherrmann, J. *Pharm. Res.* **1999**, *16*, 725–735.
(52) Nevanen, T. K.; Söderholm, L.; Kukkonen, K.; Suortti, T.; Teerinen, T.; Linder, M.; Söderlund, H.; Teeri, T. T. *J. Chromatogr. A* **2001**, *925*, 89–97.
(53) Lee, S. B. *Science* **2002**, *296*, 2198–2200.
(54) Mitchell, D. T.; Lee, S. B.; Trofin, L.; Li, N.; Nevanen, T. K.; Söderlund, H.; Martin, C. R. *J. Am. Chem. Soc.* **2002**, *124*, 11864–11865.
(55) Nevanen, T. K.; Hellman, M.-L.; Munck, N.; Wohlfahrt, G.; Koivula, A.; Soderlund, H. *Protein Eng. Des. Sel.* **2003**, *16*, 1089–1097.

(56) Vuolanto, A.; Kiviharju, K.; Nevanen, T. K.; Leisola, M.; Jokela, J. *Cryst. Growth Des.* **2003**, *3*, 777–782.
(57) Vuolanto, A.; Leisola, M.; Jokela, J. *Biotechnol. Prog.* **2004**, *20*, 771–776.
(58) Shelver, W. L.; Smith, D. J.; Berry, E. S. *J. Agric. Food Chem.* **2000**, *48*, 4020–4026.
(59) Hashimoto, M.; Sibata, T.; Wasada, H.; Toyokuni, S.; Uchida, K. *J. Biol. Chem.* **2003**, *278*, 5044–5051.
(60) Shi, Z.-D.; Yang, B.-H.; Zhao, J.-J.; Wu, Y.-L.; Ji, Y.-Y.; Yeh, M. *Bioorg. Med. Chem.* **2002**, *10*, 2171–2175.
(61) Mu, H.; Lei, H.; Wang, B.; Xu, Z.; Zhang, C.; Ling, L.; Tian, Y.; Hu, J.; Sun, Y. *J. Agric. Food Chem.* **2014**, *62*, 7804–7812.
(62) Chen, J.; Wang, L.; Lu, L.; Shen, X.; Huang, X.; Liu, Y.; Sun, X.; Wang, Z.; Eremin, S. A.; Sun, Y.; et al. *Anal. Chem.* **2017**, *89*, 6740–6748.
(63) Zhang, Y.; Wang, L.; Shen, X.; Wei, X.; Huang, X.; Liu, Y.; Sun, X.; Wang, Z.; Sun, Y.; Xu, Z.; et al. *J. Agric. Food Chem.* **2017**, *65*, 4830–4838.
(64) Hofstetter, O.; Lindstrom, H.; Hofstetter, H. *Anal. Chem.* **2002**, *74*, 2119–2125.
(65) Hofstetter, O.; Lindstrom, H.; Hofstetter, H. *J. Chromatogr. A* **2004**, *1049*, 85–95.
(66) Hofstetter, H.; Cary, J. R.; Eleniste, P. P.; Hertweck, J. K.; Lindstrom, H. J.; Ranieri, D. I.; Smith, G. B.; Undesser, L. P.; Zeleke, J. M.; Zeleke, T. K.; et al. *Chirality* **2005**, *17*, S9–S18.
(67) Dutta, P.; Tipple, C. A.; Lavrik, N. V; Datskos, P. G.; Hofstetter, H.; Hofstetter, O.; Sepaniak, M. J. *Anal. Chem.* **2003**, *75*, 2342–2348.
(68) Tsourkas, A.; Hofstetter, O.; Hofstetter, H.; Weissleder, R.; Josephson, L. *Angew. Chem. Int. Ed.* **2004**, *43*, 2395–2399.
(69) Zhang, S.; Ding, J.; Liu, Y.; Kong, J.; Hofstetter, O. *Anal. Chem.* **2006**, *78*, 7592–7596.
(70) Zeleke, T. K.; Zeleke, J. M.; Hofstetter, H.; Hofstetter, O. *J. Mol. Recognit.* **2005**, *18*, 334–340.
(71) Taran, F.; Renard, P. Y.; Bernard, H.; Mioskowski, C.; Frobert, Y.; Pradelles, P.; Grassi, J. *J. Am. Chem. Soc.* **1998**, *120*, 3332–3339.
(72) Taran, F.; Gauchet, C.; Mohar, B.; Meunier, S.; Valleix, A.; Renard, P. Y.; Créminon, C.; Grassi, J.; Wagner, A.; Mioskowski, C. *Angew. Chem. Int. Ed.* **2002**, *41*, 124–127.
(73) Tawfik, D. S.; Green, B. S.; Chap, R.; Sela, M.; Eshhar, Z. *Proc. Natl. Acad. Sci.* **1993**, *90*, 373–377.
(74) Charbonnier, J. B.; Golinelli-Pimpaneau, B.; Gigant, B.; Tawfik, D. S.; Chap, R.;

Schindler, D. G.; Kim, S. H.; Green, B. S.; Eshhar, Z.; Knossow, M. *Science* **1997**, *275*, 1140–1142.

(75) Gigant, B.; Charbonnier, J.-B.; Eshhar, Z.; Green, B. S.; Knossow, M. *Proc. Natl. Acad. Sci.* **1997**, *94*, 7857–7861.

(76) Tawfik, D. S.; Lindner, A. B.; Chap, R.; Eshhar, Z.; Green, B. S. *Eur. J. Biochem.* **1997**, *244*, 619–626.

(77) Gigant, B.; Charbonnier, J.-B.; Eshhar, Z.; Green, B. .; Knossow, M. *J. Mol. Biol.* **1998**, *284*, 741–750.

(78) D'Souza, L. J.; Gigant, B.; Knossow, M.; Green, B. S. *J. Am. Chem. Soc.* **2002**, *124*, 2114–2115.

(79) Matsushita, H.; Yamamoto, N.; Meijler, M. M.; Wirsching, P.; Lerner, R. A.; Matsushita, M.; Janda, K. D. *Mol. Biosyst.* **2005**, *1*, 303.

(80) Matsushita, M.; Meijler, M. M.; Wirsching, P.; Lerner, R. A.; Janda, K. D. *Org. Lett.* **2005**, *7*, 4943–4946.

(81) Matsushita, M.; Yoshida, K.; Yamamoto, N.; Wirsching, P.; Lerner, R. A.; Janda, K. D. *Angew. Chem. Int. Ed.* **2003**, *42*, 5984–5987.

(82) Reardan, D. T.; Meares, C. F.; Goodwin, D. A.; McTigue, M.; David, G. S.; Stone, M. R.; Leung, J. P.; Bartholomew, R. M.; Frincke, J. M. *Nature* **1985**, *316*, 265–268.

(83) Imaizumi, M.; Sisido, M. *Chem. Lett.* **1994**, *23*, 51–52.

(84) Shreder, K.; Harriman, A.; Iverson, B. L. *J. Am. Chem. Soc.* **1996**, *118*, 3192–3201.

(85) Rasmussen, B. S.; Pedersen, J. M.; Sørensen, J.; Egebjerg, J.; Schiøtt, B.; Mortensen, K. K.; Skrydstrup, T. *ChemBioChem* **2007**, *8*, 1974–1980.

(86) Linus Pauling. *Am. Sci.* **1948**, *36*, 50–58.

(87) Jencks, W. P. *Catalysis in Chemistry and Enzymology*; 1969.

(88) Pollack, S.; Jacobs, J.; Schultz, P. *Science* **1986**, *234*, 1570–1573.

(89) Tramontano, A.; Janda, K. D.; Lerner, R. A. *Science* **1986**, *234*, 1566–1570.

(90) Lerner, R. a; Tramontano, A. *Trends Biochem. Sci.* **1987**, *12*, 427–430.

(91) Schultz, P. G. *Angew. Chem. Int. Ed. Engl.* **1989**, *28*, 1283–1295.

(92) Lerner, R.; Benkovic, S.; Schultz, P. *Science* **1991**, *252*, 659–667.

(93) Benkovic, S. J. *Annu. Rev. Biochem.* **1992**, *61*, 29–54.

(94) Schultz, P.; Lerner, R. *Science* **1995**, *269*, 1835–1842.

(95) Keinan, E.; Lerner, R. a. *Isr. J. Chem.* **1996**, *36*, 113–119.

(96) Thomas, N. R. *Nat. Prod. Rep.* **1996**, *13*, 479–511.

(97) Hilvert, D. *Annu. Rev. Biochem.* **2000**, *69*, 751–793.

(98) Xu, Y.; Yamamoto, N.; Janda, K. D. *Bioorg. Med. Chem.* **2004**, *12*, 5247–5268.

(99) Reymond, J.-L.; Reber, J.-L.; Lerner, R. A. *Angew. Chem. Int. Ed. Engl.* **1994**, *33*, 475–477.
(100) Sinha, S. C.; Keinan, E. *J. Am. Chem. Soc.* **1995**, *117*, 3653–3654.
(101) Miyashita, H.; Karaki, Y.; Kikuchi, M.; Fujii, I. *Proc. Natl. Acad. Sci.* **1993**, *90*, 5337–5340.
(102) Campbell, D. a.; Gong, B.; Kochersperger, L. M.; Yonkovich, S.; Gallop, M. a.; Schultz, P. G. *J. Am. Chem. Soc.* **1994**, *116*, 2165–2166.
(103) Landry, D.; Zhao, K.; Yang, G.; Glickman, M.; Georgiadis, T. *Science* **1993**, *259*, 1899–1901.
(104) Shokat, K. M.; Leumann, C. J.; Sugasawara, R.; Schultz, P. G. *Nature* **1989**, *338*, 269–271.
(105) Janda, K. D.; Weinhouse, M. I.; Schloeder, D. M.; Lerner, R. a; Benkovic, S. J. *J. Am. Chem. Soc.* **1990**, *112*, 1274–1275.
(106) Janda, K. D.; Weinhouse, M. I.; Danon, T.; Pacelli, K. A.; Schloeder, D. M. *J. Am. Chem. Soc.* **1991**, *113*, 5427–5434.
(107) Wirsching, P.; Ashley, J. A.; Lo, C. L.; Janda, K. D.; Lerner, R. A. *Science* **1995**, *270*, 1775–1783.
(108) Björnestedt, R.; Zhong, G.; Lerner, R. a.; Barbas, C. F. *J. Am. Chem. Soc.* **1996**, *118*, 11720–11724.
(109) Lo, C. L.; Wentworth, P.; Jung, K. W.; Yoon, J.; Ashley, J. A.; Janda, K. D. *J. Am. Chem. Soc.* **1997**, *119*, 10251–10252.
(110) Suga, H.; Ersoy, O.; Williams, S. F.; Tsumuraya, T.; Margolies, M. N.; Sinskey, A. J.; Masamune, S. *J. Am. Chem. Soc.* **1994**, *116*, 6025–6026.
(111) Tsumuraya, T.; Suga, H.; Meguro, S.; Tsunakawa, A.; Masamune, S. *J. Am. Chem. Soc.* **1995**, *117*, 11390–11396.
(112) Barbas, C. F.; Kang, A. S.; Lerner, R. a; Benkovic, S. J. *Proc. Natl. Acad. Sci.* **1991**, *88*, 7978–7982.
(113) Zhou, G.; Guo, J.; Huang, W.; Fletterick, R.; Scanlan, T. *Science* **1994**, *265*, 1059–1064.
(114) Wilson, I. A.; Stanfield, R. L. *Curr. Opin. Struct. Biol.* **1994**, *4*, 857–867.
(115) Schwabacher, A. W.; Weinhouse, M. I.; Auditor, M. T. M.; Lerner, R. A. *J. Am. Chem. Soc.* **1989**, *111*, 2344–2346.
(116) Harada, A.; Okamoto, K.; Kamachi, M.; Honda, T.; Miwatani, T. *Chem. Lett.* **1990**, *19*, 917–918.
(117) Harada, A.; Okamoto, K.; Kamachi, M. *Chem. Lett.* **1991**, *20*, 953–956.
(118) Akashi, S.; Kato, K.; Torizawa, T.; Dohmae, N.; Yamaguchi, H.; Kamachi, M.;

Harada, A.; Imanaka, T.; Shimada, I.; Takio, K. *Biochem. Biophys. Res. Commun.* **1997**, *240*, 566–572.
(119) Takagi, M.; Kohda, K.; Hamuro, T.; Harada, A.; Yamaguchi, H.; Kamachi, M.; Imanaka, T. *FEBS Lett.* **1995**, *375*, 273–276.
(120) Harada, A.; Fukushima, H.; Shiotsuki, K.; Yamaguchi, H.; Oka, F.; Kamachi, M. *Inorg. Chem.* **1997**, *36*, 6099–6102.
(121) Yamaguchi, H.; Tsubouchi, K.; Kawaguchi, K.; Horita, E.; Harada, A. *Chem. Eur. J.* **2004**, *10*, 6179–6186.
(122) Cochran, A.; Schultz, P. *Science* **1990**, *249*, 781–783.
(123) Cochran, A. G.; Schultz, P. G. *J. Am. Chem. Soc.* **1990**, *112*, 9414–9415.
(124) Keinan, E.; Sinha, S. C.; Sinha-Bagchi, A.; Benory, E.; Ghozi, M. C.; Eshhar, Z.; Green, B. S. *Pure Appl. Chem.* **1990**, *62*, 2013–2019.
(125) Nimri, S.; Keinan, E. *J. Am. Chem. Soc.* **1999**, *121*, 8978–8982.
(126) Nicholas, K. M.; Wentworth, P.; Harwig, C. W.; Wentworth, A. D.; Shafton, A.; Janda, K. D. *Proc. Natl. Acad. Sci.* **2002**, *99*, 2648–2653.
(127) Girgenti, E.; Ricoux, R.; Mahy, J.-P. *Tetrahedron* **2004**, *60*, 10049–10058.
(128) Raffy, Q.; Ricoux, R.; Mahy, J.-P. *Tetrahedron Lett.* **2008**, *49*, 1865–1869.
(129) Raffy, Q.; Ricoux, R.; Sansiaume, E.; Pethe, S.; Mahy, J.-P. *J. Mol. Catal. A Chem.* **2010**, *317*, 19–26.
(130) Sansiaume, E.; Ricoux, R.; Gori, D.; Mahy, J. P. *Tetrahedron Asymmetry* **2010**, *21*, 1593–1600.
(131) Harada, A.; Yamaguchi, H.; Okamoto, K.; Fukushima, H.; Shiotsuki, K.; Kamachi, M. *Photochem. Photobiol.* **1999**, *70*, 298–302.
(132) Yamaguchi, H.; Kamachi, M.; Harada, A. *Angew. Chem. Int. Ed.* **2000**, *39*, 3829–3831.
(133) Onji, T.; Ohara, H.; Yamaguchi, H.; Ikeda, N.; Harada, A. *Chem. Lett.* **2006**, *35*, 1126–1127.
(134) Harada, A.; Shiotsuki, K.; Fukushima, H.; Yamaguchi, H.; Kamachi, M. *Inorg. Chem.* **1995**, *34*, 1070–1076.
(135) Yamaguchi, H.; Harada, A.; Kamachi, M. *React. Funct. Polym.* **1998**, *37*, 245–250.
(136) Yamaguchi, H.; Harada, A. *Chem. Lett.* **2002**, *31*, 382–383.
(137) Yamaguchi, H.; Harada, A. *Biomacromolecules* **2002**, *3*, 1163–1169.
(138) Yamaguchi, H.; Harada, A. *Top.Curr.Chem.* **2003**, *228*, 237–258.
(139) Harada, A.; Yamaguchi, H.; Tsubouchi, K.; Horita, E. *Chem. Lett.* **2003**, *32*, 18–19.
(140) Matsumoto, T.; Yamaguchi, H.; Kamijo, K.; Akiyoshi, M.; Matsunaga, T.; Harada,

A. *Bull. Chem. Soc. Jpn.* **2013**, *86*, 198–202.
(141) Yli-Kauhaluoma, J. T.; Ashley, J. A.; Lo, C.-H.; Tucker, L.; Wolfe, M. M.; Janda, K. D. *J. Am. Chem. Soc.* **1995**, *117*, 7041–7047.
(142) Yamaguchi, H.; Hirano, T.; Kiminami, H.; Taura, D.; Harada, A. *Org. Biomol. Chem.* **2006**, *4*, 3571–3573.
(143) Ghosh, P.; Shabat, D.; Kumar, S.; Sinha, S. C.; Grynszpan, F.; Li, J.; Noodleman, L.; Keinan, E. *Nature* **1996**, *382*, 339–341.
(144) Yamaguchi, H.; Harada, A. *Chem. Lett.* **2008**, *37*, 1184–1189.
(145) Mahy, J.-P.; Maréchal, J.-D.; Ricoux, R. *Chem. Commun.* **2015**, *51*, 2476–2494.

Chapter 2
Chiral Recognition by Monoclonal Antibodies against Binaphthyl Derivatives

2-1. Introduction

In biological systems, chirality plays vital roles as exemplified by the difference in activity of enantiomer of chiral molecules. Therefore, the rational design of chiral recognition element has attracted great deal of attention for synthesis, separation and detection of chiral compounds. Previously, biomolecules such as polysaccharides,[1] proteins[2,3] cyclodextrins,[4–7] as well as synthetic polymers[8,9] or supramolecules[10–14] have been used as chiral recognition elements. One promising strategy to recognize chirality precisely is to generate mAbs for each enantiomer of chiral molecules. The fact that antibody can recognize chirality was revealed at the beginning of the 20th century.[15] After the pioneering work, however, efforts on the preparation of stereoselective mAbs have mainly been focused on bioactive substances such as drug candidates,[16–29] even though the supramolecular complexation of mAbs with synthetic chiral compounds[30–32] includes the possibility of new function.

In this chapter, the author focused on the chiral recognition ability of mAbs for axially chiral binaphthyl derivatives that compose a well-known asymmetric ligand, 2,2'-bis(diphenylphosphino)-1,1'-binaphthyl (BINAP).[33] A chiral binaphthyl derivative bearing an alkyl linker and a carboxyl group (BN) was designed as a hapten to generate mAbs that bind various binaphthyl compounds in an atroposelective manner. Preparation of mAbs for BN employed two kinds of immunization strategies. First, immunization with enantiomeric pure BN was adopted to ensure the isolation of mAbs with atroposelectivity toward BN. The second strategy involved immunization with BN (*rac*) and screening of mAbs with enantiomeric pure BN. The mAbs obtained by the two strategy showed atroposelectivity for BN, 1,1’-bi-2-naphthol (BINOL) and 1,1'-binaphthyl-2,2'-diyl hydrogen phosphate (BNPA). The mechanism of chiral recognition by mAbs was discussed based on the cross reactivity of mAbs for a naphthyl derivative (N) and biphenyl derivative (BP) as well as docking simulation.

2-2. Experimental section

Materials

2-Naphthol, 1-ethyl-3-(3-dimethylaminopropyl) carbodiimide hydrochloride (EDC), 1-hydroxybenzotriazole (HOBt), KH_2PO_4, $Na_2B_4O_7 \cdot 10H_2O$, *p*-nitrophenyl phosphate sodium salt, RPMI 1640 medium, and Blocking One were purchased from Nakalai Tesque, Inc. (*R*), (*S*), (*rac*)-1,1'-bi-2-naphthol (BINOL), (*R*), (*S*)-1,1'-binaphthyl-2,2'-diyl hydrogen phosphate (BNPA), 2, 2'-biphenol were obtained from Tokyo Chemical Industry Co. Ltd. Bovine serum albumin **(**BSA) was purchased from Medical & Biological Laboratories Co. Ltd. Keyhole limpet hemocyanin (KLH), hypoxanthine thymidine (HT), hypoxanthine aminopterin thymidine (HAT) supplement, and alkaline phosphatase labeled anti-mouse IgG were obtained from Sigma Aldrich Co. BCA protein assay reagents A and B, and Freund's complete adjuvant (FCA) were purchased from Thermo Scientific Co. Ltd. Female Balb/c mice were purchased from Japan SLC, Inc. Poly(ethylene glycol)(PEG; 1,500 Da, PEG 50% w/v in 75 mM 4-(2-hydroxyethyl)-1-piperazineethanesulfonic acid) was obtained from Roche Applied Science. Myeloma cell (SP2/0-Ag14) was purchased from RIKEN Bio Resource Center. Fetal bovine serum (FBS) was obtained from MP Biomedicals, LLC. 2,6,10,14-Tetramethylpentadecane (pristane) was purchased from Funakoshi Co., Ltd. HiTrap Protein G HP was purchased from GE healthcare. IsoStrip^{TM} mouse monoclonal antibody isotyping kit was obtained from Roche Diagnostics. Other reagents were used without further purification. The buffer compositions are as follows. 0.1 M phosphate borate buffer (PBB): KH_2PO_4 3.97 g, $Na_2B_4O_7 \cdot 10H_2O$ 26.2 g/H_2O 1 L.Washing buffer: 10 mM PBS containing 20 mM NaN_3 and 10 mM of Tween 20. Substrate buffer was prepared by dissolving 1 M di-ethanolamine, 3 mM sodium azide, and 1 mM MgCl in water and pH was adjusted to 9.8 by hydrochloric acid solution.

Measurements

The ^{1}H NMR and ^{13}C NMR spectra were recorded at 500 MHz with a JEOL JNM-ECA 500 NMR spectrometer. The absorption spectra were measured with a JASCO V-650 at room temperature. Optical rotations were measured by using JASCO P2100 polarimeter. Absorbance at 405 nm for the product of the enzymatic reaction on the enzyme-linked immunosorbent assay (ELISA) was measured by an iMark microplate absorbance reader.

General Procedure for (ELISA)

Each well of 96 well microplates was coated with 100 μL of BN (*R*)-BSA or BN (*S*)-BSA and incubated at 4 °C overnight. After the removal of the solutions, 180 μL of Blocking One (1:5 dilution) was added and the plates were incubated at 4 °C overnight. After removal of the solutions, sample was added to each well of the plates and the plates were incubated at 37 °C for 90 min. After removal of the solutions, the well was washed twice with 150 μL of washing buffer. Then 100 μL of alkaline phosphatase labeled anti-mouse IgG (1:1000 dilution) solution was added to each well and the plates were incubated at 37 °C for 90 min. After removal of the solutions, the well was washed with three times with 150 μL of washing buffer. Then 150 μL of *p*-nitrophenyl phosphate sodium salt in substrate buffer (1.0 mg/mL) was added. Absorbance at 405 nm derived from the product the enzymatic hydrolysis reaction was recorded.

Synthesis

BN (*R*), BN (*S*) and BN (*rac*)[34,35]

Scheme 2-1. Synthesis of **BN (*R*)**.

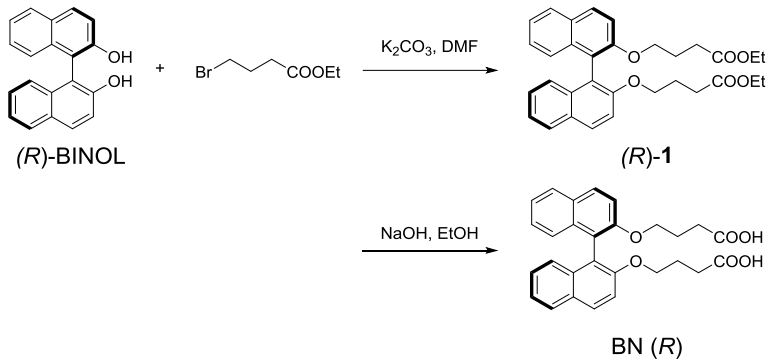

A mixture of *R*-BINOL (450 mg, 1.57 mmol), ethyl 4-bromobutyrate (0.919 g, 4.71 mmol), and K_2CO_3 (0.868 g, 6.28 mmol) was refluxed in DMF (20 mL) under N_2 for 20 h. The solvent was removed under reduced pressure, and the residue was partitioned between CH_2Cl_2 and water. The organic layer was separated, dried with $MgSO_4$ and evaporated to dryness. Purification by column chromatography (hexane: ether, 5:1) gave (*R*)-1. Compound (*R*)-1 was dissolved in a 1:1 mixture of 2 M NaOH and EtOH (20 mL) and refluxed overnight followed by removal of the solvent under reduced pressure. The residue was dissolved in water, which was then acidified with 1 M HCl. The precipitate was filtered off, washed with water and dissolved in CH_2Cl_2 and

filtered. The solvent was removed under reduced pressure to give BN (*R*) as a white powder (290 mg, 40%, **Scheme 2-1**, **Figures 2-1** and **2-2**). BN (*S*) and BN (*rac*) were synthesized in the same way. ^{1}H NMR ($CDCl_3$, 500 MHz): δ 1.59–1.69 (m, 2H, Alkyl), 1.75–1.84 (m, 2H, Alkyl), 1.90–1.99 (m, 2H, Alkyl), 2.03–2.11 (m, 2H, Alkyl), 3.88–3.95 (m, 2H, Alkyl), 4.01–4.08 (m, 2H, Alkyl), 7.10–7.42 (6H, Ar-C*H*), 7.86 (d, 2H, Ar-C*H*), 7.94 (d, 2H, Ar-C*H*). ^{13}C NMR ($CDCl_3$, 150 MHz): δ 24.17, 29.57, 68.11, 115.54, 120.44, 123.55, 125.24, 126.17, 129.25, 129.30, 133.98, 153.93, 179.67. IR (KBr pellet): 2940, 1706, 1263 cm^{-1}. MALDI-TOF-MS (*m/z*): [M + H^+] Calcd.. for $C_{28}H_{27}O_6$, 459.18; found, 458.6. EA: Calcd. for $C_{28}H_{26}O_6 0.25H_2O$: C, 72.63; H, 5.77. Found: C, 72.65; H, 5.80. **BN (*R*)**:$[\alpha]_D^{25}$ 60.4 (THF, *c*=1.00, **BN (*S*)**:$[\alpha]_D^{25}$ -59.6 (THF, *c*=1.00)

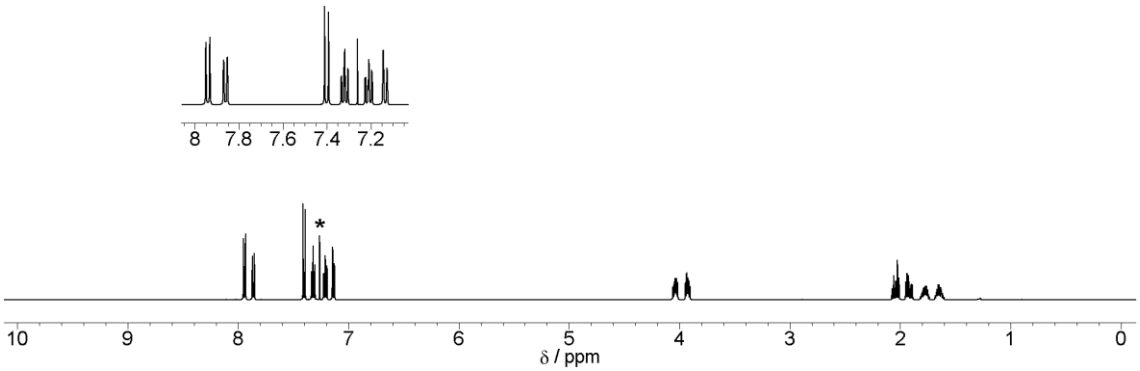

Figure 2-1. ^{1}H NMR spectrum of BN (*S*) in $CDCl_3$ at 303K. The asterisk (*) indicates the solvent peak.

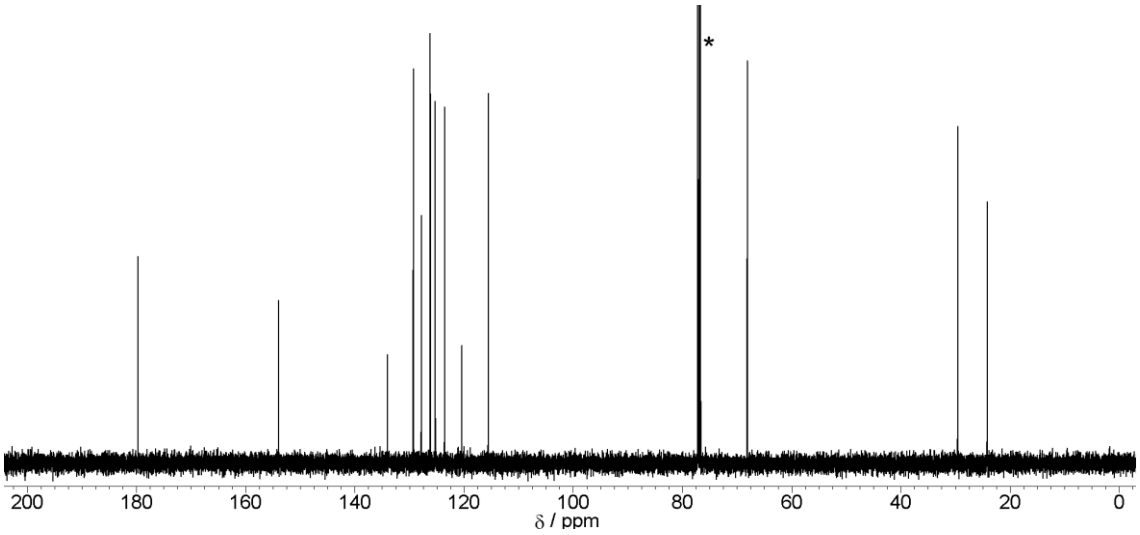

Figure 2-2. ^{13}C NMR spectrum of BN (*S*) in $CDCl_3$ at 303K. The asterisk (*) indicates the solvent peak.

4-(naphthalen-2-yloxy)butanoic acid (N)

Scheme 2-2. Synthesis of N.

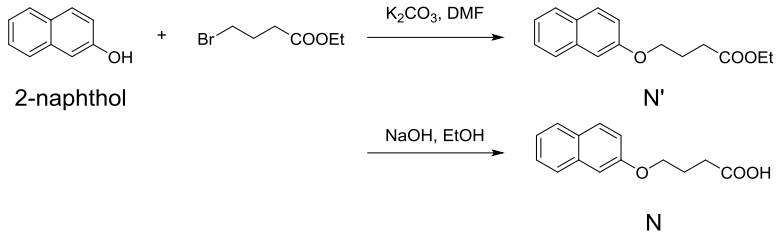

A mixture of 2-naphthol (1.005 g 6.98 mmol), ethyl 4-bromobutyrate (5.40 g 327.7 mmol), K_2CO_3 (2.15 g, 15.5 mmol) was stirred in DMF (25 mL) under Ar at 90 °C for 4 h. The solvent was removed under reduced pressure, and the residue was partitioned between CH_2Cl_2 and water. The organic layer was separated, dried with $MgSO_4$ and evaporated to dryness. Purification by column chromatography (hexane:ethyl acetate, 7:1) gave N'. Compound N' was dissolved in a mixture of 7 M NaOH (30 mL) and THF (20 mL) and stirred at 90 °C for 20 h followed by removal of the solvent under reduced pressure. The residue was dissolved in water, which was then acidified with 6 M HCl, extracted with CH_2Cl_2 and washed with 0.1 M HCl. The organic layer was separated, dried with $MgSO_4$ and evaporated to dryness to give N as a white powder (0.943 g, 59%, **Scheme 2-2**, **Figures 2-3** and **2-4**). ^{1}H NMR (DMSO-d_6, 500 MHz):δ 2.02 (m, 2H, Alkyl), 2.44 (t, J = 7.3 Hz, 2H, Alkyl), 4.11 (t, J = 6.5 Hz, 2H, Alkyl), 7.16 (dd, J = 8.9 Hz, J = 2.6 Hz, 1H, Ar-C*H*), 7.30-7.35 (m, 2H, Ar-C*H*), 7.45 (td, J = 7.5 Hz, J = 1.3 Hz, 1H, Ar-C*H*), 7.78-7.82 (3H, Ar-C*H*), 12.14(s, 1H, COO*H*). ^{13}C NMR (DMSO-d_6, 150 MHz):δ 24.20, 30.14, 66.64, 106.68, 118.65, 123.47, 126.30, 126.61, 127.43, 128.43, 129.21, 134.26, 156.38, 174.05. EA: Calcd. for $C_{14}H_{14}O_3$: C, 73.03; H, 6.13. Found: C, 72.85; H, 6.02.

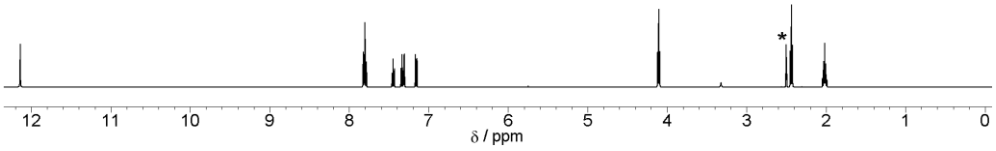

Figure 2-3. ^{1}H NMR spectrum of N in DMSO-d_6 at 303K. The asterisk (*) indicates the solvent peak.

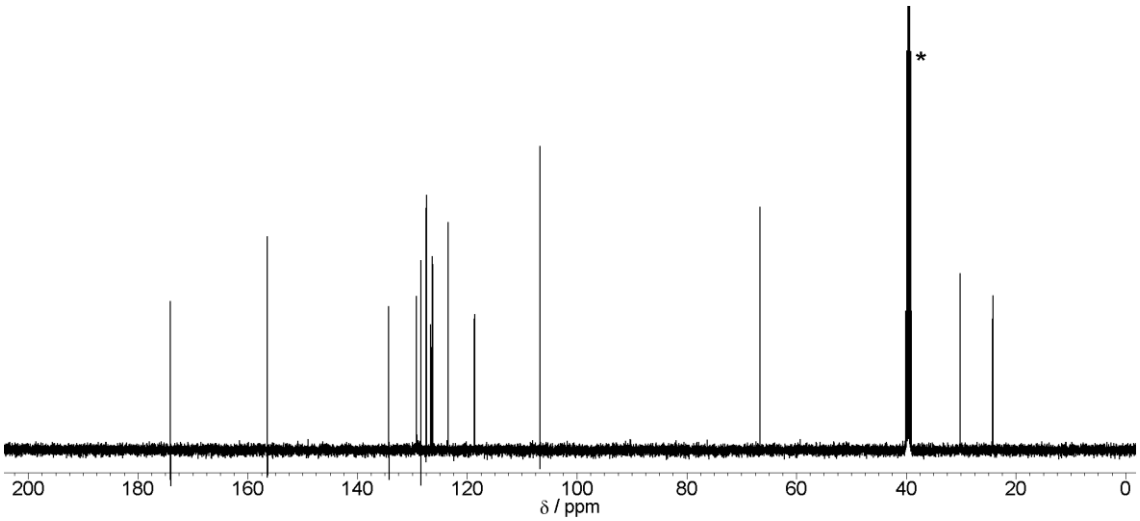

Figure 2-4. ^{13}C NMR spectrum of N in DMSO-d_6 at 303K. The asterisk (*) indicates the solvent peak.

4,4'-([1,1'-biphenyl]-2,2'-diylbis(oxy))dibutanoic acid (BP)

Scheme 2-3. Synthesis of BP.

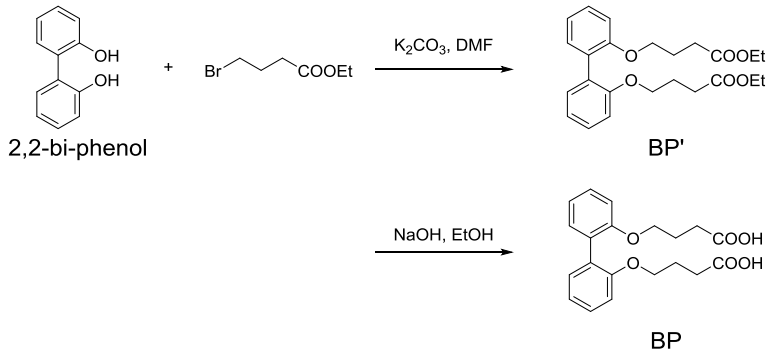

A mixture of 2, 2'-biphenol (1.05 g 5.67 mmol), ethyl 4-bromobutyrate (6.21 g 32.1 mmol), K_2CO_3 (2.93 g, 21.2 mmol) was stirred in DMF (20 mL) under Ar at 90 °C for 22 h. The solvent was removed under reduced pressure, and the residue was partitioned between CH_2Cl_2 and water. The organic layer was separated, dried with $MgSO_4$ and evaporated to dryness. Purification by column chromatography (hexane: ethyl acetate, 95:5) gave BP'. Compound BP' was dissolved in a 1:1 mixture of 6 M NaOH (40 mL) and THF (20 mL) and stirred at 90 °C for 22 h followed by removal of the solvent under reduced pressure. The residue was dissolved in water and washed with CH_2Cl_2 (60 mL×3). The aqueous layer was then acidified with 1 M HCl and extracted with CH_2Cl_2 (60 mL×3). The organic layer was separated, dried with $MgSO_4$ and

evaporated to dryness to give BP as a white powder (470 mg, 23%, **Scheme 2-3**, **Figures 2-5** and **2-6**). ^{1}H NMR (DMSO-d_6, 500 MHz): 1.76 (m, 4H, Alkyl), 2.18 (t, J = 7.4 Hz, 4H, Alkyl), 3.92 (t, J = 6.4 Hz, 4H, Alkyl), 6.95 (td, J = 7.4 Hz, J = 1.1 Hz, 2H, Ar-C*H*), 7.03 (dd, J = 8.4 Hz, J = 1.0 Hz, 2H, Ar-C*H*), 7.15 (dd, J = 7.4 Hz, J = 1.8 Hz, 2H, Ar-C*H*), 7.28 (m, 2H, Ar-C*H*), 12.02(s, 2H, COO*H*). ^{13}C NMR (DMSO-d_6, 150 MHz): 24.23, 29.77, 66.67, 112.14, 119.97, 127.61, 128.45, 131.01, 155.82, 174.03. MALDI-TOF-MS (*m/z*): [M + Na^+], [M + K^+] Calcd. for $C_{20}H_{22}O_6$, 381.13, 397.11; found, 381.5, 397.5. EA: Calcd. for $C_{20}H_{22}O_6$0.08MeCN: C, 66.95; H, 6.20; N, 0.31%. Found: C, 66.68; H, 6.15; N, 0.30%.

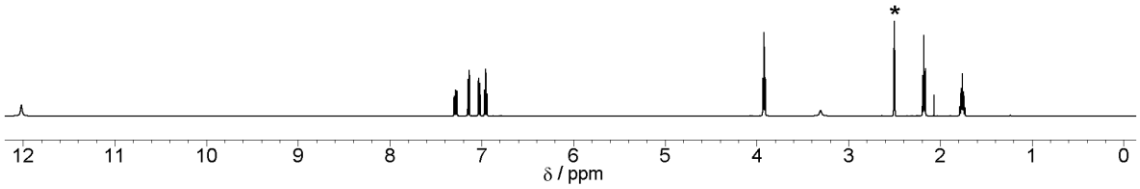

Figure 2-5. ^{1}H NMR spectrum of BP in DMSO-d_6 at 303K. The asterisk (*) indicates the solvent peak.

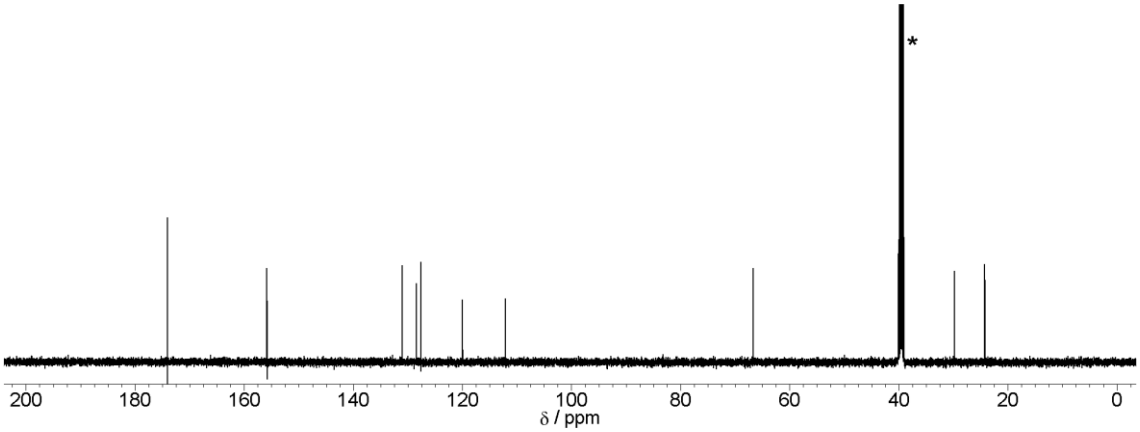

Figure 2-6. ^{13}C NMR spectrum of BP in DMSO-d_6 at 303K. The asterisk (*) indicates the solvent peak.

Preparation of antigen for immunization

BN (*rac*) (4.55 mg, 9.94 μmol), EDC・HCl (5.85 mg, 30.5 μmol), and HOBt (4.05 mg, 30.0 μmol) were dissolved in DMF (2.0 mL) and stirred at 0 °C for 2 hours. Subsequently, this solution was added dropwise to a solution of keyhole limpet hemocyanin (KLH) solution (1.16 nmol in 0.1M PBB) over a period of 1.5 hours and stirred overnight at 0 °C. The resulting solution was purified using ultrafiltration membrane with 10 kDa molecular weight cutoff (Sartorius). BN (*R*) and BN (*S*) was conjugated to KLH in the same way.

Preparation of antigen for assay

BN (*R*) (1.19 mg, 2.61 μmol), EDC・HCl (1.98 mg, 10.3 μmol), and HOBt (1.29 mg, 9.53 μmol) were dissolved in DMF (2.0 mL) and stirred at 0 °C for 2 hours. Subsequently, this solution was added dropwise to a solution of bovine serum albumin (BSA) (0.124 μmol) over a period of 1.5 hours and stirred overnight at 0 °C. The resulting solution was purified using ultrafiltration membrane with 10 kDa molecular weight cutoff (Sartorius). BN (*S*) was conjugated to BSA in the same way.

Characterization of antigens for immunization and assay

The concentration of the antigen for immunization or the antigen for assay was determined by bicinchoninic acid method and adjusted to 0.3 mg/mL. UV-Vis spectra of antigens were measured. The number of conjugated BN is determined by using standard curve of BN (ε_{333}=5750 $M^{-1}cm^{-1}$).

Procedure of immunization

BN (*rac*)-KLH, BN (*R*)-KLH, and BN (*S*)-KLH (0.3 mg/mL) was emulsified with equal amount of Freund's complete adjuvant (FCA). Three groups of Balb/c mice were immunized with 37.5 μg of BN (*rac*)-KLH, BN (*R*)-KLH or BN (*S*)-KLH 3 times at 2 weeks interval, respectively. At boost, each group of mice were immunized with 90 μg of BN (*rac*)-KLH, BN (*R*)-KLH or BN (*S*)-KLH without the adjuvant.

Evaluation of immunoresponse

Dilution series of blood of mice immunized with BN (*rac*) was added to BN (*R*)-BSA and BN (*S*)-BSA-coated plates, respectively. The antibodies adsorbed on BN-coated plates were detected by ELISA. The immunoresponse of mice immunized with BN (*R*) or BN (*S*) was analyzed in the same way as BN (*rac*).

Preparation of mAbs

Three days after the final injection, the spleen cells were removed from the mice and fused with myeloma cells using PEG. The hybridomas which produce antibodies specific for one of the enantiomers of BN were cloned by limited dilution method. The antibodies produced were assayed again and selected. The hybridomas selected were injected to pristane-primed mice. After 7 to 14 days, the ascites fluid was obtained. The ascites fluid was centrifuged and the supernatant was stored at −20 °C. Monoclonal antibodies were purified by affinity chromatography using HiTrap Protein G HP. The subclass of mAbs obtained was determined by using IsoStrip^{TM} mouse monoclonal antibody isotyping kit.

Six and seven mAbs were prepared by immunization with BN (*R*) and BN (*S*), respectively. The mAb R44E1 and mAb S1E11 were selected as mAb for BN (*R*) and BN (*S*), respectively. Among thirty-three mAbs prepared by immunization with BN (*rac*), mAb 34H12 and mAb 9H3 were selected based on the selectivity for BN enantiomer. The four mAbs were all IgG and subclass of them were IgG_1 (R44E1), IgG_{2b} (S1E11), IgG_1 (34H12) and IgG_{2b} (9H3). All four mAbs have κ light chain.

Determination of the dissociation constants (K_d) of the complexes between monoclonal antibody (mAb) and BN, N, and BP

Solutions of mAbs (60 μL in 0.1M PBB) were mixed with solution of substrates in various concentrations (10^{-8} M to 10^{-2} M, 60 μL) on a BSA-coated plate. The mixed solutions were incubated at 4 °C overnight and added to a BN (*R*)-BSA coated plate (in the case of mAbs specific for BN (*R*)) or a BN (*S*)-BSA coated plate (in the case of mAbs specific for BN (*S*)). The plates were incubated at 37 °C for 90 min. After removal of the solutions, the well was washed twice with 150 μL washing buffer. Then 100 μL of alkaline phosphatase labeled anti-mouse IgG (1:1000 dilution) was added and the plates were incubated at 37 °C for 90 min. After removal of the solution, the well was washed with three times with 150 μL of washing buffer. Then 150 μL *p*-nitrophenyl phosphate sodium salt in substrate buffer (1.0 mg / mL) was added. Absorbance at 405 nm derived from the product of the enzyme reaction was recorded.

Dissociation constants were determined by the Klotz plot

$$\frac{A_0}{A_0 - A} = 1 + K_d(\frac{1}{c})$$

where A_0 and A indicate absorbance at 405 nm in the absence or presence of competitive molecules, respectively. The character c shows the concentration of dilution series of competitive molecule such as BN (*R*), BN (*S*), N, and BP. K_d represents the

dissociation constant.

Sequence analysis of variable region of mAb R44E1 and mAb S1E11

Total RNA of hybridoma cell lines secreting mAb R44E1 and mAb S1E11 were isolated using RNeasy Mini Kit（QIAGEN）and was converted to cDNA by reverse transcription reaction. The cDNA obtained was converted to duplex and adaptor ligation was carried out to prepare cDNA-adaptor. DNA sequence was determined by ABI3730xl.

Docking simulation of mAb R44E1 with BN (*R*), and mAb S1E11 with BN (*S*)

The variable region of mAb R44E1 and mAb S1E11 were modeled using Rosetta Online Server that Includes Everyone (ROSIE).[36–41] The model structures of L chain of mAb R44E1 were constructed using PDB 1H0D as template for frame work region and CDRs. Construction of model structure of H chain of mAb R44E1 employed PDB 1UYW for the template for frane work region and H1. Model structures of H2 and H3 of mAb R44E1 used PDB 2A6I and PDB 1AY1 as template, respectively. The L chain of mAb S1E11 was modeled using PDB 2BDN for the template of frame work region and PDB 3CVI for L1, L2 and L3. The H chain of mAb S1E11 was constructed using PDB 2OZ4, PDB 1FGV and PDB 3CLF as the template for frame work region, H1 and H2, respectively. Docking simulation of mAbs with BN enantiomer was carried out using LigandDocking.[42-45]

2-3. Results and Discussion

Characterization of antigens for immunization and assay

The number of BN (*R*), BN (*S*) and BN (*rac*) conjugated to KLH were 1.0×10^3 per KLH molecule (**Fig. 2-7a**). The UV-Vis spectra of BN (*R*)-KLH and that for BN (*S*)-KLH are overlapped. The number of BN (*R*) and BN (*S*) attached to BSA was 5 (**Fig. 2-7b**).

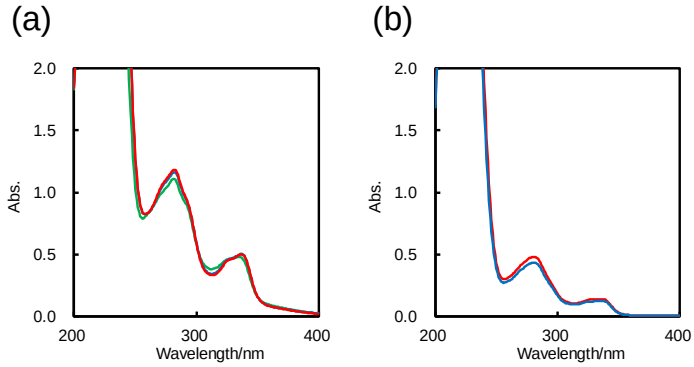

Figure 2-7. UV-Vis spectra of 0.25 mg/mL of BN (*R*)-KLH (blue), BN (*S*)-KLH (red) and BN (*rac*)-KLH (green) (a) and that for 0.30 mg/mL of BN (*R*)-BSA (blue) and BN (*S*)-BSA (red) (b).

Immune response against BN (*R*), BN (*S*) and BN (*rac*)

Antibodies in blood of mice immunized with BN (*R*)-KLH adsorbed mainly on BN (*R*)-BSA (**Figure 2-8 a**). In contrast, the amount of antibodies adsorbed on BN (*S*)-BSA was larger than that on BN (*R*)-BSA in the case of immunization with BN (*S*)-KLH (**Figure 2-8 b**). Immune system clearly recognizes the chirality of BN. In the case of immunization with BN (*rac*)-KLH, no difference is observed in the amounts of antibodies adsorbed on BN (*R*)-BSA and BN (*S*)-BSA (**Figure 2-8 c**). This result raises two possible interpretation. First, the mixture of anti-BN (*R*) mAbs and anti-BN (*S*) mAbs yielded the results. Another interpretation is that the antibodies with no atroposelectivity were dominant in the mice. These two possibilities are validated later from the specificity of isolated mAbs. The immune response toward BN (*R*) and BN (*S*) induced by immunization with BN (*rac*) is equivalent to that induced by immunization with pure enantiomer (**Figure 2-8 d**), even though the number of BN (*R*) and BN (*S*) attached to BN (*rac*)-KLH was the half the enantiomeric pure antigens. This result highlights the superiority of immunization with BN (*rac*) in the induction of immunoresponse to BN enantiomer. Interestingly, the result obtained herein is opposite to a report on nicotine

vaccination where enantiomeric pure hapten induced stronger immunoresponse compared with racemic hapten.[46] Structural difference of hapten might result in this difference.

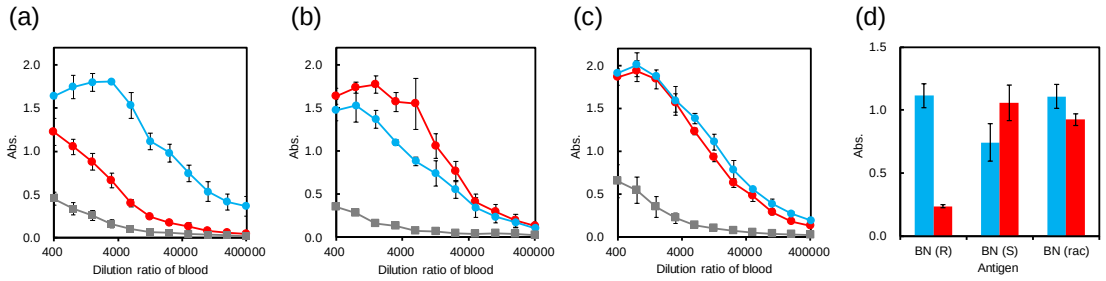

Figure 2-8. The ELISA for blood from mice immunized three times with BN (*R*) (a), BN (*S*) (b) or BN (*rac*)-KLH (c), respectively. The absorbance for blood of mice at 1:12800 dilution (d). Serial dilution of blood was added to the BN (*R*)-BSA (blue), BN (*S*)-BSA (red), and BSA-coated plates (gray)) and bound antibodies were detected by ELISA.

Chiral recognition of mAbs for BN enantiomer

The affinity of mAbs was determined by competitive ELISA (**Table 2-1**). The dissociation constant (K_d) of mAb R44E1 for BN (*R*) is 1.6×10^{-7} M, while that for BN (*S*) is 1.3×10^{-4} M (**Figure 2-9**). The mAb R44E1 recognizes the atropisomerism of BN with an 810-fold difference in affinity. The mAb S1E11 has higher affinity for BN (*S*) than BN (*R*). The K_d values for BN (*R*) and BN (*S*) are 4.8×10^{-7} M and 9.0×10^{-4} M, respectively (**Figure 2-10**). The mAb S1E11 has 1900-fold higher affinity for BN (*S*) than BN (*R*). These results indicate that the atroposelectivity of mAbs can be controlled directly by immunization with enantiomeric pure BN.

mAbs prepared by racemic immunization can be divided in four groups; BN (*R*) selective mAbs, BN (*S*) selective mAbs, mAbs with no atroposelectivity, and mAbs with no affinity for BN (**Figure 2-11**). Among the mAbs with atroposelectivity, mAb 34H12 and mAb 9H3 were selected from their high selectivity for BN (*R*) and BN(*S*), respectively. Their binding affinity was evaluated in detail. The mAb 34H12 binds BN (*R*) with a K_d value of 8.5×10^{-8} M, contrary the K_d value for BN (*S*) is 1.4×10^{-4} M. mAb 34H12 has a 1700-fold higher affinity for BN (*R*) than BN (*S*) (**Figure 2-12**). The mAb 9H3 prefers to bind the opposite enantiomer of BN. The affinity for BN (*S*) ($K_d = 6.7\times10^{-8}$M) is higher than that for BN (*R*) ($K_d = 9.6\times10^{-4}$ M) (**Figure 2-13**). Among the four mAbs, mAb 9H3 has the highest affinity for the targeted enantiomer and the weakest affinity toward the opposite enantiomer. mAb 9H3 recognizes the axial chirality of BN with a 14000-fold difference in affinity. Based on these results, it is reasonable that the mixture

of anti-BN (*R*) mAbs and anti-BN (*S*) mAbs yielded the immunoresponse of mice immunized with BN (*rac*). (**Figure 2-8 c**). Some of previous studies concluded based on the analysis of specificity of antisera that immunization with racemic mixture of hapten does not induce stereoselective antibodies.[47–49] However, the analysis of binding specificity of isolated mAbs should be taken into consideration. This study shows that the stereoselective mAbs can be isolated by immunization with racemic mixture based on the combination of analysis of polyclonal antibodies in blood and isolated mAbs. Notably, atroposelective antibodies for both enantiomer can be developed at one time by immunization with BN (*rac*). This finding provides a strategy to rapidly diverse the pool of mAbs for BN enantiomer.

The affinity of mAb R44E1 and mAb 34H12 for N and the BP (**Figures 2-14**, **2-15**, **2-16** and **2-17**) are *ca*. ten-thousandth compared with that for BN (*R*) (**Figures 2-9** and **2-12**). Furthermore, mAb S1E11 and mAb 9H3 do not show cross reactivities toward N and BP in the measured concentration range (**Figures 2-18**, **2-19**, **2-20**, and **2-21**). These low cross reactivities for N and BP suggest that mAbs recognize the crossing moiety of the two naphthyl rings.

Table 2-1. Dissociation constants (K_d) of complexes of mAbs with (*R*), (*S*)-BN, (*R*), (*S*)-BINOL, (*R*), (*S*)-BNPA, N and BP.

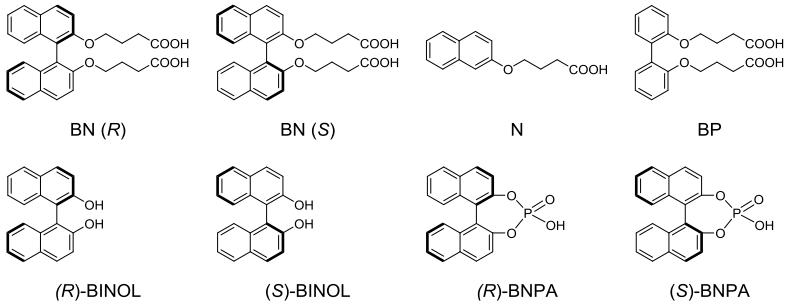

mAbs	R44E1	S1E11	34H12	9H3
Specificity	*R*	*S*	*R*	*S*
Immunogen	*R*	*S*	*R*/*S*	*R*/*S*
$K_{BN\ (R)}$ / M	1.6×10^{-7}	9.0×10^{-4}	8.5×10^{-8}	9.6×10^{-4}
$K_{BN\ (S)}$ / M	1.3×10^{-4}	4.8×10^{-7}	1.4×10^{-4}	6.7×10^{-8}
Selectivity[a]	810	1900	1700	14000
$K_{(R)\text{-BINOL}}$ / M	2.8×10^{-7}	2.1×10^{-5}	2.7×10^{-7}	4.3×10^{-5}
$K_{(S)\text{-BINOL}}$ / M	1.7×10^{-6}	2.2×10^{-6}	2.6×10^{-5}	2.5×10^{-6}
Selectivity[a]	6.3	9.7	95	17
$K_{(R)\text{-BNPA}}$ / M	4.3×10^{-7}	4.3×10^{-6}	2.5×10^{-5}	1.2×10^{-5}
$K_{(S)\text{-BNPA}}$ / M	1.6×10^{-5}	2.1×10^{-6}	1.0×10^{-3}	1.9×10^{-6}
Selectivity[a]	37	2.1	40	6.6
K_N / M	9.8×10^{-4}	ND[b]	4.0×10^{-3}	ND[b]
K_{BP} / M	2.2×10^{-3}	ND[b]	1.8×10^{-3}	ND[b]

[a]Selectivity is calculated by dividing the higher K_d value by the lower one.

[b]Interaction is not detected in competitive ELISA.

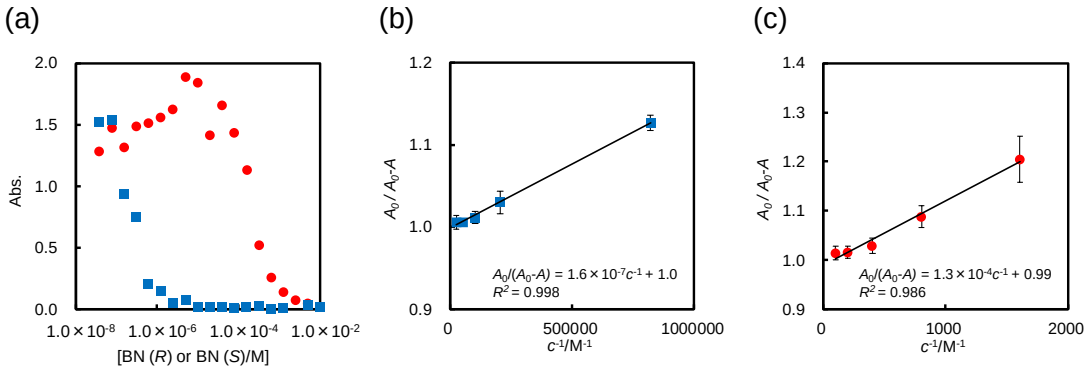

Figure 2-9. Competitive ELISA of mAb R44E1 for BN (*R*) (■) and BN (*S*) (●) (a). Klotz plot for mAb R44E1 with BN (*R*) (b) and BN (*S*) (c).

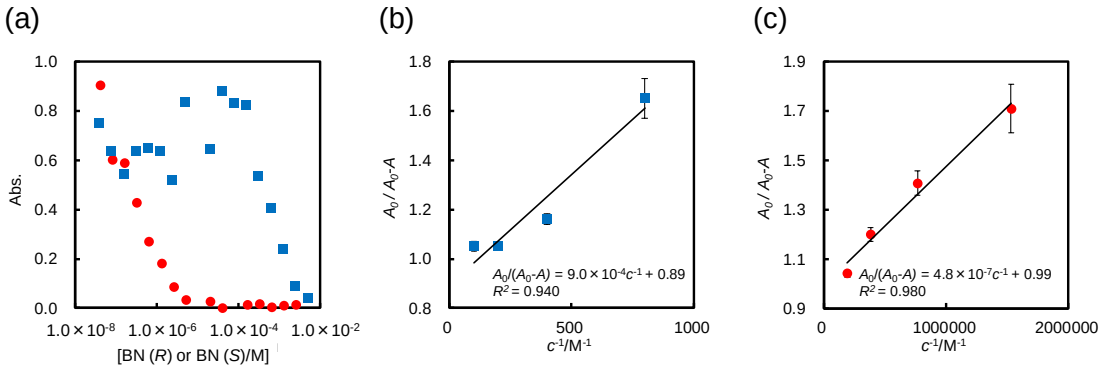

Figure 2-10. Competitive ELISA of mAb S1E11 for BN (*R*) (■) and BN (*S*) (●) (a). Klotz plot for mAb S1E11 with BN (*R*) (b) and BN (*S*) (c).

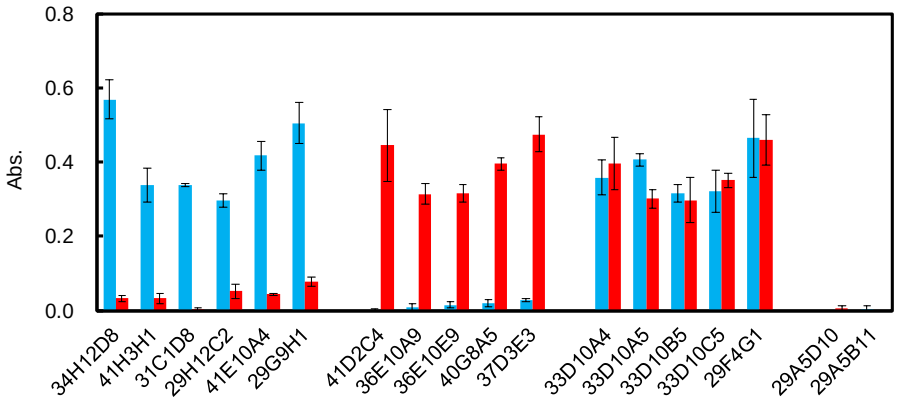

Figure 2-11. Typical examples of the ELISA for culture supernatant of monoclonal hybridomas established from a mouse immunized with BN (*rac*). The mAbs contained in was captured by BN (*R*)-BSA (blue) and BN (*S*)-BSA-coated plates (red)) and detected by ELISA.

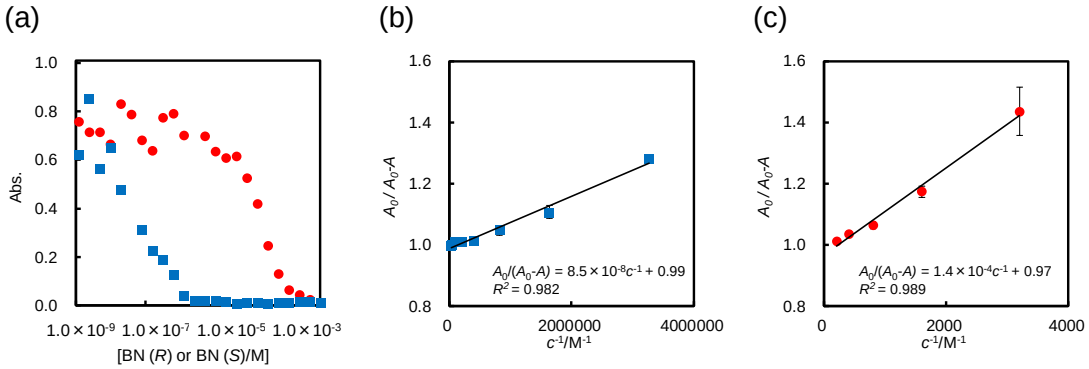

Figure 2-12. Competitive ELISA of mAb 34H12 for BN (*R*) (■) and BN (*S*) (●) (a). Klotz plot for mAb 34H12 with BN (*R*) (b) and BN (*S*) (c).

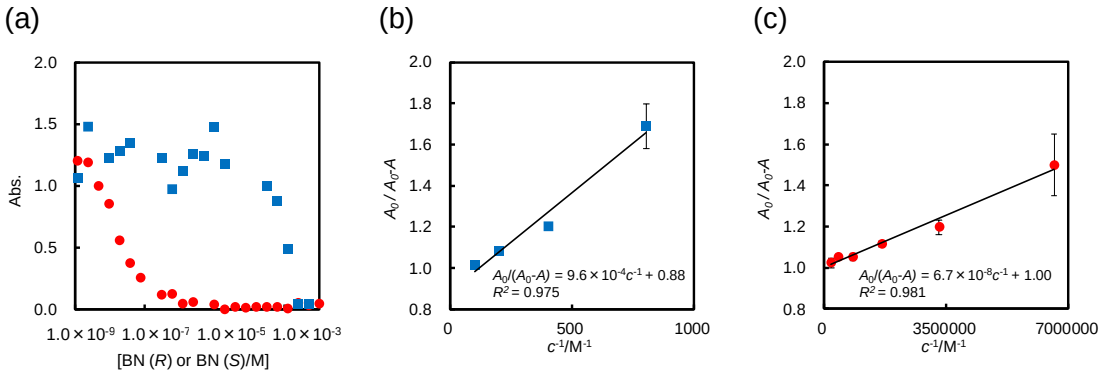

Figure 2-13. Competitive ELISA of mAb 9H3 for BN (*R*) (■) and BN (*S*) (●) (a). Klotz plot for mAb 9H3 with BN (*R*) (b) and BN (*S*) (c).

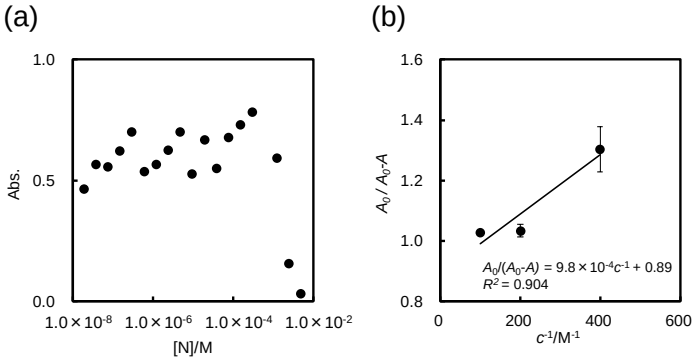

Figure 2-14. Competitive ELISA of mAb R44E1 for N (a) and the corresponding Klotz plot (b).

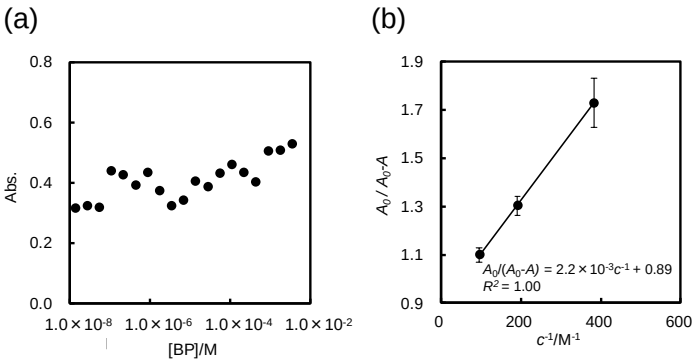

Figure 2-15. Competitive ELISA of mAb R44E1 for BP (a) and the corresponding Klotz plot (b).

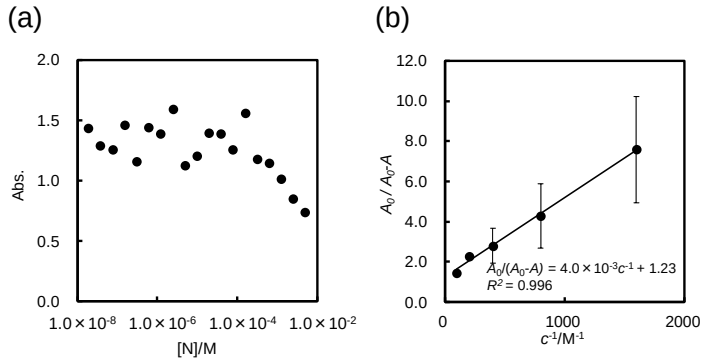

Figure 2-16. Competitive ELISA of mAb 34H12 for N (a) and the corresponding Klotz plot (b).

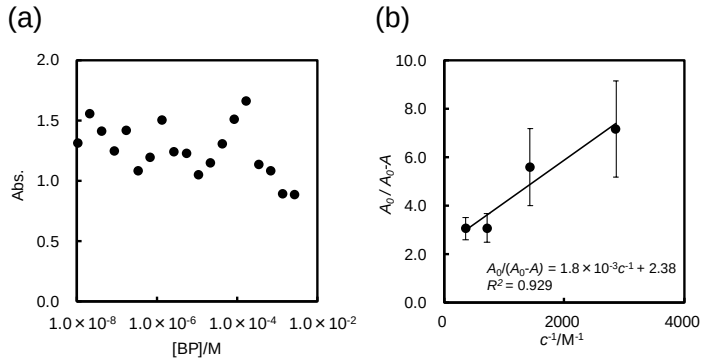

Figure 2-17. Competitive ELISA of mAb 34H12 for BP (a) and the corresponding Klotz plot (b).

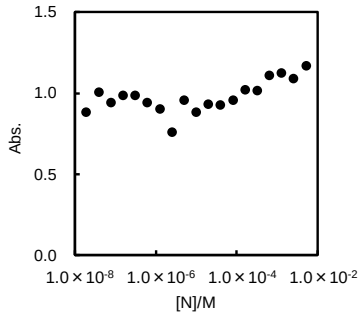

Figure 2-18. Competitive ELISA of mAb S1E11 for N.

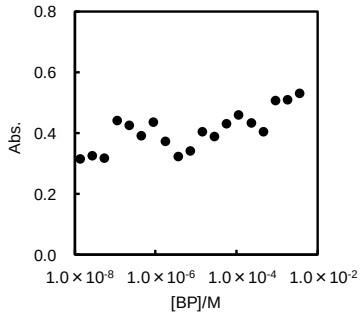

Figure 2-19. Competitive ELISA of mAb S1E11 for BP.

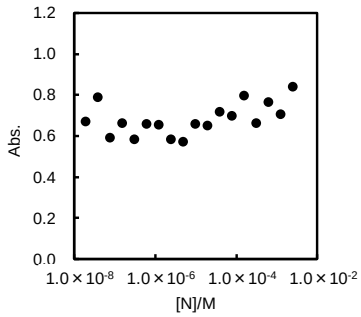

Figure 2-20. Competitive ELISA of mAb 9H3 for N.

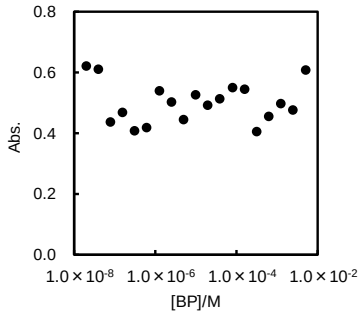

Figure 2-21. Competitive ELISA of mAb 9H3 for BP.

Binding scope of mAbs toward binaphthyl compounds other than BN

The affinity of mAbs for binaphthyl derivatives other than BN was investigated (**Figure 2-22**). BINOL and BNPA were selected as target molecules. BINOL is an important building block in the synthesis of various binaphthyl derivatives.[50,51] BNPA is a chiral organic catalyst with binaphthyl backbone.[52–58] All four mAbs bind BINOL in an enantioselective manner (**Figure 2-22 b**). The affinity of mAb 9H3 for (*S*)-BINOL is 37-fold lower compared with that for BN (*S*) (**Figure 2-23**). In contrast, mAb R44E1, mAb S1E11 and mAb 34H12 show similar affinity for BN and BINOL (**Figures 2-24**, **2-25**, and **2-26**). In addition, all four mAbs also bind enantiomer of BNPA (**Figure 2-22 c**). Although, mAb 34H12 and mAb 9H3 have relatively lower affinity for BNPA than that for BN (**Figures 2-27** and **2-28**), mAb R44E1 and mAb S1E11 bind BNPA with similar affinity for BN (**Figures 2-29** and **2-30**).

Although, the affinity of mAbs for BINOL and BNPA is lower compared with that for BN enantiomer, anti-BN mAbs also bind enantiomer of BINOL and BNPA in an enantioselective manner. These results validate our strategy to create chiral recognition element for axially chiral binaphthyl derivatives. The cross reactivity of anti-BN mAbs for enantiomer of BINOL and BNPA depends on mAbs. Especially, the cross reactivities of mAb 9H3 for BINOL and BNPA are very low. This result indicates that mAb 9H3 has specificity for BN among axially chiral compounds. The affinity and atroposelectivity of mAbs for BINOL and BNPA are lower compared with that for BN. This is presumably due to the participation of alkyl linker and carboxyl group of BN in the binding of mAbs, or the difference in the bite angle of BN, BINOL and BNPA. Notably, chiral supramolecular complexes of mAbs with a chiral organic catalyst with binaphthyl backbone is developed for the first time in this study

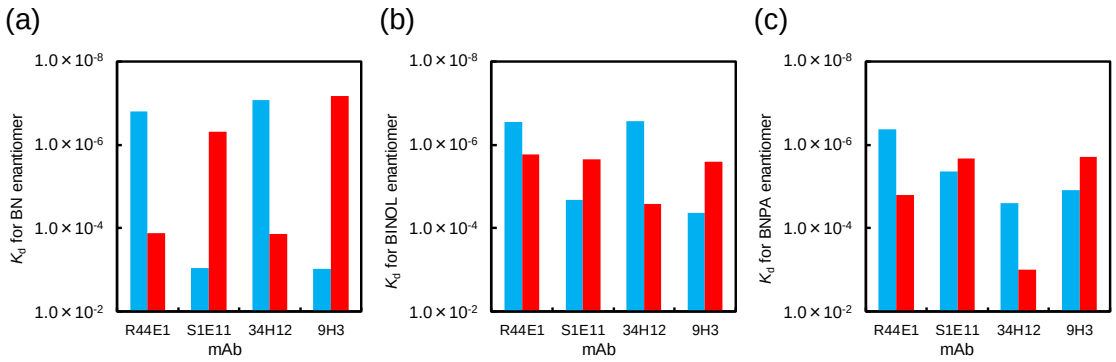

Figure 2-22. K_d values of mAbs for *R* (blue) or *S* (red) isomer of BN (a), BINOL (b) and BNPA (c).

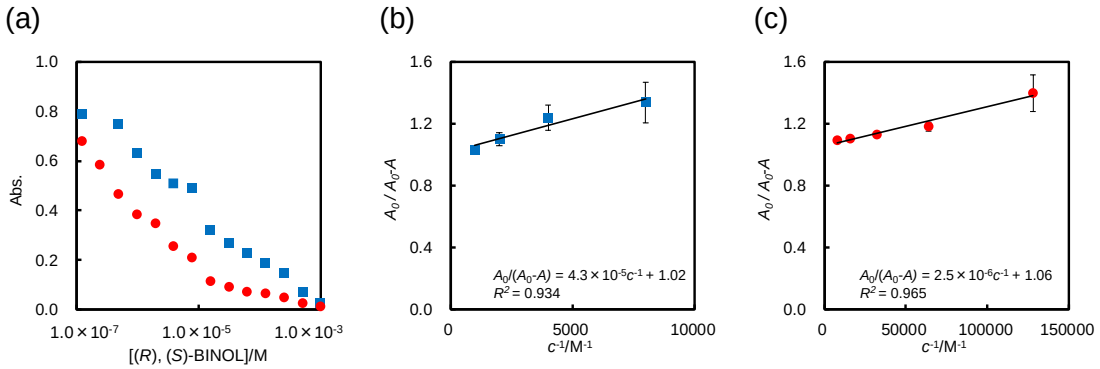

Figure 2-23. Competitive ELISA of mAb 9H3 for (*R*)-BINOL (■) and (*S*)-BINOL (●) (a). Klotz plot for mAb R44E1 with (*R*)-BINOL (b) and (*S*)-BINOL (c).

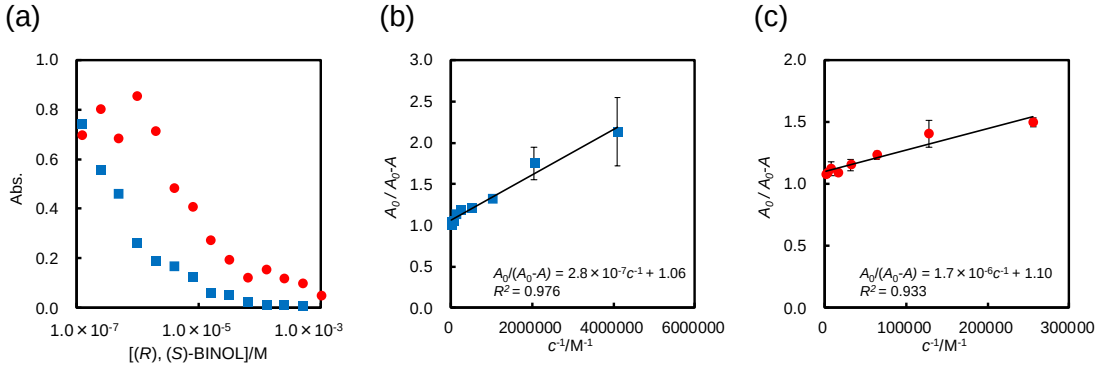

Figure 2-24. Competitive ELISA of mAb R44E1 for (*R*)-BINOL (■) and (*S*)-BINOL (●) (a). Klotz plot for mAb R44E1 with (*R*)-BINOL (b) and (*S*)-BINOL (c).

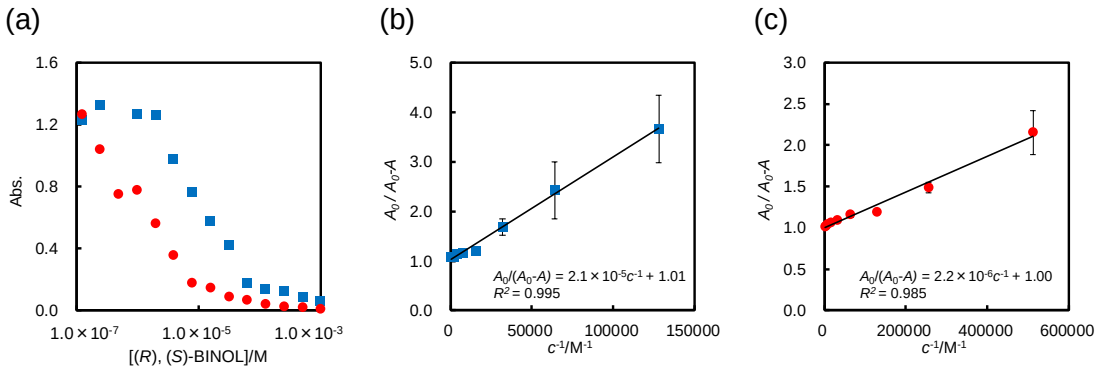

Figure 2-25. Competitive ELISA of mAb S1E11 for (*R*)-BINOL (■) and (*S*)-BINOL (●) (a). Klotz plot for mAb R44E1 with (*R*)-BINOL (b) and (*S*)-BINOL (c).

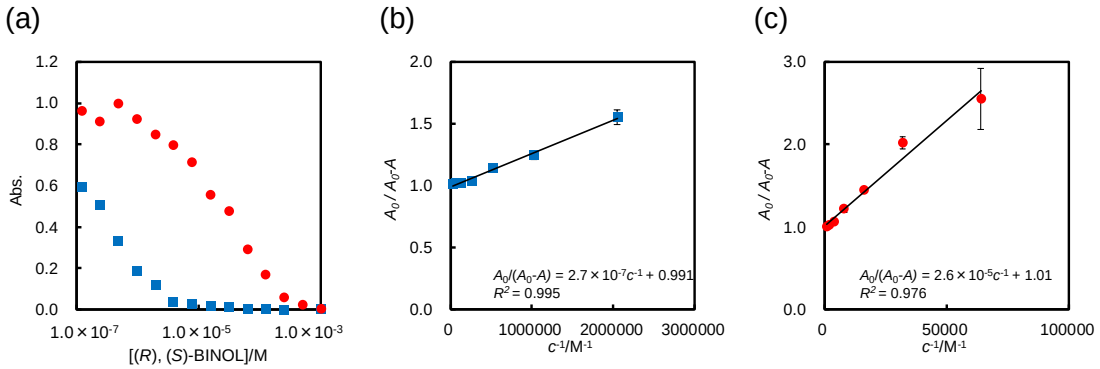

Figure 2-26. Competitive ELISA of mAb 34H12 for (*R*)-BINOL (■) and (*S*)-BINOL (●) (a). Klotz plot for mAb R44E1 with (*R*)-BINOL (b) and (*S*)-BINOL (c).

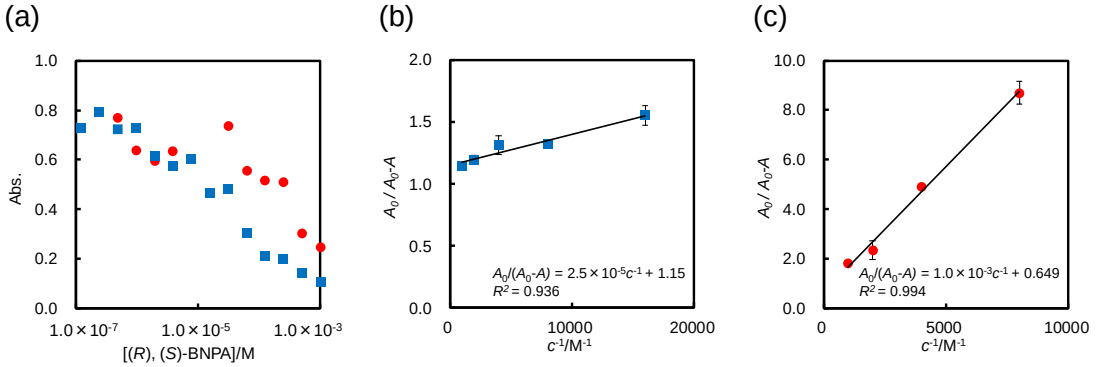

Figure 2-27. Competitive ELISA of mAb 34H12 for (*R*)-BNPA (■) and (*S*)-BNPA (●) (a). Klotz plot for mAb R44E1 with (*R*)-BNPA (b) and (*S*)-BNPA (c).

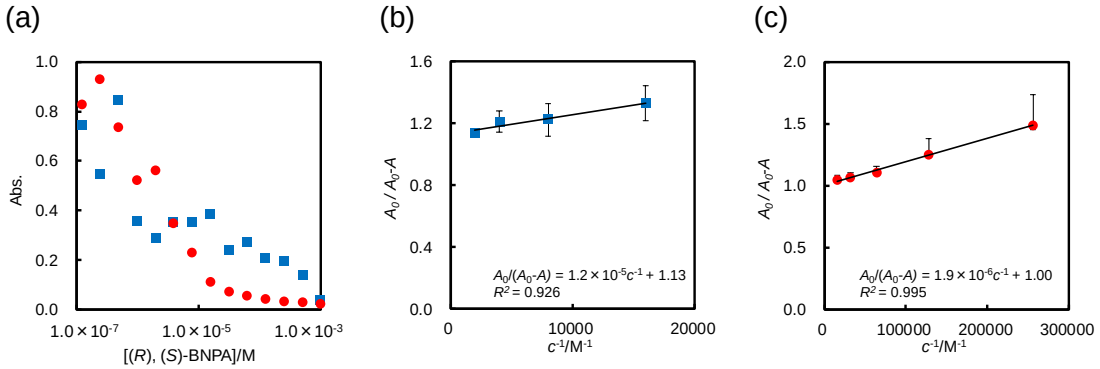

Figure 2-28. Competitive ELISA of mAb 9H3 for (*R*)-BNPA (■) and (*S*)-BNPA (●) (a). Klotz plot for mAb R44E1 with (*R*)-BNPA (b) and (*S*)-BNPA (c).

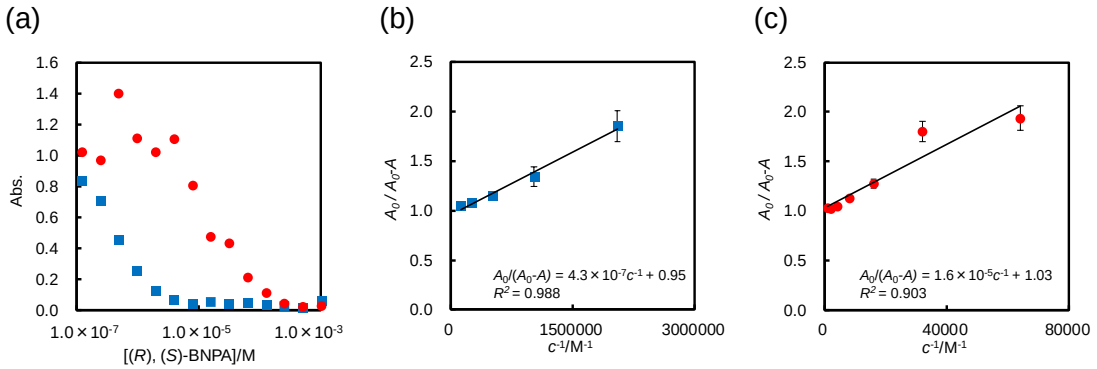

Figure 2-29. Competitive ELISA of mAb R44E1 for (*R*)-BNPA (■) and (*S*)-BNPA (●) (a). Klotz plot for mAb R44E1 with (*R*)-BNPA (b) and (*S*)-BNPA (c).

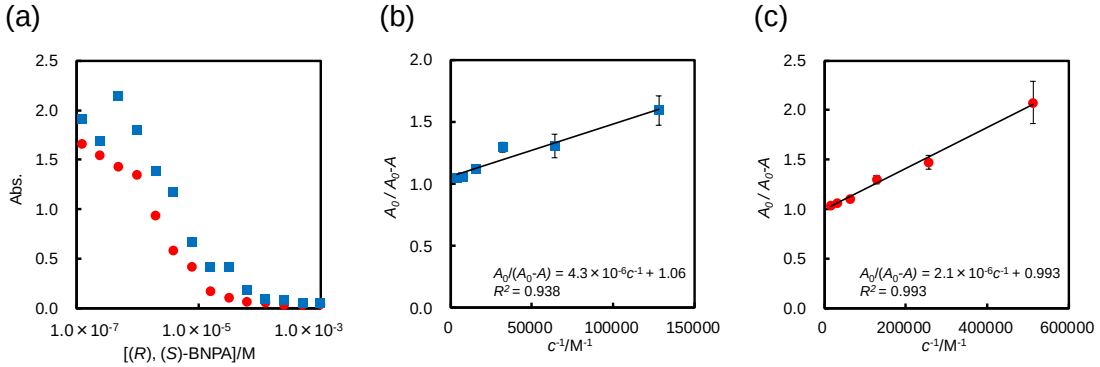

Figure 2-30. Competitive ELISA of mAb S1E11 for (*R*)-BNPA (■) and (*S*)-BNPA (●) (a). Klotz plot for mAb R44E1 with (*R*)-BNPA (b) and (*S*)-BNPA (c).

Sequence analysis and homology modeling of variable region of mAb R44E1 and mAb S1E11

Amino acid sequences of variable region of mAb R44E1 and mAb S1E11 were determined (**Figure 2-31**). The sequence similarity of H chain and L chain of these two mAbs are 79% and 54%. These values are relatively low compared with anti-amino acid mAbs.[63,64] The homology of these two mAbs is also low in CDRs compared with anti-amino acid mAbs (L1 13%, L2 0%, L3 56%, H1 77%, H2 60%, H3 0%).[63,64] The clusters of CDRs of mAb R44E1 (**Table 2-2**) and mAb S1E11 (**Table 2-3**) were determined following the definition by North et al.[61] Although the cluster of H3 of mAb S1E11 cannot be assigned to any cluster, the difference in the two mAbs are only observed in L1. As is observed generally, [62–64] the ratios of aromatic amino acid residues in H1 and H3 of both mAbs are high compared with that of the other CDRs.

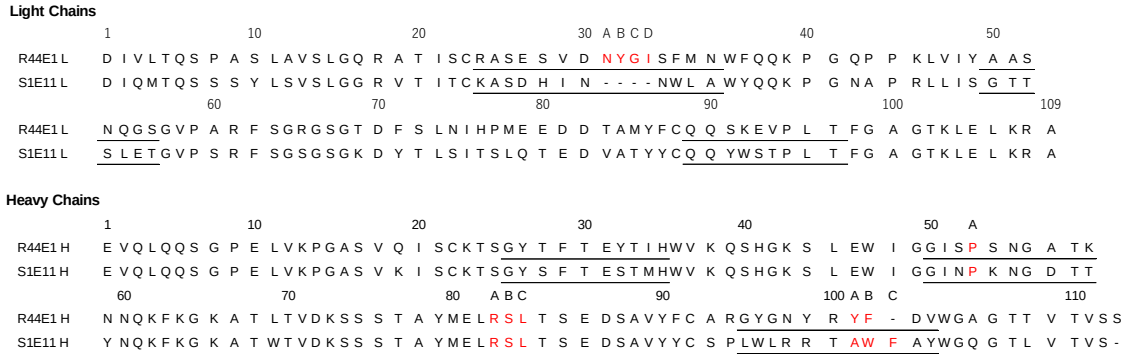

Figure 2-31. Sequence alignment of the variable domains of mAb R44E1 and mAb S1E11. Chothia numbering scheme is used. Insertions are shown in red. The CDRs are determined based on the definition provided by North et al.

Table 2-2. Amino acid sequence, cluster, length of CDRs of mAb R44E1 and the ratio of aromatic, polar and nonpolar amino acids in CDRs.

CDR	Sequence	Cluster	Length	Distribution/% of amino acid residues		
				Aromatic	Polar	Nonpolar
L1	RASESVDNYGISFMN	L1-15-1	15	13	60	40
L2	YAASNQGS	L2-8-1	8	13	63	38
L3	QQSKEVPLT	L3-9-cis7-1	9	0	67	33
H1	KTSGYTFTEYTIH	H1-13-1	13	23	69	31
H2	GISPSNGATK	H2-10-1	10	0	50	50
H3	ARGYGNYRYFDV	H3-12-1	12	40	58	42

Table 2-3. Amino acid sequence, cluster, length of CDRs of mAb S1E11 and ratio of aromatic, polar and nonpolar amino acids in CDRs.

CDR	Sequence	Cluster	Length	Distribution/% of amino acid residues		
				Aromatic	Polar	Nonpolar
L1	KASDHINNWLA	L1-11-2	11	9	55	45
L2	SGTTSLET	L2-8-1	8	0	75	25
L3	QQYWSTPLT	L3-9-cis7-1	9	22	67	33
H1	KTSGYSFTESTMH	H1-13-1	13	8	77	23
H2	GINPKNGDTT	H2-10-1	10	0	60	40
H3	SPLWLRRTAWFAY	NA[a]	13	31	38	62

[a]H3 of mAb S1E11 cannot be assigned to any cluster.

Three dimensional structures of variable region of mAb R44E1 and mAb S1E11 were constructed using ROSIE.[36–41] Although relatively large difference in amino acid sequences of mAb R44E1 and mAb S1E11 is observed, the overall structures of the two mAbs are similar (**Figure 2-32 a, b**). The difference is observed in the loop structures of L1 and L3 (**Figure 2-32 c**). The modeled structures of both mAb R44E1 and mAb S1E11 have binding pockets that seem to be compartmentalized into two parts (**Figure 2-33 a, b**). The docked structure of mAb R44E1 with BN (R), and mAb S1E11 with BN (S) suggest that these mAbs recognize the axial chirality of BN by binding the binaphthyl moiety of BN (**Figure 2-34**).

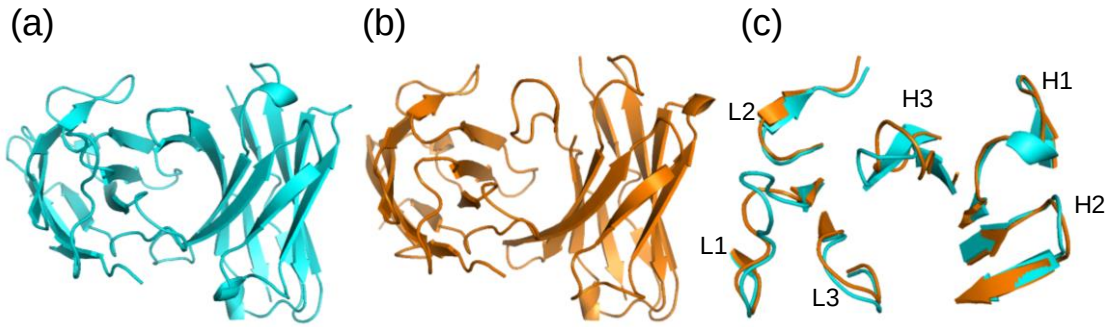

Figure 2-32. Overall structures of the modeling structure of antigen binding site of mAb R44E1 (a) and mAb S1E11 (b). Overlay of the CDR loops of mAb R44E1 (cyan) and mAb S1E11 (orange) (c).

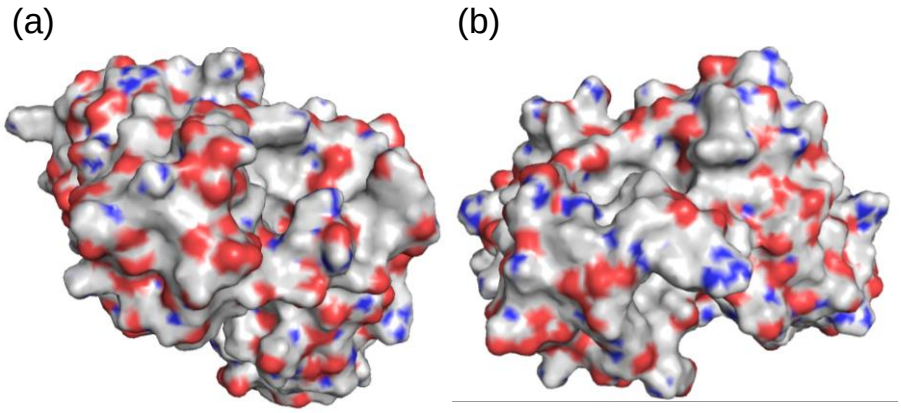

Figure 2-33. Surface representations of the modeling structure of antigen binding site of mAb R44E1 (a) and mAb S1E11 (b).

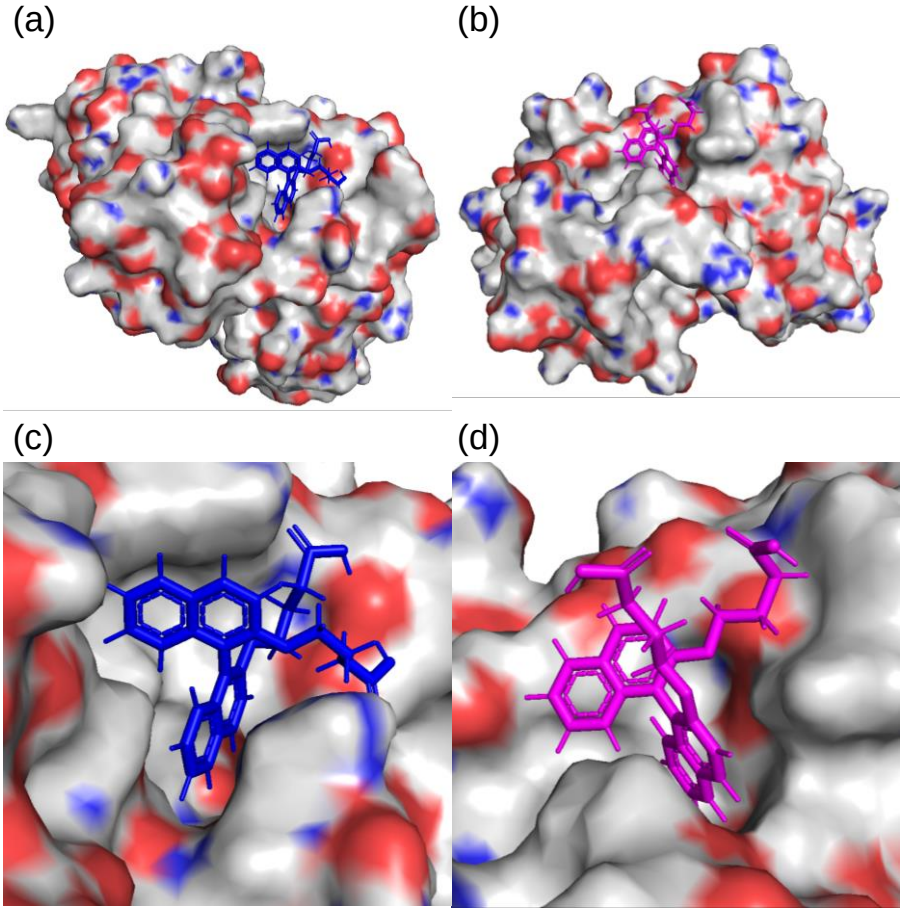

Figure 2-34. Docked structure of mAb R44E1 with BN (*R*) (a) mAb S1E11 with BN (*S*) (b) and their close up view (c), (d).

2-4. Conclusion

In this chapter, mAbs precisely recognizing the axial chirality of binaphthyl derivatives were successfully developed by immunization with enantiomeric pure BN and racemic mixture of BN. Immunization with pure enantiomer of BN yields the mAbs with atroposelectivity toward their hapten. This results indicate that the atroposelectivities of antigen binding sites can be rationally designed by the use of enantiomeric pure BN. In the case of immunization with racemic mixture, atroposelective antibodies for both BN (*R*) and BN (*S*) can be isolated at one time. This finding provides a strategy to rapidly diverse the antigen binding sites for BN enantiomer. The obtained mAbs show high affinity and high atroposelectivity for BN enantiomer, whereas very weak affinity for N and BP was observed. These result suggests that mAbs bind the crossing moiety of the two naphthyl rings of BN. All four mAbs also bind chiral BINOL and chiral BNPA in an atroposelective manner. These results support that the mAbs bind the binaphthyl moiety of BN. Although the affinity and selectivity of mAbs for BINOL and BNPA are low compared with that for BN enantiomer, the binding pockets of mAbs designed by immunization with BN enantiomer accept BINOL and BNPA as guest molecules. Notably, chiral supramolecular complexes of mAbs with a chiral organic catalyst with binaphthyl backbone are developed for the first time in this study. Atroposelective complexation of mAbs with axially chiral molecules will open up a new supramolecular functions such as detection, separation and creation of chirality.

References

(1) Shen, J.; Okamoto, Y. *Chem. Rev.* **2016**, *116*, 1094–1138.

(2) Haginaka, J. *J. Chromatogr. B* **2008**, *875*, 12–19.

(3) Nishijima, M.; Chang, J.-W.; Yang, C.; Fukuhara, G.; Mori, T.; Inoue, Y. *Res. Chem. Intermed.* **2013**, *39*, 371–383.

(4) Rekharsky, M.; Inoue, Y. *J. Am. Chem. Soc.* **2000**, *122*, 4418–4435.

(5) Rekharsky, M. V.; Inoue, Y. *J. Am. Chem. Soc.* **2002**, *124*, 813–826.

(6) Xiao, Y.; Ng, S.-C.; Tan, T. T. Y.; Wang, Y. *J. Chromatogr. A* **2012**, *1269*, 52–68.

(7) Zheng, Y.; Kobayashi, Y.; Sekine, T.; Takashima, Y.; Hashidzume, A.; Yamaguchi, H.; Harada, A. *Commun. Chem.* **2018**, *1*, 4.

(8) Maier, N. M.; Lindner, W. *Anal. Bioanal. Chem.* **2007**, *389*, 377–397.

(9) Shimomura, K.; Ikai, T.; Kanoh, S.; Yashima, E.; Maeda, K. *Nat. Chem.* **2014**, *6*, 429–434.

(10) Kyba, E. B.; Koga, K.; Sousa, L. R.; Siegel, M. G.; Cram, D. J. *J. Am. Chem. Soc.* **1973**, *95*, 2692–2693.

(11) Kubo, Y.; Maeda, S.; Tokita, S.; Kubo, M. *Nature* **1996**, *382*, 522–524.

(12) de Loos, M.; van Esch, J.; Kellogg, R. M.; Feringa, B. L. *Angew. Chem. Int. Ed.* **2001**, *40*, 613–616.

(13) Hayashi, T.; Aya, T.; Nonoguchi, M.; Mizutani, T.; Hisaeda, Y.; Kitagawa, S.; Ogoshi, H. *Tetrahedron* **2002**, *58*, 2803–2811.

(14) Gao, Z.; Lin, R.; Bai, D.; Tao, Z.; Liu, J.; Xiao, X. *Sci. Rep.* **2017**, 2–8.

(15) Landsteiner, K.; van der Scheer, J. *J. Exp. Med.* **1928**, *48*, 315–320.

(16) Sawutz, D. G.; Sylvestre, D.; Homcy, C. J. *J. Immunol.* **1985**, *135*, 2713–2718.

(17) Got, P.; Raimbaud, E.; Bussey, C.; Caron, G.; Carrupt, P.; Walther, B.; Bensussan, A.; Scherrmann, J. *Pharm. Res.* **1999**, *16*, 725–735.

(18) Mu, H.; Lei, H.; Wang, B.; Xu, Z.; Zhang, C.; Ling, L.; Tian, Y.; Hu, J.; Sun, Y. *J. Agric. Food Chem.* **2014**, *62*, 7804–7812.

(19) Chen, J.; Wang, L.; Lu, L.; Shen, X.; Huang, X.; Liu, Y.; Sun, X.; Wang, Z.; Eremin, S. A.; Sun, Y.; et al. *Anal. Chem.* **2017**, *89*, 6740–6748.

(20) Zhang, Y.; Wang, L.; Shen, X.; Wei, X.; Huang, X.; Liu, Y.; Sun, X.; Wang, Z.; Sun, Y.; Xu, Z.; et al. *J. Agric. Food Chem.* **2017**, *65*, 4830–4838.

(21) Hofstetter, H.; Hofstetter, O. *Trends Anal. Chem.* **2005**, *24*, 869–879.

(22) Nevanen, T. K.; Söderholm, L.; Kukkonen, K.; Suortti, T.; Teerinen, T.; Linder, M.; Söderlund, H.; Teeri, T. T. *J. Chromatogr. A* **2001**, *925*, 89–97.

(23) Lee, S. B. *Science* **2002**, *296*, 2198–2200.

(24) Mitchell, D. T.; Lee, S. B.; Trofin, L.; Li, N.; Nevanen, T. K.; Söderlund, H.;

Martin, C. R. *J. Am. Chem. Soc.* **2002**, *124*, 11864–11865.
(25) Nevanen, T. K.; Hellman, M.-L.; Munck, N.; Wohlfahrt, G.; Koivula, A.; Soderlund, H. *Protein Eng. Des. Sel.* **2003**, *16*, 1089–1097.
(26) Vuolanto, A.; Kiviharju, K.; Nevanen, T. K.; Leisola, M.; Jokela, J. *Cryst. Growth Des.* **2003**, *3*, 777–782.
(27) Vuolanto, A.; Leisola, M.; Jokela, J. *Biotechnol. Prog.* **2004**, *20*, 771–776.
(28) Shelver, W. L.; Smith, D. J.; Berry, E. S. *J. Agric. Food Chem.* **2000**, *48*, 4020–4026.
(29) Shi, Z.-D.; Yang, B.-H.; Zhao, J.-J.; Wu, Y.-L.; Ji, Y.-Y.; Yeh, M. *Bioorg. Med. Chem.* **2002**, *10*, 2171–2175.
(30) Reardan, D. T.; Meares, C. F.; Goodwin, D. A.; McTigue, M.; David, G. S.; Stone, M. R.; Leung, J. P.; Bartholomew, R. M.; Frincke, J. M. *Nature* **1985**, *316*, 265–268.
(31) Imaizumi, M.; Sisido, M. *Chem. Lett.* **1994**, *23*, 51–52.
(32) Rasmussen, B. S.; Pedersen, J. M.; Sørensen, J.; Egebjerg, J.; Schiøtt, B.; Mortensen, K. K.; Skrydstrup, T. *ChemBioChem* **2007**, *8*, 1974–1980.
(33) Miyashita, A.; Yasuda, A.; Takaya, H.; Toriumi, K.; Ito, T.; Souchi, T.; Noyori, R. *J. Am. Chem. Soc.* **1980**, *102*, 7932–7934.
(34) Rasmussen, B. S.; Elezcano, U.; Skrydstrup, T. *J. Chem. Soc. Perkin 1* **2002**, *2*, 1723–1733.
(35) Robertson, M.; Bremner, J. B.; Coates, J.; Deadman, J.; Keller, P. a; Pyne, S. G.; Somphol, K.; Rhodes, D. I. *Eur. J. Med. Chem.* **2011**, *46*, 4201–4211.
(36) Sivasubramanian, A.; Sircar, A.; Chaudhury, S.; Gray, J. J. *Proteins Struct. Funct. Bioinforma.* **2009**, *74*, 497–514.
(37) Sircar, A.; Kim, E. T.; Gray, J. J. *Nucleic Acids Res.* **2009**, *37*, W474–W479.
(38) Lyskov, S.; Chou, F.-C.; Conchúir, S. Ó.; Der, B. S.; Drew, K.; Kuroda, D.; Xu, J.; Weitzner, B. D.; Renfrew, P. D.; Sripakdeevong, P.; et al. *PLoS One* **2013**, *8*, e63906.
(39) Marze, N. A.; Lyskov, S.; Gray, J. J. *Protein Eng. Des. Sel.* **2016**, *29*, 409–418.
(40) Weitzner, B. D.; Jeliazkov, J. R.; Lyskov, S.; Marze, N.; Kuroda, D.; Frick, R.; Adolf-Bryfogle, J.; Biswas, N.; Dunbrack, R. L.; Gray, J. J. *Nat. Protoc.* **2017**, *12*, 401–416.
(41) Weitzner, B. D.; Gray, J. J. *J. Immunol.* **2017**, *198*, 505–515.
(42) Lyskov, S.; Chou, F.-C.; Conchúir, S. Ó.; Der, B. S.; Drew, K.; Kuroda, D.; Xu, J.; Weitzner, B. D.; Renfrew, P. D.; Sripakdeevong, P.; et al. *PLoS One* **2013**, *8*, e63906.
(43) Combs, S. A.; DeLuca, S. L.; DeLuca, S. H.; Lemmon, G. H.; Nannemann, D. P.;

Nguyen, E. D.; Willis, J. R.; Sheehan, J. H.; Meiler, J. *Nat. Protoc.* **2013**, *8*, 1277–1298.

(44) Kothiwale, S.; Mendenhall, J. L.; Meiler, J. *J. Cheminform.* **2015**, *7*, 47.

(45) DeLuca, S.; Khar, K.; Meiler, J. *PLoS One* **2015**, *10*, e0132508.

(46) Lockner, J. W.; Lively, J. M.; Collins, K. C.; Vendruscolo, J. C. M.; Azar, M. R.; Janda, K. D. *J. Med. Chem.* **2015**, *58*, 1005–1011.

(47) Satoh, H.; Hayashi, M.; Satoh, S. *J. Pharm. Pharmacol.* **1982**, *34*, 429–433.

(48) Sahui-Gnassi, A.; Pham-Huy, C.; Galons, H.; Warnet, J.-M.; Claude, J.-R.; Duc, H.-T. *Chirality* **1993**, *5*, 448–454.

(49) Chikhi-Chorfi, N.; Galons, H.; Pham-Huy, C.; Thevenin, M.; Warnet, J.-M.; Claude, J.-R. *Chirality* **2001**, *13*, 187–192.

(50) Brunel, J. M. *Chem. Rev.* **2005**, *105*, 857–898.

(51) Brunel, J. M. *Chem. Rev.* **2007**, *107*, PR1-PR45.

(52) Courant, T.; Kumarn, S.; He, L.; Retailleau, P.; Masson, G. *Adv. Synth. Catal.* **2013**, *355*, 836–840.

(53) Shi, F.; Tan, W.; Zhang, H.-H.; Li, M.; Ye, Q.; Ma, G.-H.; Tu, S.-J.; Li, G. *Adv. Synth. Catal.* **2013**, *355*, 3715–3726.

(54) Li, G.; Liang, T.; Wojtas, L.; Antilla, J. C. *Angew. Chem. Int. Ed.* **2013**, *52*, 4628–4632.

(55) Zhou, J.-Q.; Sheng, W.-J.; Jia, J.-H.; Ye, Q.; Gao, J.-R.; Jia, Y.-X. *Tetrahedron Lett.* **2013**, *54*, 3082–3084.

(56) Enders, D.; Stöckel, B. A.; Rembiak, A. *Chem. Commun.* **2014**, *50*, 4489–4491.

(57) Beceño, C.; Chauhan, P.; Rembiak, A.; Wang, A.; Enders, D. *Adv. Synth. Catal.* **2015**, *357*, 672–676.

(58) Zhu, G.; Wei, Q.; Chen, H.; Zhang, Y.; Shen, W.; Qu, J.; Wang, B. *Org. Lett.* **2017**, *19*, 1862–1865.

(59) Ranieri, D. I.; Corgliano, D. M.; Franco, E. J.; Hofstetter, H.; Hofstetter, O. *Chirality* **2008**, *20*, 559–570.

(60) Ranieri, D. I.; Hofstetter, H.; Hofstetter, O. *J. Sep. Sci.* **2009**, *32*, 1686–1695.

(61) North, B.; Lehmann, A.; Dunbrack, R. L. *J. Mol. Biol.* **2011**, *406*, 228–256.

(62) Padlan, E. A. *Proteins Struct. Funct. Genet.* **1990**, *7*, 112–124.

(63) Bogan, A. A.; Thorn, K. S. *J. Mol. Biol.* **1998**, *280*, 1–9.

(64) Nagumo, Y.; Oguri, H.; Tsumoto, K.; Shindo, Y.; Hirama, M.; Tsumuraya, T.; Fujii, I.; Tomioka, Y.; Mizugaki, M.; Kumagai, I. *J. Immunol. Methods* **2004**, *289*, 137–146.

Chapter 3
Direct Chiral Separation of Binaphthyl Derivatives Using Atroposelective Antibodies

3-1. Introduction

Chirality is crucial in various scientific fields such as pharmaceuticals,[1] chemistry,[2–4] and materials science.[5] For example, in pharmaceutical applications employing a specific enantiomer is especially important. Often one enantiomer displays the desired effect, while the other elicits serious side effects. Therefore, chiral separations on both industrial and laboratory scales are important. High-performance liquid chromatography is a popular chiral separation methodology.[6] To date, many researchers have devoted much effort to develop chiral stationary phases (CSPs) such as synthetic polymers,[7] saccharides,[8,9] biomacromolecules, etc.[10–12] However, trial and error is still required to optimize condition for chiral separation for each molecule. One promising approach toward a straightforward chiral separation strategy is to use antibodies that precisely recognize the chirality of the target molecule.[13] With the advent of cell technology, it is now possible to prepare mAbs in large amounts and in a homogeneous form semi-permanently.[14]

Many researchers have developed mAbs against chiral molecules for various purposes.[15–20] Among them, the use of mAbs as CSP of immuno affinity chiral columns has been extensively studied.[21] However, harsh elution conditions are necessary due to the high affinity of mAbs against target molecules. Eluting a tightly bound enantiomer while maintaining the stability of mAbs is problematic.[22–24] In addition, optimization of the immobilization method of mAbs onto columns is necessary to retain the binding affinity of mAbs.[25] To fully utilize the characteristic of mAbs, a more convenient methodology without columns for chiral separation is necessary.

In this chapter, an operationally-simple methodology for chiral separation is developed. This research focuses on the basic properties of mAbs, including high specificity for the target molecule and the molecular weight. Chiral separation is achieved by carrying out ultrafiltration of the solution of BN (*rac*) and atroposelective antibodies. The large difference in the molecular weights of mAbs and BN realized direct chiral separation via a simple one-step procedure. Neither immobilizing mAbs onto chromatographic supports nor releasing the target molecules from mAbs is required. Intact mAbs can be used directly. In addition, both enantiomers can be obtained by this procedure where mAbs are prepared for each enantiomer.

3-2. Experimental section

Materials

Bovine serum albumin **(**BSA) was purchased from Medical & Biological Laboratories Co. Ltd. Other reagents were used without further purification. The buffer compositions are as follows. 0.1M phosphate borate buffer (PBB): KH_2PO_4 3.97 g, $Na_2B_4O_7 \cdot 10H_2O$ 26.3 g/H_2O 1L.Washing buffer: 10 mM PBS containing 20 mM NaN_3 and 10 mM of Tween 20.

Measurements

The absorption spectra were measured with a JASCO V-650 at room temperature. Circular dichroism spectra were recorded with a JASCO J820 spectrometer.

General procedure for chiral separation using atroposelective antibodies

Solutions of mAbs (6.7 μM, 1000 μL) or BSA (6.7 μM) in 0.1M PBB (pH 9.0) were mixed with BN (*rac*) (160 μM, 84 μL for mAbs or 42 μL for BSA) and steered 1 min at room temperature. The molar ratio of antigen binding sites to BN (*rac*) is one-to-one in this case (13.4 nmol each). These solutions were ultrafiltrated (4000 rpm, 4 min) using Amicon®Ultra 4 (MWCO 10,000). The UV-Vis and CD spectra of filtrates were recorded. The concentration of free BN were quantified from the absorbance at 333 nm derived from BN. The ee value was determined using the molar circular dichroism at 237 nm of major enantiomer.

Procedure for releasing bound BN from antigen binding sites.

To the high molecular weight fraction obtained by ultrafiltration, 2000 μL of 0.1M PBB was added and ultrafiltrated. This washing procedure was repeated 5 times. The high molecular weight fraction was concentrated to ca. 250 μL. To this fraction, 2000 μL of 1% sodium dodecyl sulfate 50 mM PBB (pH 9) was added and steered 10 min. The high molecular weight fractions were washed 10 times by 2000 μL of 0.1M PBB and the UV-Vis spectra of high molecular weight fractions were recorded.

3-3. Results and Discussion

Direct chiral separation was carried out following the general procedure by using mAb R44E1 and mAb S1E11, respectively. The eluted solutions contain BN (*S*) with 97 ± 2% ee using mAb R44E1 as a chiral separator (**Figure 3-1**). In contrast, BN (*R*) is obtained with 96 ± 2% ee by mAb S1E11 (**Figure 3-2**). Free BN is easily separated by ultrafiltration because the molecular weight of the complex of mAbs with BN is three orders of magnitude higher than that of BN alone.

As a control experiment, mAb 2B6 elicited against a water soluble porphyrin was used.[26,27] In this case, BN (*rac*) is obtained (**Figure 3-3**) because this mAb does not have an affinity for BN enantiomer (**Figure 3-4**). Another control experiment used bovine serum albumin (BSA) (Mw 66 kDa). In this case, BSA and BN (*rac*) were mixed in a one-to-one ratio because it is assumed that one BN molecule is bound per BSA molecule from a study on the complexation of BINOL with BSA.[28–30] Although one enantiomer (*R*-isomer) is eluted preferentially, the ee of the eluted fraction is low (16 ± 2%) (**Figure 3-5**). This result shows that the low affinity and the low enantioselectivity of BSA for the binaphthyl group ($K_d = 10^3 \sim 10^4$ M for both of *R*- and *S*-BINOL)[28–30] are insufficient to realize chiral separation with this procedure. These two control experiments demonstrate the importance of a high atroposelectivity of mAbs prepared as a tailor-made chiral selector to realize direct chiral separation (**Table 3-1**). Actually, magnetic particles coated with albumins have yet to realize direct separation of the enantiomers.[31,32] Moreover, another group tried direct chiral separation using metal-organic frameworks, but a complicated procedure was required to remove the chiral separator with a low molecular weight.[33]

To make the current approach practically viable, reuse of mAbs in a direct chiral separation is tried. The bound BN is released from the antigen binding sites by treatment with PBB containing 1% sodium dodecyl sulfate. The free BN and mAb are separated by ultrafiltration, and the buffer condition for mAb is exchanged to PBB. The second use of mAb R44E1 gives the pure BN (*S*) in 83% ee (**Figure 3-6**). On the other hand, treatment with PBB containing 30% dimethyl sulfoxide or 30% ethanol does not completely dissociate the bound BN (**Figures 3-7** and **3-8**). These results highlight the importance of the experimental conditions when releasing bound enantiomer. At the same time, this observation shows the simplicity of the direct chiral separation where mAbs are prepared for each enantiomer.

Atroposelective binding of mAbs is applied in chiral sensing. The mAb S1E11 even recognizes the chirality of BN attached on a thermoresponsive polymer, poly-*N*-isopropylacrylamide (pNIPAM). The aqueous solution of pNIPAM bearing BN (*S*)

(pNIPAM-BN (*S*)) is cloudy at 32 °C (**Figure 3-9**). However, the addition of mAb S1E11 resolves the turbidity by increasing the lower critical solution temperature from 31.5 °C to 33.0 °C. The binding of mAb S1E11 alters the hydration behavior of pNIPAM-based polymer. The addition of BN (*S*) to the mixture of pNIPAM-BN (*S*) and mAb S1E11 reclouds the solution, whereas BN (*R*) does not cause any change (**Figure 3-9**). It is suggested that mAb S1E11 switches the binding partner from pNIPAM BN (*S*) to BN (*S*). Modification of pNIPAM to BN (*S*) allows visualization of association and dissociation of mAb S1E11 to pNIPAM-BN (*S*) by the naked eye. Furthermore, the presence of chiral BN is atroposelectively detected just adding BN to the mixture of pNIPAM-BN (*S*) and mAb S1E11. Rapid and operationally simple chiral detection system is developed.

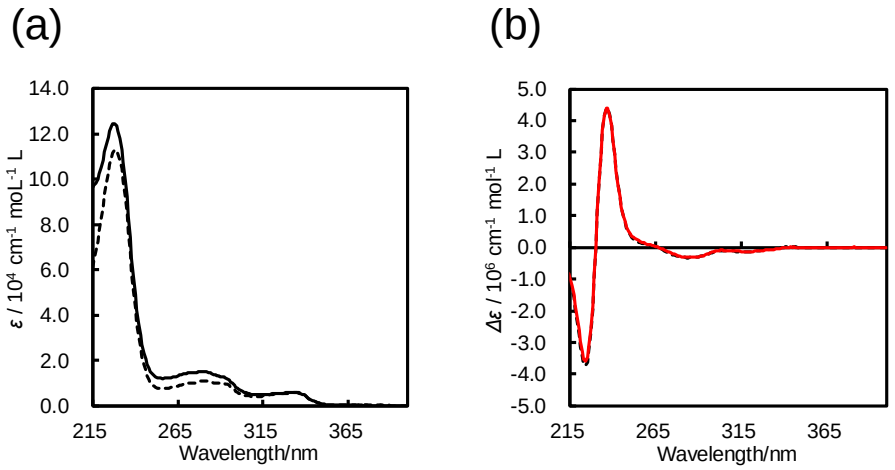

Figure 3-1. UV-Vis (a) and CD spectra (b) of BN separated by ultrafiltration after mixing aqueous solutions of BN (*rac*) with mAb R44E1 (solid line in (a), (b)). Dotted lines are the UV-Vis and CD spectra of pure BN (*S*).

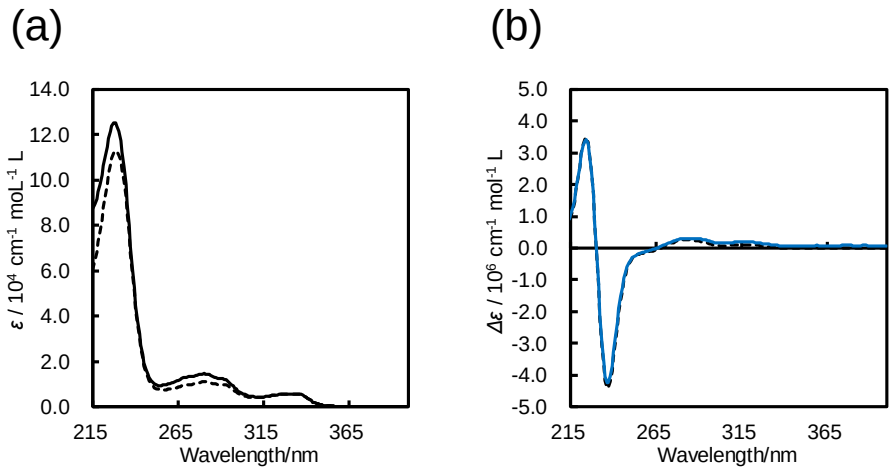

Figure 3-2. UV-Vis (a) and CD spectra (b) of BN separated by ultrafiltration after mixing aqueous solutions of BN (*rac*) with mAb S1E11 (solid line in (a), (b)). Dotted lines are the UV-Vis and CD spectra of pure BN (*R*).

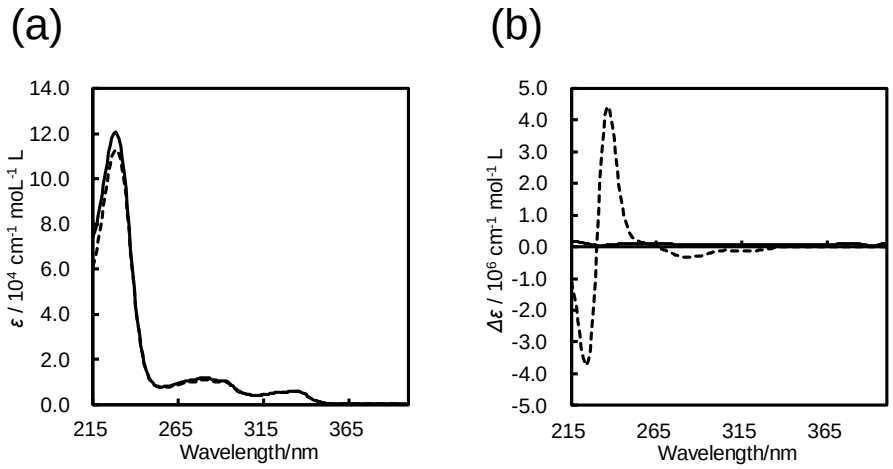

Figure 3-3. UV-Vis (a) and CD spectra (b) of BN separated by ultrafiltration after mixing aqueous solutions of BN (*rac*) with anti-porphyrin mAb 2B6 (solid line in (a), (b)). Dotted lines are the UV-Vis and CD spectra of pure BN (*S*).

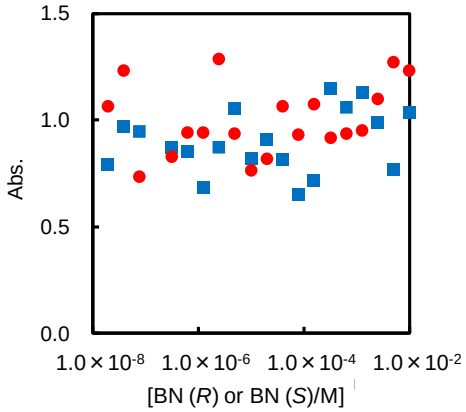

Figure 3-4. Competitive ELISA of mAb 2B6 for BN (*R*) (■) and BN (*S*) (●).

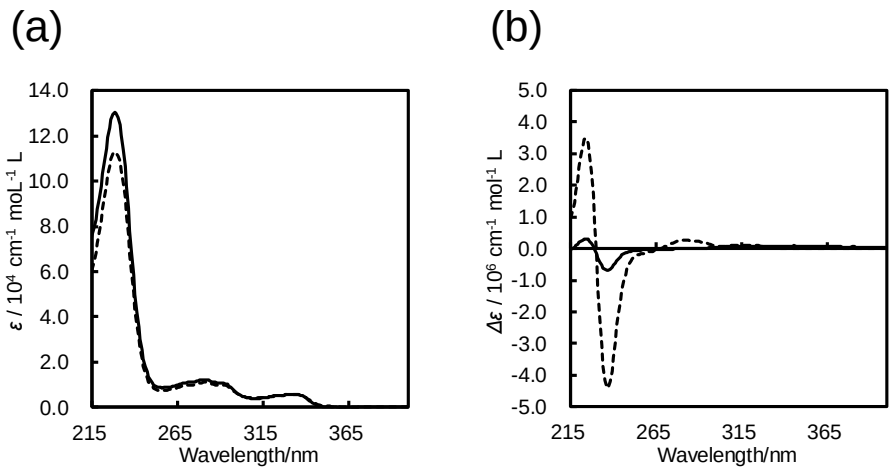

Figure 3-5. UV-Vis (a) and CD spectra (b) of BN separated by ultrafiltration after mixing aqueous solutions of BN (*rac*) with BSA (solid line in (a), (b)). Dotted lines are the UV-Vis spectrum of pure BN (*R*).

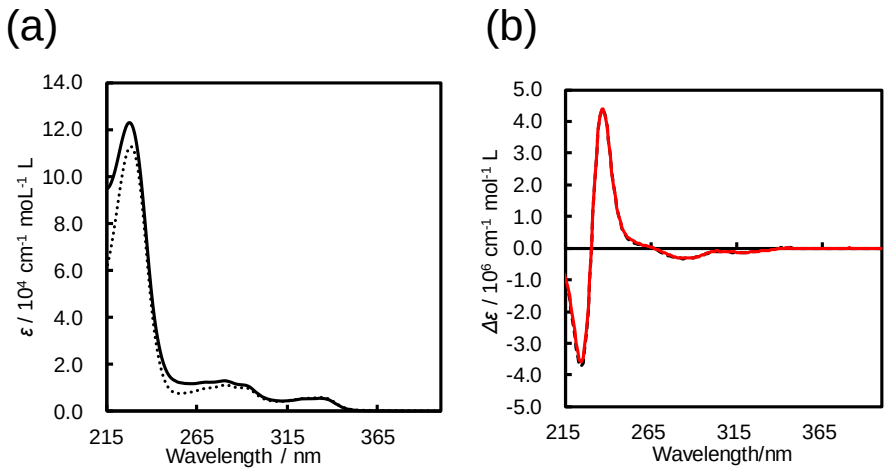

Figure 3-6. UV-Vis (a) and CD spectra (b) of BN separated by ultrafiltration after mixing aqueous solutions of BN (*rac*) with reused-mAb R44E1 (solid line in (a), (b)). Dotted lines are the UV-Vis and CD spectra of pure BN (*S*).

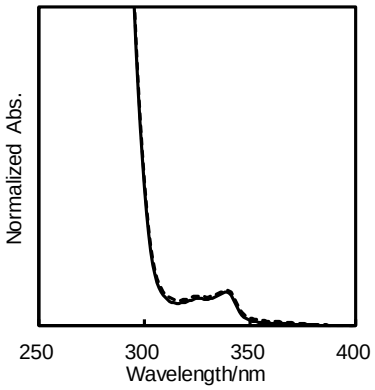

Figure 3-7. Normalized UV-Vis spectra of **BN** complexed with mAb R44E1 before (solid line) and after (dotted line) treatment with PBB (pH 9)/DMSO (7:3 (w/w)).

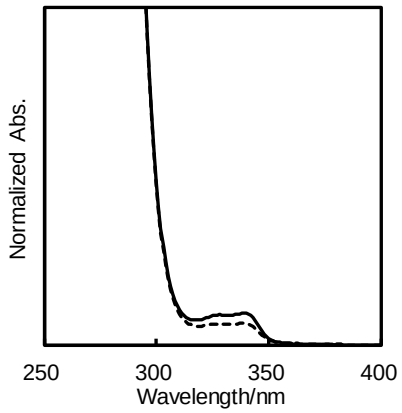

Figure 3-8. Normalized UV-Vis spectra of **BN** complexed with mAb R44E1 before (solid line) and after (dotted line) treatment with PBB (pH 9)/EtOH (7:3 (w/w)).

Table 3-1. The ee of BN separated by direct chiral separation using atroposelective antibodies.

Protein	Specificity	ee of purified BN/%
mAb R44E1	*R*	97 ± 2 (*S*)
mAb S1E11	*S*	96 ± 2 (*R*)
mAb 2B6	-	0
BSA	*S*	16 ± 2 (*R*)

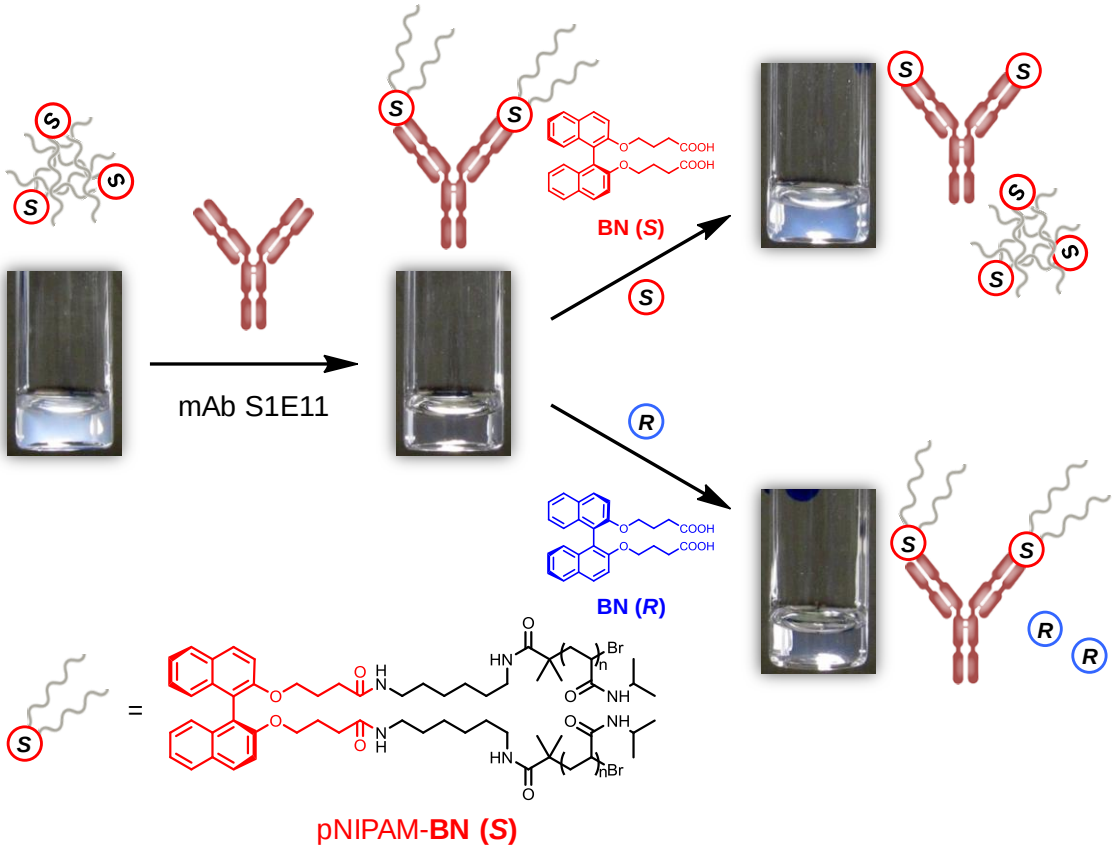

Figure 3-9. Visual chiral sensing system based on atroposelective antibodies and thermoresponsive polymers. Photo images of pNIPAM-BN (*S*) (the initial state), the mixture of pNIPAM-BN (*S*) and mAb S1E11 (the second state) and the solutions including the polymer, mAb S1E11 and mAb S1E11 (the third state, upper) or BN (*R*) (the third state, lower). [mAb S1E11] = 1.2 μM. [BN (*R*) or BN (*S*)] = 2.4 μM. All samples contain 3.2 μM of pNIPAM-BN (*S*). Pictures are taken at 32.0 °C after 10min incubation.

3-4. Conclusion

In this chapter, an operationally-simple methodology for chiral separation was developed. Chiral separation of BN is achieved via ultrafiltration of mixtures of BN and atroposelective antibodies. The difference of molecular weight of mAbs and BN enables the direct use of intact antibodies without any pre-processing or immobilization of mAbs on chromatographic supports. Unlike previous reports where the processes to immobilize antibodies or release bound enantiomer must be optimized,[22–24] the chiral separation methodology presented herein is easy and rapid. Atroposelective binding of mAbs was applied to the chiral sensing using a thermoresponsive polymer. Association and dissociation of mAbs to BN on the polymer were visualized. The author expects that enantioselective complex formation of mAbs with artificial chiral molecules[34–36] will be expanded to new applications such as chiral biocatalysts.

References

(1) Agranat, I.; Caner, H.; Caldwell, J. *Nat. Rev. Drug Discov.* **2002**, *1*, 753–768.

(2) Knowles, W. S. *Angew. Chem. Int. Ed.* **2002**, *41*, 1998.

(3) Noyori, R. *Angew. Chem. Int. Ed.* **2002**, *41*, 2008.

(4) Sharpless, K. B. *Angew. Chem. Int. Ed.* **2002**, *41*, 2024.

(5) Kuzyk, A.; Schreiber, R.; Fan, Z.; Pardatscher, G.; Roller, E.-M.; Högele, A.; Simmel, F. C.; Govorov, A. O.; Liedl, T. *Nature* **2012**, *483*, 311–314.

(6) Shen, J.; Okamoto, Y. *Chem. Rev.* **2016**, *116*, 1094–1138.

(7) Kempe, M.; Mosbach, K. *J. Chromatogr. A* **1995**, *694*, 3–13.

(8) Yashima, E. *J. Chromatogr. A* **2001**, *906*, 105–125.

(9) Xiao, Y.; Ng, S.-C.; Tan, T. T. Y.; Wang, Y. *J. Chromatogr. A* **2012**, *1269*, 52–68.

(10) Haginaka, J. *J. Chromatogr. B* **2008**, *875*, 12–19.

(11) Yu, Y.; Ren, Y.; Shen, W.; Deng, H.; Gao, Z. *TrAC Trends Anal. Chem.* **2013**, *50*, 33–41.

(12) Shimomura, K.; Ikai, T.; Kanoh, S.; Yashima, E.; Maeda, K. *Nat. Chem.* **2014**, *6*, 429–434.

(13) Landsteiner, K.; van der Scheer, J. *J. Exp. Med.* **1928**, *48*, 315–320.

(14) Köhler, G.; Milstein, C. *Nature* **1975**, *256*, 495–497.

(15) Janda, K.; Benkovic, S.; Lerner, R. *Science* **1989**, *244*, 437–440.

(16) Créminon, C.; Taran, F. *Chem. Commun.* **2015**, *51*, 7996–8009.

(17) Geva, M.; Frolow, F.; Eisenstein, M.; Addadi, L. *J. Am. Chem. Soc.* **2003**, *125*, 696–704.

(18) Lenz, D. E.; Yourick, J. J.; Dawson, J. S.; Scott, J. *Immunol. Lett.* **1992**, *31*, 131–135.

(19) Mu, H.; Lei, H.; Wang, B.; Xu, Z.; Zhang, C.; Ling, L.; Tian, Y.; Hu, J.; Sun, Y. *J. Agric. Food Chem.* **2014**, *62*, 7804–7812.

(20) Hashimoto, M.; Sibata, T.; Wasada, H.; Toyokuni, S.; Uchida, K. *J. Biol. Chem.* **2003**, *278*, 5044–5051.

(21) Hofstetter, H.; Hofstetter, O. *Trends Anal. Chem.* **2005**, *24*, 869–879.

(22) Hofstetter, O.; Lindstrom, H.; Hofstetter, H. *J. Chromatogr. A* **2004**, *1049*, 85–95.

(23) Nevanen, T. K.; Söderholm, L.; Kukkonen, K.; Suortti, T.; Teerinen, T.; Linder, M.; Söderlund, H.; Teeri, T. T. *J. Chromatogr. A* **2001**, *925*, 89–97.

(24) Nevanen, T. K.; Hellman, M.-L.; Munck, N.; Wohlfahrt, G.; Koivula, A.; Soderlund, H. *Protein Eng. Des. Sel.* **2003**, *16*, 1089–1097.

(25) Franco, E. J.; Hofstetter, H.; Hofstetter, O. *J. Sep. Sci.* **2006**, *29*, 1458–1469.

(26) Onji, T.; Ohara, H.; Yamaguchi, H.; Ikeda, N.; Harada, A. *Chem. Lett.* **2006**, *35*,

1126–1127.

(27) Yamaguchi, H.; Onji, T.; Ohara, H.; Ikeda, N.; Harada, A. *Bull. Chem. Soc. Jpn.* **2009**, *82*, 1341–1346.

(28) Nishijima, M.; Chang, J.-W.; Yang, C.; Fukuhara, G.; Mori, T.; Inoue, Y. *Res. Chem. Intermed.* **2013**, *39*, 371–383.

(29) Levi-Minzi, N.; Zandomeneghi, M. *J. Am. Chem. Soc.* **1992**, *114*, 9300–9304.

(30) Ouchi, A.; Zandomeneghi, G.; Zandomeneghi, M. *Chirality* **2002**, *14*, 1–11.

(31) Wang, Y.; Su, P.; Wang, S.; Wu, J.; Huang, J.; Yang, Y. *J. Mater. Chem. B* **2013**, *1*, 5028.

(32) Wu, J.; Su, P.; Yang, Y.; Huang, J.; Wang, Y.; Yang, Y. *J. Mater. Chem. B* **2014**, *2*, 775–782.

(33) Chang, C.-L.; Qi, X.-Y.; Zhang, J.-W.; Qiu, Y.-M.; Li, X.-J.; Wang, X.; Bai, Y.; Sun, J.-L.; Liu, H.-W. *Chem. Commun.* **2015**, *51*, 3566–3569.

(34) Reardan, D. T.; Meares, C. F.; Goodwin, D. A.; McTigue, M.; David, G. S.; Stone, M. R.; Leung, J. P.; Bartholomew, R. M.; Frincke, J. M. *Nature* **1985**, *316*, 265–268.

(35) Imaizumi, M.; Sisido, M. *Chem. Lett.* **1994**, *23*, 51–52.

(36) Shreder, K.; Harriman, A.; Iverson, B. L. *J. Am. Chem. Soc.* **1996**, *118*, 3192–3201.

Chapter 4

Creation of Artificial Metalloenzymes based on Atroposelective Antibodies as a Designed Protein Scaffold

4-1. Introduction

Artificial metalloenzymes, which consist of transition metal catalysts and biomolecular scaffolds, offer new reactivities or selectivities that are not observed in nature or synthetic catalysts.[1,2,11–14,3–10] One way to create artificial metalloenzymes is to engineer natural enzymes to yield non-natural reactivities that combine the attractive features of both the metal catalyst and bio-molecular scaffold.[15,16,25–27,17–24] Another strategy is to incorporate synthetic metal catalysts into bimolecular scaffolds by covalent,[28,29,38–40,30–37] dative[16,41–46] or supramolecular interaction.[47,48,57,49–56] This strategy has also been applied to non-enzymatic proteins or DNAs. However, there are a limited number of existing protein scaffolds that can be used to implement the aforementioned design strategies. Therefore, the choice and engineering of biomolecular scaffolds along with the synthetic optimization of cofactors or conjugation technologies are also routinely required.[1,2,7] An alternative to these strategies is the *de novo* creation of tailored protein scaffolds with immunological optimization to provide a chiral environment around the metal complex. Monoclonal antibodies (mAbs), which are chemically homogeneous antibodies[58] have received much attention as designable protein scaffolds for artificial metalloenzymes.[50,59,68,69,60–67]

One of the most attractive features of mAbs as a protein scaffold of artificial metalloenzymes is the ability to provide specific protein environment even for chiral molecules.[70–75] Binaphthyl group was chosen as a target to complex with mAbs.[76–78] 2,2'-Bis(diphenylphosphino)-1,1'-binaphthyl (BINAP) has a unique structure where two phosphine atoms located at the 2,2' position of the BN groups play a key role in stabilizing the unique chiral structure and coordination behavior.[79] Due to atropisomeric instability, structurally similar ligands with binaphthyls such as 1,1'-bi-isoquinoline (BIQ) have not been used in asymmetric catalysis.[80] In this context, the author expect that supramolecular complexation of BIQ-based metal catalysts with mAbs will enhance the diversity of available asymmetric catalysts. In this chapter, enantioselective artificial metalloenzymes for the Friedel-Crafts alkylation reaction are developed based on the supramolecular complexation of BIQ-based metal catalysts with atroposelective antibodies generated against BN (**Figure 4-1**).

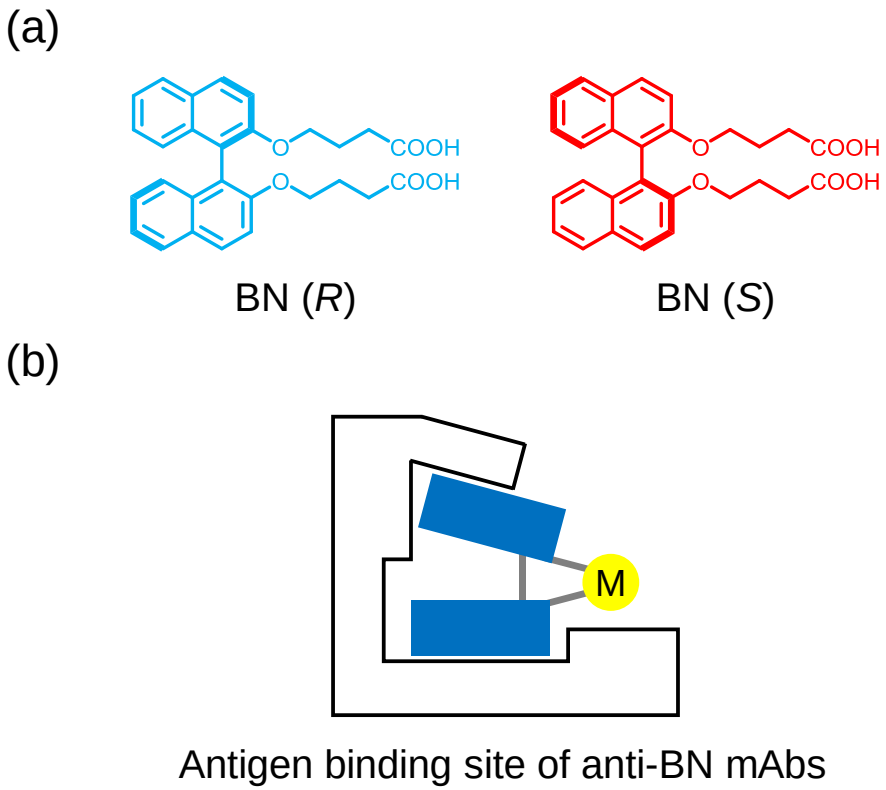

Figure 4-1. Design strategy for artificial metalloenzymes based on atroposelective antibodies. Atroposelective antibodies generated against BN (a) are used to accommodate various BIQ-based metal catalysts (b).

4-2. Experimental section

Materials

KH_2PO_4, $Na_2B_4O_7 \cdot 10H_2O$, $MgSO_4$, Na_2SO_4, $NaHCO_3$, NaCl, , $CuNO_3 \cdot 3H_2O$, Zn, NH_3 aq., and *p*-nitrophenyl phosphate sodium salt were purchased from Nakalai Tesque, Inc. 1-Chloroisoquinoline, tetramethylammonium iodide (Et_4NI), 1-methyl-1H-imidazole, crotonic acid, 2-methyl-1H-indole, $PdCl_2(CH_3CN)_2$, $Pd(OAc)_2$, 2-phenyl quinolone were purchased from Tokyo Kasei Inc. Dibromobis(triphenylphosphine)nickel(II) ($NiBr_2(PPh_3)$) was purchased from Sigma Aldrich Inc. K_2PtCl_4 was purchased from Wako Pure Chemical Industries, Ltd. *n*-BuLi was purchased from Kanto Chemical Co., Inc. BSA was purchased from Medical & Biological Laboratories Co. Ltd. Alkaline phosphatase labeled anti-mouse IgG were obtained from Sigma Aldrich Co. Reagents were used without further purification. The buffer compositions are as follows. 0.1M PBB: KH_2PO_4 3.97 g, $Na_2B_4O_7 \cdot 10H_2O$ 26.3 g/H_2O 1L.Washing buffer: 10 mM PBS containing 20 mM NaN_3 and 10 mM of Tween 20. Substrate buffer was prepared by dissolving 1 M di-ethanolamine, 3 mM sodium azide and 1 mM MgCl in water and pH was adjusted to 9.8 by hydrochloric acid solution.

Measurements

The ^1H NMR and ^{13}C NMR spectra were recorded at 500 MHz with a JEOL JNM-ECA 500 NMR spectrometer. The absorption spectra were measured with a JASCO V-650 and a Shimadzu UV-2500 PC spectrometer at room temperature. Circular dichroism spectra were recorded with a JASCO J820 spectrometer. Absorbance at 405 nm for ELISA was measured by an iMark microplate absorbance reader (Bio-Rad). The chiral HPLC analyses were carried out using JASCO HPLC system equipped with a HPLC pump (PU-2080), an UV-Vis detector (UV-2075), a CD detector (CD-4095) and a Daicel ChiralPak AD-H (4.6×250 nm). Condition for HPLC analyses is hexane/2-propanol (90/10), 40°C, 1.0 mL/min, UV and CD detection at 275 and 280 nm.

General Procedure for Friedel-Crafts alkylation reaction

Catalytic reaction was performed in 150 μL total volume containing 1.0 mM of substrates, 50 μM of BIQ-Cu (5.0%) and 50 μM of mAb (5.0%) in 20 mM MOPS buffer (pH 6.5), 150 mM NaCl. The reaction mixture was incubated at 4 °C for 72 h followed by addition of 2-phenyl quinolone as an internal standard for HPLC analysis. The mixture was extracted with diethyl ether (300μL×3) and the combined organic layer was dried over Na_2SO_4 and evaporated under reduced pressure. The residue was dissolved in hexane

and analyzed by chiral HPLC. Yields are determined based on peal area at 275 nm using 2-phenylisoquinoline as an internal standard.

Determination of dissociation constants (K_d) of the complexes of mAbs and metal complexes, substrates, and product of Friedel-Crafts alkylation reaction

60 μL of solutions of mAbs in 20 mM MOPS buffer (pH 6.5) containing 150 mM NaCl were mixed with 60 μL of solutions of metal complexes in various concentrations (10^{-7} M to 10^{-3} M) on a BSA-coated plate. The mixed solutions were incubated at 4 °C overnight and added to a BN(*R*)-BSA coated plate (in the case of mAbs specific for BN (*R*)) or a BN(*S*)-BSA coated plate (in the case of mAbs specific for BN (*R*)). The plates were incubated at 37 °C for 90 min. After removal of the solutions, the wells were washed twice with 150 μL of washing buffer. Then 100 μL of alkaline phosphatase labeled anti-mouse IgG (1:1000 dilution, in 20 mM PBS) was added and the plates were incubated at 37 °C for 90 min. After removal of the solutions, the wells were washed three times with 150 μL of washing buffer. Then 150 μL *p*-nitrophenyl phosphate sodium salt in substrate buffer (1.0 mg/mL) was added. Absorbance at 405 nm derived from the product of the enzyme reaction was recorded.

Dissociation constants were determined by Klotz plot:

$$\frac{A_0}{A_0 - A} = 1 + K_d(\frac{1}{c})$$

where A_0 and A indicate absorbance at 405 nm in the absence or presence of competitive molecules, respectively. The character c shows the concentration of dilution series of competitive molecule such as BIQ-based metal complexes and substrates, and product of the Friedel-Crafts reaction. K_d represents the dissociation constant.

Synthesis

1,1'-Bi-isoquinoline (BIQ)[81]

Scheme 4-1. Synthesis of 1,1'-bi-isoquinoline (BIQ).

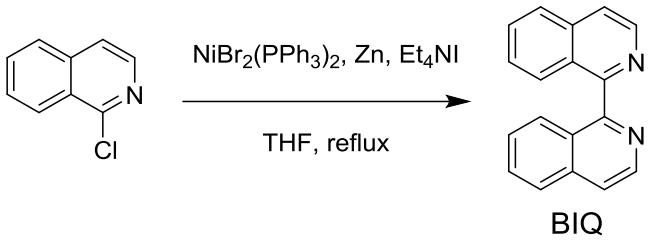

THF (20.0 mL) was added to $NiBr_2(PPh_3)$ (2.27 g, 3.04 mmol), Zn (1.03 g. 25.8 mmol), Et_4NI (2.71 g, 10.5 mmol). The reaction mixture was stirred for 30 minutes under nitrogen atmosphere and then a solution of 1-chloroisoquinoline (1.05 g, 6.37 mmol) in THF (10.0 mL) was added. The resulting mixture was refluxed for 23 h and solvent was removed under reduced pressure. CH_2Cl_2 (50 mL) was added to black solid and filtered. 2M NH_3 aq. (60 mL) was added to the filtrate and was extracted with CH_2Cl_2 (50 mL×3). The combined organic phase was washed with 2 M NH_3 aq. (30 mL×2), water (30 mL×1) and sat. NaCl aq. (30 mL×1) and dried over $MgSO_4$. The solvent was removed under reduced pressure. Purification by column chromatography (SiO_2, hexane/EtOAc (95/5), $CHCl_3$/MeOH (96/4)) gave BIQ as a yellow solid (603 mg, 74%, **Scheme 4-1**, **Figures 4-2** and **4-3**). ^{1}HNMR (500 MHz, $CDCl_3$) δ 7.48 (td, *J*=1.4, 6.0 Hz, 1H), 7.70 (m, 1H), 7.75 (d, *J*=7.4 Hz, 1H), 7.82 (d, *J*=5.7 Hz, 1H), 7.95 (d, *J*=8.3 Hz, 1H), 8.71 (d, *J*=5.7 Hz, 1H). ^{13}CNMR (125 MHz, $CDCl_3$) δ 121.18, 127.98, 130.48, 136.99, 142.10, 158.28. ESI-TOF-MS: *m*/*z* Calcd. for $C_{18}H_{12}N_2Na$ ($[M+Na]^+$) 279.09; Found 279.10

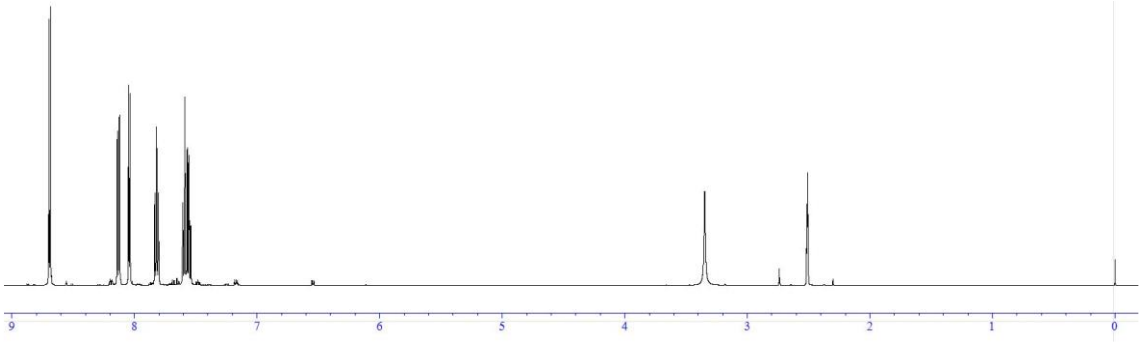

Figure 4-2. ^{1}HNMR spectrum of BIQ (500 MHz, $CDCl_3$).

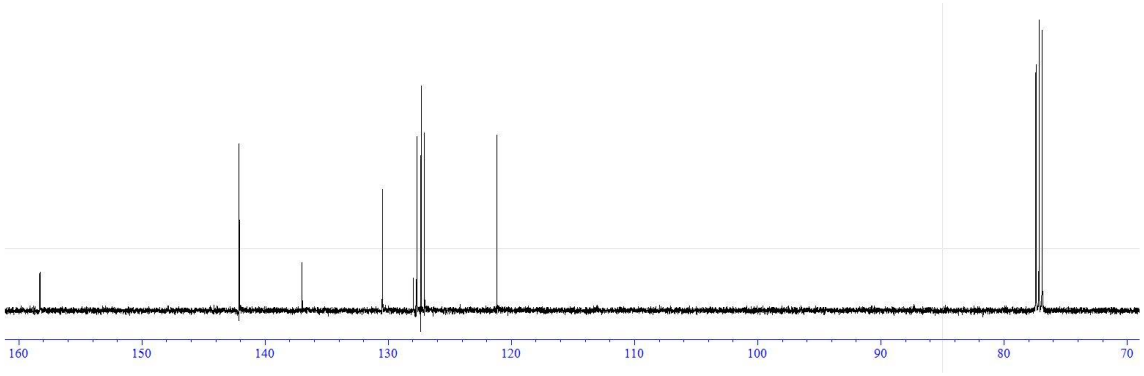

Figure 4-3. Partial ^{13}C NMR spectrum of BIQ (125 MHz, $CDCl_3$).

BIQ-Cu

Scheme 4-2. Synthesis of BIQ-Cu.

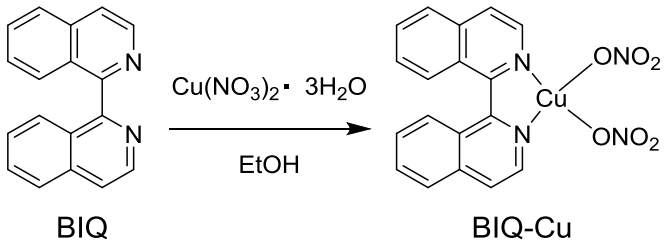

To a solution of BIQ (106 mg, 0.414 mmol) in ethanol (10 mL) was added a solution of $CuNO_3 \cdot 3H_2O$ (109 mg, 0.452 mmol) in ethanol (5.0 mL). The resulting mixture was stirred for 2 h at room temperature under air. The suspension was filtered and the solid was washed with cold ethanol. Dark green solid 108 mg, 59% (**Scheme 4-2**).

BIQ-$PdCl_2$

Scheme 4-3. Preparation of BIQ-$PdCl_2$. [82,83]

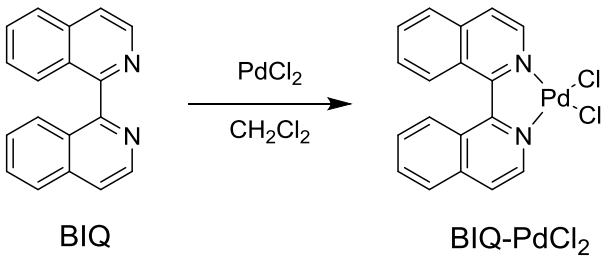

To a solution of BIQ (102 mg, 0.398 mmol) in CH_2Cl_2 (1.0 mL) was added a suspension of $PdCl_2(CH_3CN)_2$ (104 mg, 0.402 mmol) in CH_2Cl_2 (8.0 mL). The resulting

mixture was stirred for 2 hours at room temperature under air. Hexane (20.0 mL) was added, and the precipitate was filtered and dried under reduced pressure. Dark green solid 166 mg, 96% (**Scheme 4-3**, **Figures 4-4** and **4-5**). ^{1}HNMR (500 MHz, DMSO-d_6) δ 7.72 (t, *J*=7.5, 15.5 Hz, 1H), 7.85 (d, *J*=8.5 Hz, 1H), 8.04 (t, *J*=7.0, 15.0 Hz, 1H), 8.29 (d, *J*=8.0 Hz, 1H), 8.43 (d, *J*=6.0 Hz, 1H), 9.15 (d, *J*=6.5Hz, 1H). ^{13}CNMR (500 MHz, DMSO-d_6) δ 125.42, 126.89, 127.51, 128.25, 129.04, 133.37, 137.91, 141.00, 157.90

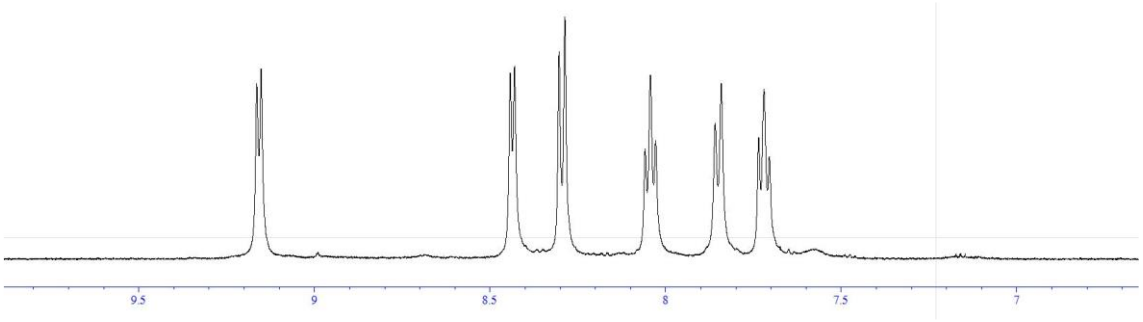

Figure 4-4. Partial ^{1}HNMR spectrum of BIQ-$PdCl_2$ (500 MHz, DMSO-d_6).

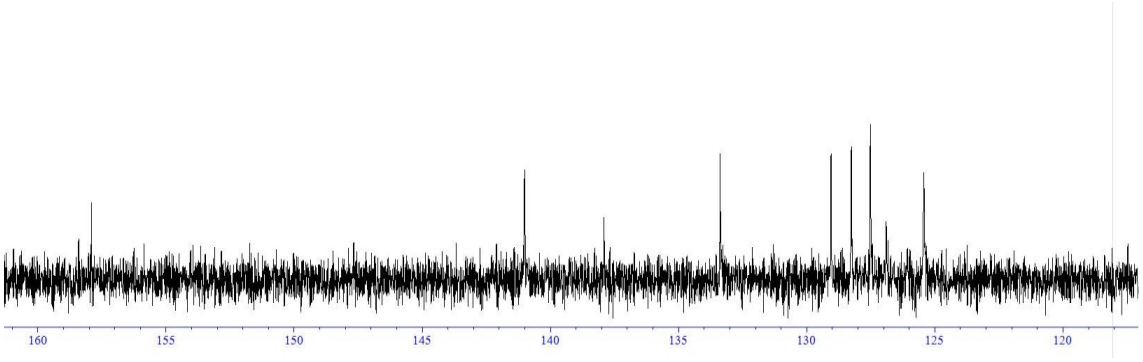

Figure 4-5. Partial ^{13}CNMR spectrum of BIQ-$PdCl_2$ (125 MHz, DMSO-d_6).

BIQ-Pd(OAc)$_2$

Scheme 4-4. Preparation of BIQ-Pd(OAc)$_2$.

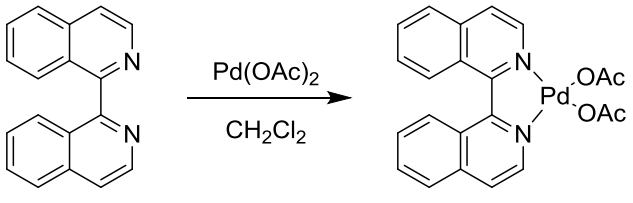

BIQ BIQ-Pd(OAc)$_2$

To a solution of BIQ (102 mg, 0.398 mmol) in CH_2Cl_2 (5.0 mL) was added a suspension of Pd(OAc)$_2$ (92.5 mg, 0.413 mmol) in CH_2Cl_2 (10.0 mL). The resulting

mixture was stirred for 2 h at room temperature under air. Hexane (60.0 mL) was added, and the precipitate was filtered and dried under reduced pressure. Brown solid 72.4 mg, 38% (**Scheme 4-4**, **Figures 4-6** and **4-7**). ^{1}HNMR (500 MHz, DMSO-d_6) δ 7.74 (m, 1H), 7.89 (d, *J*=9.0 Hz, 1H), 8.03 (t, *J*=7.5, 15 Hz, 1H), 8.18 (d, *J*=6.0 Hz, 1H), 8.30 (d, *J*=8.5 Hz, 1H), 8.41 (d, *J*=10 Hz, 1H). ^{13}CNMR (500 MHz, DMSO-d_6) δ 23.48, 125.76, 126.61, 127.62, 127.84, 129.14, 137.94, 140.66, 156.70, 175.73, 180.26

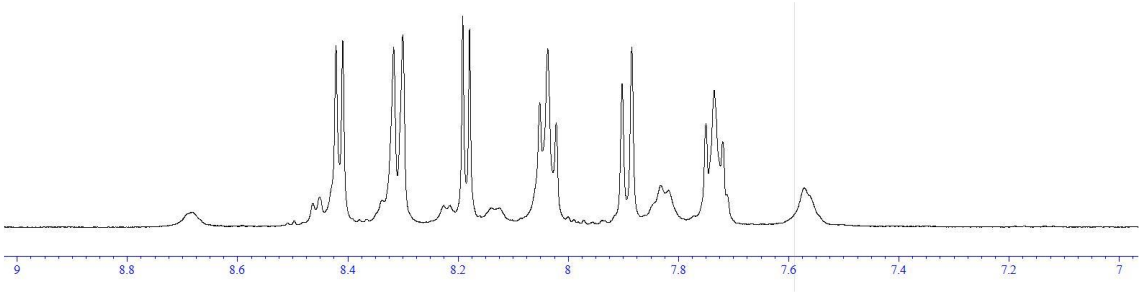

Figure 4-6. Partial ^{1}HNMR spectrum of BIQ-Pd(OAc)$_2$ (500 MHz, DMSO-d_6).

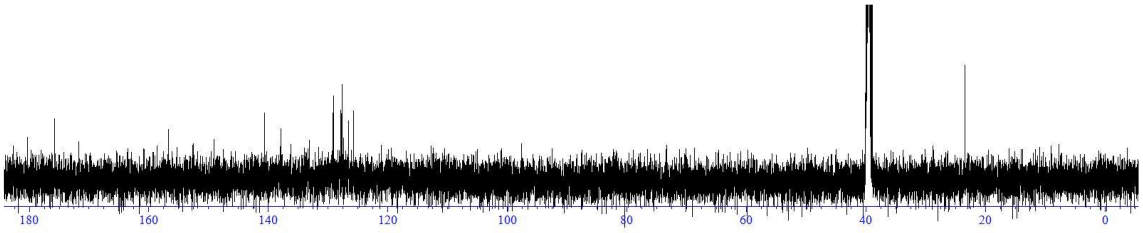

Figure 4-7. ^{13}CNMR spectrum of BIQ-Pd(OAc)$_2$ (125 MHz, DMSO-d_6).

BIQ-PtCl$_2$[84]

Scheme 4-5. Preparation of BIQ-PtCl$_2$.

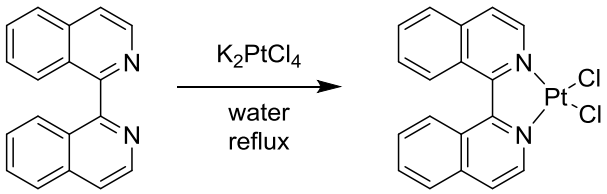

BIQ (280 mg, 1.09 mmol) and K_2PtCl_4 (445 mg, 1.07 mmol) were refluxed in water (80 mL) for 2 h. The reaction mixture was cooled to 0 °C. The solid precipitate was filtered and washed with EtOH, 1M HCl and water. Orange solid, 460 mg (82%, **Scheme 4-5**).

Compound 1[85]

Scheme 4-6. Preparation of **1**.

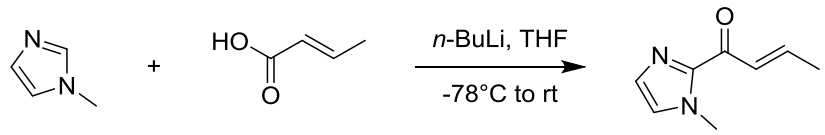

4 **5** **1**

1-methyl-1H-imidazole (**4**, 1.50 mL, 19.0 mmol) and THF (25.0 mL) were added to an oven-dried schlenk tube under nitrogen atmosphere. The solution was cooled to −78 °C and *n*-BuLi (1.5M in hexane, 17.0 mL, 25.5 mmol) was added dropwise over 25 min. The mixture was warmed to room temperature and stirred for 20 min, then cooled back to −78 °C. Crotonic acid (**5**, 793 mg, 9.2 mmol) in THF (10.0 mL) was added dropwise over 5 min. The resulting solution was stirred at −78 °C for 20 min, then warmed to room temperature and stirred for additional 2 h. The reaction was quenched with sat $NaHCO_3$ solution (50 mL) and the aqueous phase was extracted with EtOAc (40 mL×3). The combined organic phase was washed with brine (30 mL×2), dried over $MgSO_4$, and the solvent was removed under reduced pressure. Purification by column chromatography (SiO_2, hexane/EtOAc (72/28) gave 1-(1-methyl-1H-imidazol-2-yl)but-2-en-1-one (**1**) as a yellow liquid (291 mg, 21%, **Scheme 4-6**, **Figures 4-8** and **4-9**). ^{1}HNMR (500 MHz, $CDCl_3$) δ 1.99 (dd, J= 2.0, 7.0 Hz, 3H), 4.04 (s, 3H), 7.04 (s, 1H), 7.14 (m, 2H), 7.42 (m, 1H). ^{13}CNMR (500 MHz, DMSO-d_6) δ 18.57, 36.38, 127.16, 127.97, 129.26, 143.79, 144.00, 180.80. ESI-TOF-MS: *m*/*z* Calcd. for $C_8H_{10}N_2ONa$ ($[M+Na]^+$) 173.07; Found 173.07

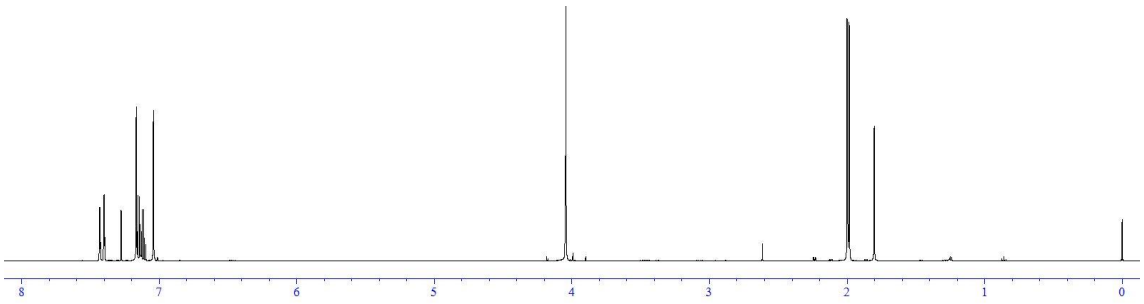

Figure 4-8. ^{1}HNMR spectrum of **1** (500 MHz, $CDCl_3$).

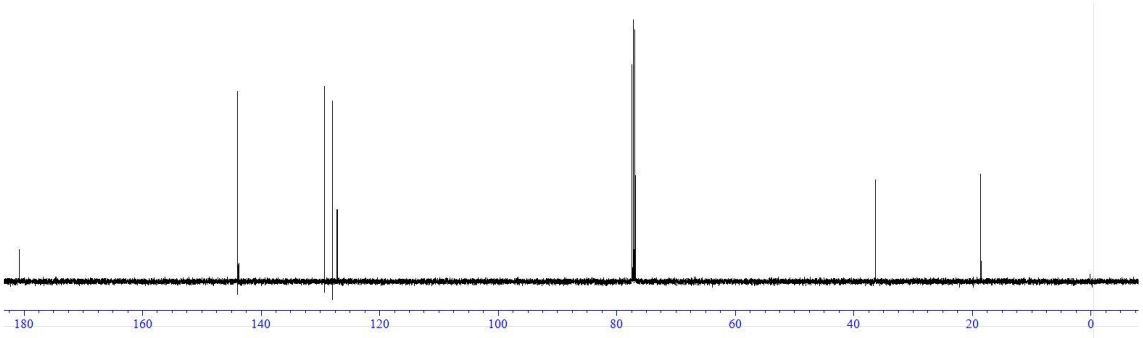

Figure 4-9. ^{13}CNMR spectrum of **1** (125 MHz, $CDCl_3$).

Compound 3[57]

Scheme 4-7. Preparation of **3**.

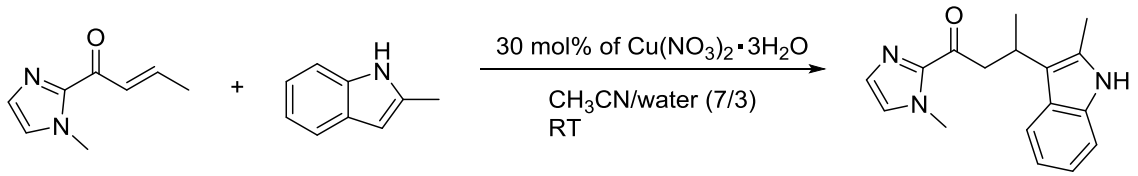

1 **2** **3**

A solution of **1** (202 mg, 1.34 mmol) in 2.0 mL of CH_3CN/water (7/3) was added to a solution of 2-methyl-1H-indole (**2**, 356 mg, 2.72 mmol) and $Cu(NO_3)_2 \cdot 3H_2O$ (98.6 mg, 0.334 mmol) in 3.0 mL of CH_3CN/water (7/3). The resulting mixture was stirred at room temperature for 2 days. CH_3CN was removed under reduced pressure and diluted with water (30 mL). The aqueous phase was extracted with CH_2Cl_2 (30 mL×3), dried over $MgSO_4$, and the solvent was removed under reduced pressure. Purification by column chromatography (SiO_2, hexane/EtOAc (70/30) gave **3** as a brown liquid (152 mg, 41%, **Scheme 4**-7, **Figures 4-10** and **4-11**). ^{1}HNMR (500 MHz, $CDCl_3$) δ 1.46 (d, J= Hz, 3H), 2.41 (s, 3H), 3.60 (m, 2H), 3.78 (m, 1H), 3.86 (s, 3H), 6.93 (s, 1H), 7.04 (m, 2H), 7.09 (m, 1H), 7.22 (m, 1H), 7.66 (d, 1H), 7.70 (s, 1H). ^{13}CNMR (500 MHz, DMSO-d_6) δ 12.38, 21.20, 27.15, 36.12, 46.33, 110.28, 115.59, 119. 02, 119.37, 120.67, 126.69, 127.49, 128.94, 130.45, 135.44, 143.42, 192.46. ESI-TOF-MS: *m/z* Calcd. for $C_{17}H_{19}N_3ONa$ ($[M+Na]^+$) 304.14; Found 304.15

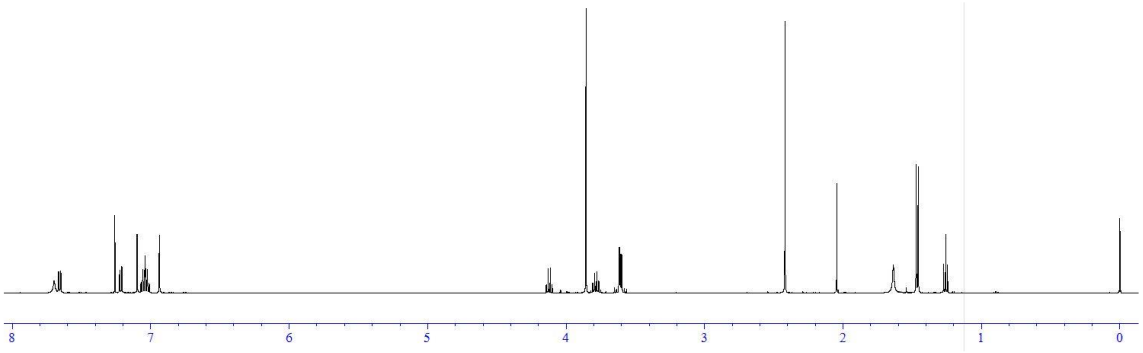

Figure 4-10. ^{1}HNMR spectrum of **3** (500 MHz, $CDCl_3$).

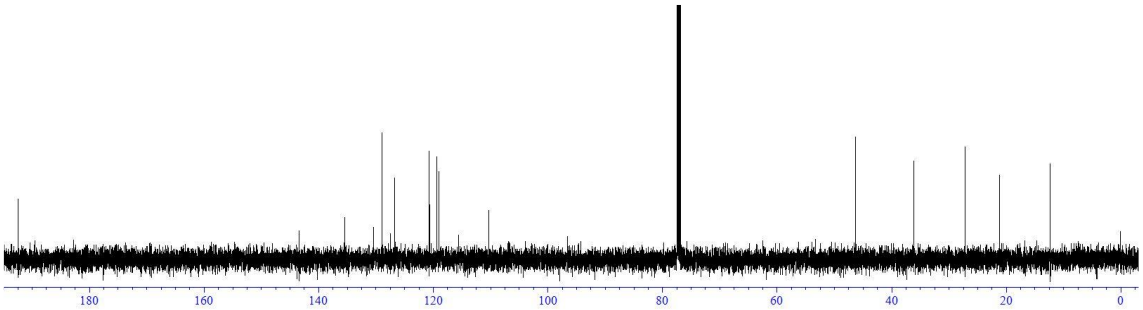

Figure 4-11. ^{13}CNMR spectrum of **3** (125 MHz, $CDCl_3$).

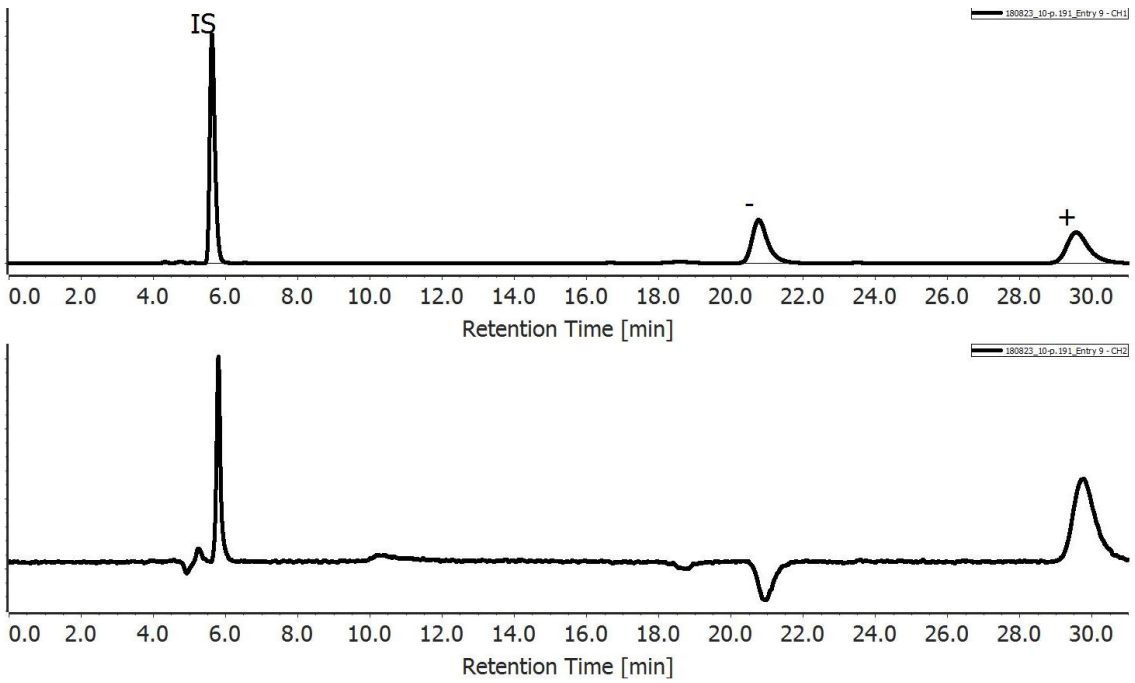

Figure 4-12. HPLC chart of a mixture of 2-phenylquinolone and **3**. Daicel Chiralpak AD-H, hexane/2-propanol (90/10), 1.0 mL/min, UV and CD detection at 275 and 280 nm. (−) and (+) isomer of **3** are defined based on the HPLC analysis with UV and CD detector.

4-3. Results and Discussion

Creation of artificial metalloenzymes consisting of atroposelective antibodies and BIQ-based metal catalysts

Four kinds of BIQ-based metal complexes: BIQ-Cu, BIQ-$PdCl_2$, BIQ-$Pd(OAc)_2$, and BIQ-$PtCl_2$ were prepared. The binding affinity of mAbs to four kinds of BIQ-based metal complexes was evaluated by competitive ELISA. The K_d values of mAbs are ranged from 10^{-4} M to 10^{-5} M, with an exception of mAb 9H3 for BIQ-$PtCl_2$ (**Table 4-1**, **Figures 4-13** to **4-28**). The mAbs prepared for BN also bind BIQ-based metal catalysts. All four mAbs show the highest affinity toward BIQ-Cu among the four metal complexes evaluated. Especially, mAb R44E1 shows the highest affinity for BIQ-Cu among the four mAbs (K_d =1.0×10^{-5}M, **Figure 4-13**). The other three mAbs have similar affinities for BIQ-Cu (K_d =4.0×10^{-5}M for mAb S1E11 and mAb 34H12, K_d =3.8×10^{-5}M for mAb 9H3, **Figure 4-14**, **4-15**, **4-16**). Importantly, supramolecular complexes consist of four kinds of BIQ-based metal catalysts and atroposelective antibodies are successfully developed. Complexes of mAbs with BIQ-Cu were selected for further investigation

Table 4-1. Dissociation constants (K_d) of the complexes of mAbs and BIQ-based metal complexes.

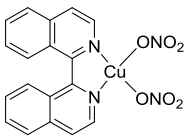

BIQ-Cu

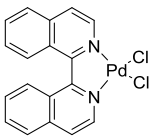

BIQ-$PdCl_2$

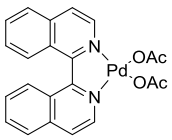

BIQ-$Pd(OAc)_2$

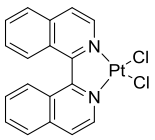

BIQ-$PtCl_2$

mAb	K_d/M			
	BIQ-Cu	BIQ-$PdCl_2$	BIQ-$Pd(OAc)_2$	BIQ-$PtCl_2$
R44E1	1.0×10^{-5}	3.1×10^{-5}	4.9×10^{-5}	1.6×10^{-4}
S1E11	4.0×10^{-5}	~10^{-5}	~10^{-5}	2.3×10^{-4}
34H12	4.0×10^{-5}	3.6×10^{-4}	6.3×10^{-5}	5.8×10^{-5}
9H3	3.8×10^{-5}	~10^{-5}	7.6×10^{-5}	~10^{-5}

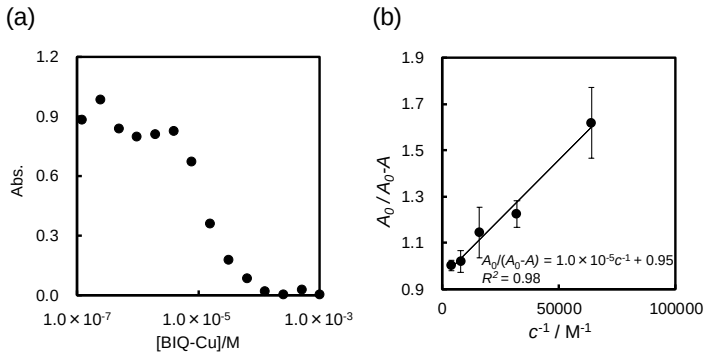

Figure 4-13. Competitive ELISA of mAb R44E1 for BIQ-Cu (a) and corresponding Klotz plot (b).

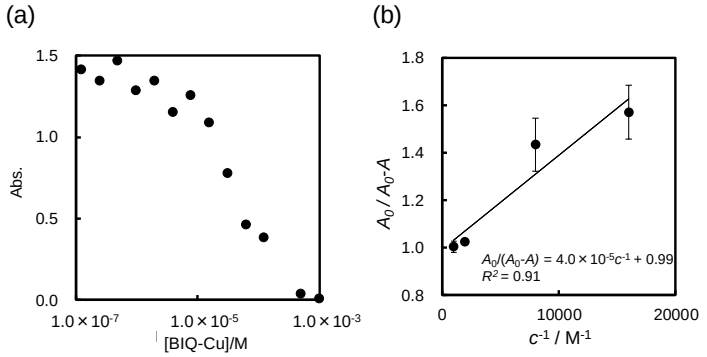

Figure 4-14. Competitive ELISA of mAb S1E11 for BIQ-Cu (a) and corresponding Klotz plot (b).

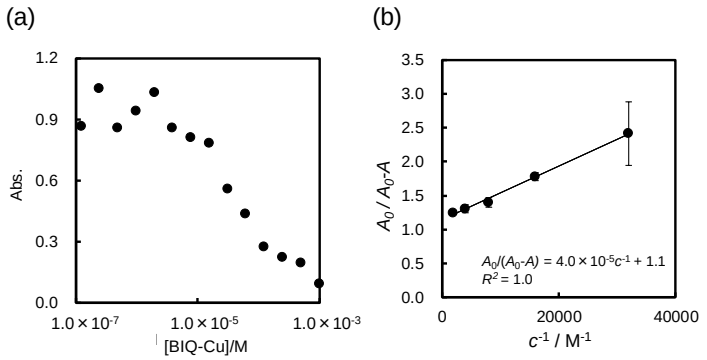

Figure 4-15. Competitive ELISA of mAb 34H12 for BIQ-Cu (a) and corresponding Klotz plot (b).

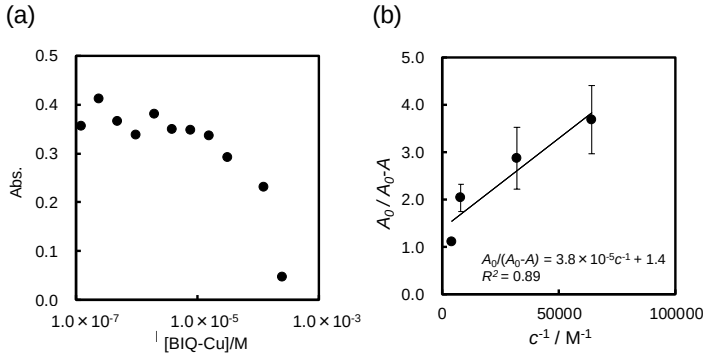

Figure 4-16. Competitive ELISA of mAb 9H3 for BIQ-Cu (a) and corresponding Klotz plot (b).

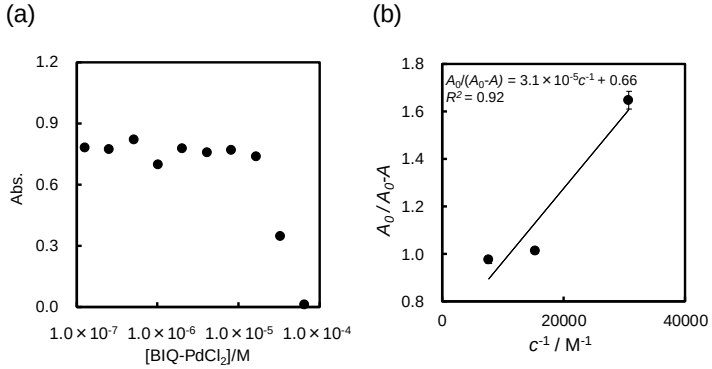

Figure 4-17. Competitive ELISA of mAb R44E1 for BIQ-$PdCl_2$ (a) and corresponding Klotz plot (b).

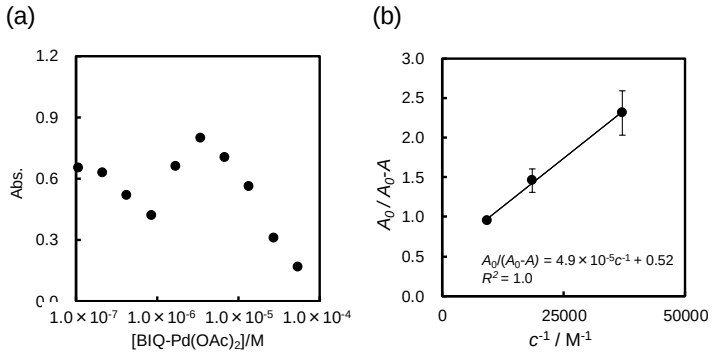

Figure 4-18. Competitive ELISA of mAb R44E1 for BIQ-$Pd(OAc)_2$ (a) and corresponding Klotz plot (b).

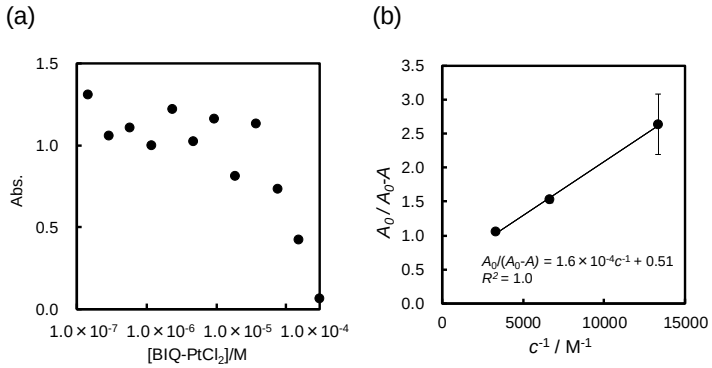

Figure 4-19. Competitive ELISA of mAb R44E1 for BIQ-$PtCl_2$ (a) and corresponding Klotz plot (b).

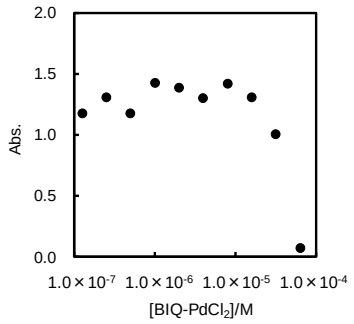

Figure 4-20. Competitive ELISA of mAb S1E11 for BIQ-$PdCl_2$.

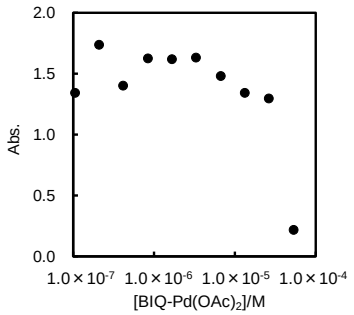

Figure 4-21. Competitive ELISA of mAb S1E11 for BIQ-$Pd(OAc)_2$.

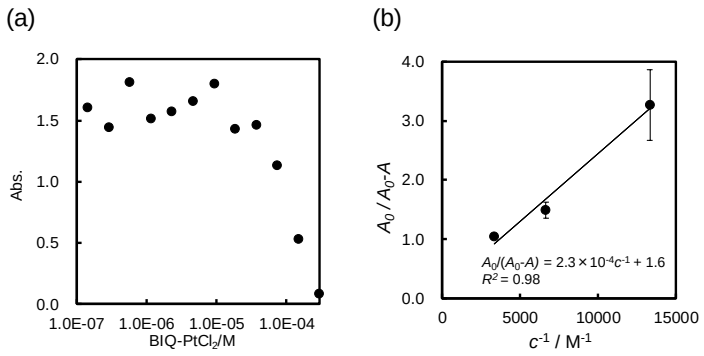

Figure 4-22. Competitive ELISA of mAb S1E11 for BIQ-$PtCl_2$ (a) and corresponding Klotz plot (b).

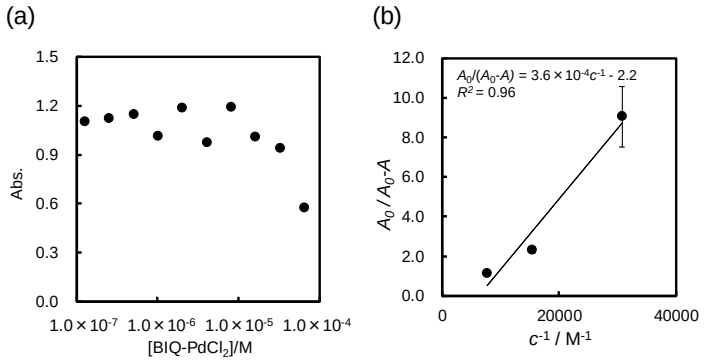

Figure 4-23. Competitive ELISA of mAb 34H12 for BIQ-$PdCl_2$ (a) and corresponding Klotz plot (b).

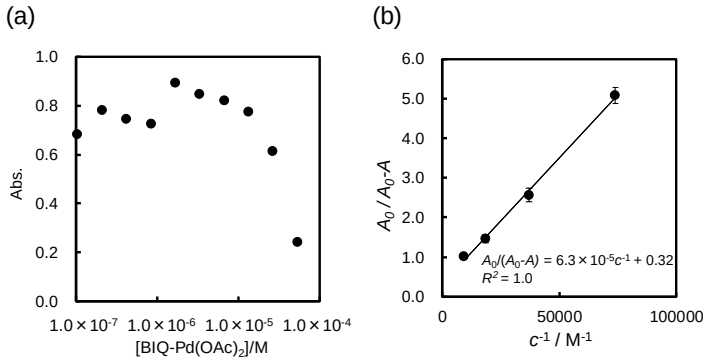

Figure 4-24. Competitive ELISA of mAb 34H12 for BIQ-$Pd(OAc)_2$ (a) and corresponding Klotz plot (b).

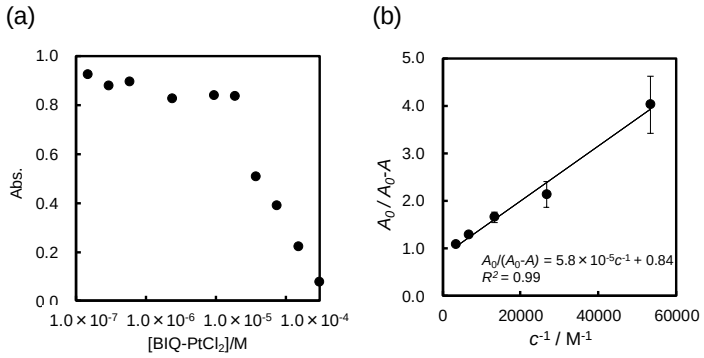

Figure 4-25. Competitive ELISA of mAb 34H12 for BIQ-$PtCl_2$ (a) and corresponding Klotz plot (b).

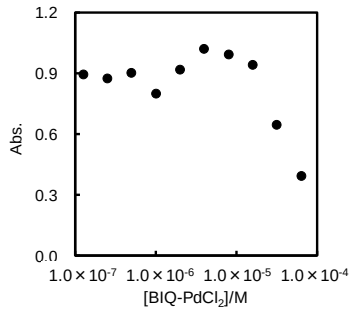

Figure 4-26. Competitive ELISA of mAb 9H3 for BIQ-$PdCl_2$.

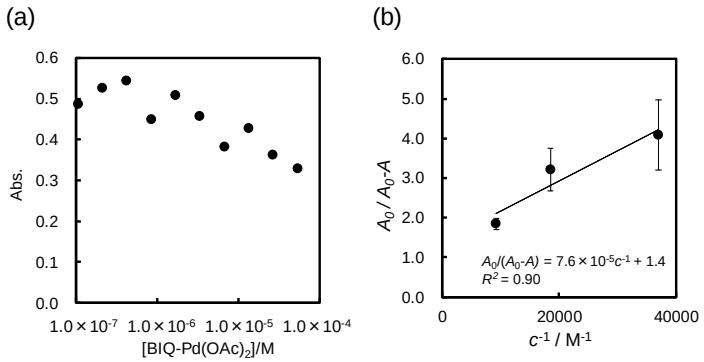

Figure 4-27. Competitive ELISA of mAb 9H3 for BIQ-$Pd(OAc)_2$ (a) and corresponding Klotz plot (b).

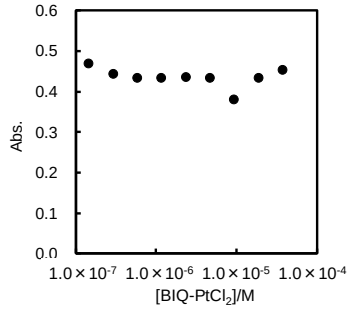

Figure 4-28. Competitive ELISA of mAb 9H3 for BIQ-$PtCl_2$.

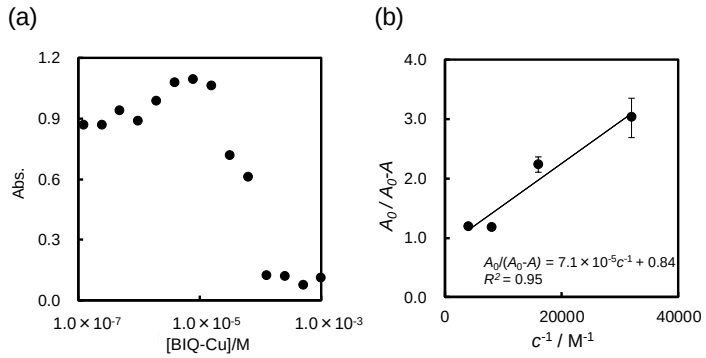

Figure 4-29. Competitive ELISA of mAb 2B6 (anti-porphyrin antibody) for BIQ-Cu (a) and corresponding Klotz plot (b).

Friedel-Crafts alkylation reactions catalyzed by atroposelective antibody-based artificial metalloenzymes

The Friedel-Crafts alkylation reaction was carried out by mixing atroposelective antibodies (50 μM) with BIQ-Cu (50 μM) in 20 mM MOPS buffer (pH 6.5) containing 150 mM NaCl followed by the addition of substrates (1.0 mM). Under these conditions, the molar ratio of antigen binding sites to BIQ-Cu is two to one. The reactions were carried out at 4 °C for 72 h. The product was analyzed by chiral HPLC. Although BIQ-Cu affords racemic **3** with 6% yield (**Entry 1** in **Table 4-2**, **Figure 4-31**), the supramolecular complex of mAb S1E11 with BIQ-Cu (S1E11+BIQ-Cu) yields **3** with 2% yield, 65% ee (**Entry 2** in **Table 4-2**, **Figure 4-32**). The complex of mAb R44E1 and BIQ-Cu (R44E1+BIQ-Cu) catalyzes the reaction with 10% yield, 88% ee (**Entry 3** in **Table 4-2**, **Figure 4-33**). In contrast, mAb 34H12 and mAb 9H3-based ones (34H12+BIQ-Cu, 9H3+BIQ-Cu) do not show enantioselectivity in this reaction (**Entry 4** and **5** in **Table 4-2**, **Figures 4-34** and **4-35**). However, 9H3+BIQ-Cu shows a five-fold increased catalytic activity (TON 6.4) compared with BIQ-Cu (TON 1.3; **Entry 5** in **Table 4-2**, **Figure 4-35**). These results suggest that precisely designed second coordination spheres control the reactivity and enantioselectivity of the asymmetric catalysis. Although anti-porphyrin mAb 2B6 has an unexpected affinity for BIQ-Cu (**Figure 4-29**, $K_d = 7.1\times10^{-5}$ M), presumably due to hydrophobic interaction, 2B6+BIQ-Cu gives racemic **3** (**Entry 6** in **Table 4-2**, **Figure 4-36**). In another control experiment, bovine serum albumin (BSA) does not affect the reactivity and enantioselectivity of the catalytic reaction (**Entry 7** in **Table 4-2**, **Figure 4-37**). These two control experiments indicate that the protein scaffolds must be optimized immunologically to prepare enantioselective artificial metalloenzymes. Hence, the artificial metalloenzyme R44E1+BIQ-Cu was subjected to further investigations.

The effect of the ratio of supramolecular complexation on the yield and enantioselectivity of the artificial metalloenzyme R44E1+BIQ-Cu was evaluated. Although the catalytic experiments with less than 5% of catalyst loading do not have an ee (**Table 4-2**, **Entry 8**, **9**, and **10**), increasing the concentration of BIQ-Cu to a certain level ([BIQ-Cu] = 5.0×10^{-5} M) while maintaining a constant ratio of the antigen binding site to BIQ-Cu (2:1) results in an enantioselective catalytic reaction (**Table 4-2**, **Entry 3**). Given the affinity of mAb R44E1 for BIQ-Cu ($K_d = 1.0\times10^{-5}$M), this behavior strongly supports that the enantioselectivity of the reaction is derived from the complexation of BIQ-Cu with mAb R44E1. Along with an enhanced enantioselectivity, the yield of the catalytic reaction decreases at a 5% catalyst loading. This behavior is attributed to the inherent nature of BIQ-Cu from the control experiments without mAbs (**Table 4-3**). The

data, including control experiments using only BIQ-Cu, mAb 2B6, and BSA, and the dependency of enantioselectivity on the ratio of supramolecular complexation indicate that the enantioselective reaction occurs inside the binding sites of mAbs.

To obtain mechanistic insight into the artificial metalloenzyme based on atroposelective antibodies, the affinity of mAbs toward substrates **1**, **2**, and product **3** of the Friedel-Crafts alkylation reaction was evaluated by competitive ELISA (**Figures 4-38** to **4-49**). All four mAbs do not bind substrate **1**. In contrast, mAb R44E1, mAb S1E11 and mAb 34H12 show weak affinity for substrate **2** with K_d value ranging from 1.8×10^{-3} M to 6.5×10^{-3} M, even though interaction with substrate **2** is not immunologically installed (**Table 4-4**). Apparently, the weak affinity appears to be non-specific binding of hydrophobic indole derivative **2**. However, mAb 9H3 does not bind it at all. Therefore, the interaction of mAbs to **2** is attributed to the structural nature of each mAb. Interestingly, mAb R44E1 and mAb 34H12 also bind product **3** with higher affinity (**Table 4-4**; K_d =4.8×10^{-5} M and 1.6×10^{-4} M, respectively) compared with substrate **2**, whereas no interaction is observed between mAbs S1E11 or mAb 9H3 and **3**. The observed diversity in the binding affinity of mAbs for **1**, **2**, **3**, and BIQ-based metal catalysts highlights a unique feature of mAb as a protein scaffold for artificial Friedel-Crafts-ase.[57,86–92]

Plausible mechanisms of the atroposelective antibody-based artificial metalloenzymes are proposed based on the catalytic and the binding behavior of mAbs. The mAb R44E1 binds *ca*. 90% of BIQ-Cu under the reaction conditions based on competitive ELISA (K_d = 1.0×10^{-5} M). As the catalytic reaction progresses, product **3** (up to 1.0×10^{-4} M in 10% yield) competes with BIQ-Cu to bind with mAb R44E1 (K_d = 4.8×10^{-5} M). This competition causes reactions outside the binding sites to reduce the enantioselectivity. The affinity of mAb R44E1 for substrate **2** (K_d = 4.8×10^{-3} M) seems to contribute to the slight increase in yield compared with BIQ-Cu. The mAb S1E11 binds *ca*. 70% of BIQ-Cu under the reaction conditions (K_d = 4.0×10^{-5} M). The moderate enantioselectivity is attributed to the reaction outside the binding sites. The yield is lower than that of BIQ-Cu, although mAb S1E11 has an affinity for substrate **2** (K_d = 6.5×10^{-3} M). The lower yield is attributed to the second coordination sphere where the accessibility of the substrate to the reaction center is regulated. The mAb 34H12 binds *ca*. 50% of BIQ-Cu under the condition (K_d = 4.0×10^{-5} M). It is assumed that no competitive binding of product **3** to mAb 34H12 occurred until the completion of reaction based on the binding constants (K_d for **3**: 1.6×10^{-4} M, [**3**]: upto 6.0×10^{-5}). Although mAb 34H12 has the highest affinity for substrate **2** (K_d = 1.8×10^{-3} M) among the four mAbs, no significant accretion or selectivity is observed. This is attributed to the effect of protein environment and/or

low complexation ratio of mAbs with BIQ-Cu under the condition. The mAb 9H3 binds *ca*. 50% of BIQ-Cu under the condition ($K_d = 3.8\times10^{-5}$ M). This mAb has no affinity for product **3** ensuring smooth diffusing after the reaction. The significant acceleration observed in 9H3+BIQ-Cu is remarkable, considering the low complexation ratio under the condition and no affinity for substrates **1** and **2**. These results suggest that the specific second coordination effect provided by mAb 9H3 results in the acceleration of the reaction. It should be emphasized that the immunologically optimized atroposelective antibodies as a protein scaffold realize acceleration and stereocontrol of the catalytic reaction.

Table 4-2. Friedel-Crafts Alkylation Reactions Catalyzed by Atroposelective Antibodies-based Artificial Metalloenzymes

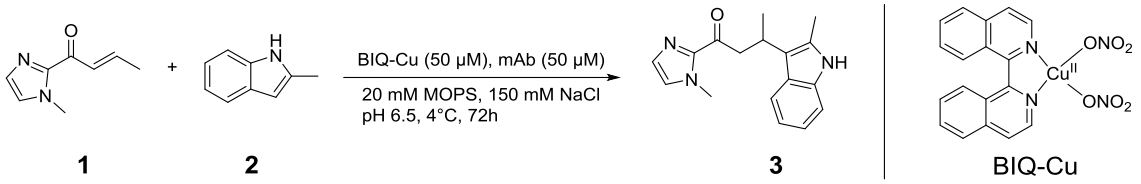

1 **2** **3** BIQ-Cu

Entry	Catalyst	Yield / %[a]	ee / %[b]
1	BIQ-Cu (5.0%)	6	<5
2	S1E11+BIQ-Cu (5.0%)	2	65
3	R44E1+BIQ-Cu (5.0%)	10	88
4	34H12+BIQ-Cu (5.0%)	6	<5
5	9H3+BIQ-Cu (5.0%)	32	<5
6	2B6+BIQ-Cu (5.0%)	17	<5
7	BSA+BIQ-Cu (5.0%)	8	<5
8	R44E1+BIQ-Cu (1.0%)	29	<5
9	R44E1+BIQ-Cu (0.5%)	24	<5
10	R44E1+BIQ-Cu (0.1%)	4	<5

Reaction condition: 1.0 mM of substrate **1** and **2**, 50 μM of mAb (5.0%), 50 μM of BIQ-Cu (5.0%) in 20 mM MOPS buffer (pH 6.5), 150 mM NaCl at 4 °C for 72h. Conditions for HPLC analysis: Daicel ChiralPak AD-H, hexane/2-propanol (90/10), 1.0 mL/min, 40 °C, UV and CD detector at 275 nm and 280 nm. [a]Yields were determined by HPLC using 2-phenylquinoline as an internal standard. [b]ee of (+) isomer. (−) and (+) isomers of **3** are defined based on the HPLC analysis with UV and CD detector (**Figure 4-12**).

Table 4-3. Friedel-Crafts Alkylation Reactions Catalyzed by BIQ-Cu.

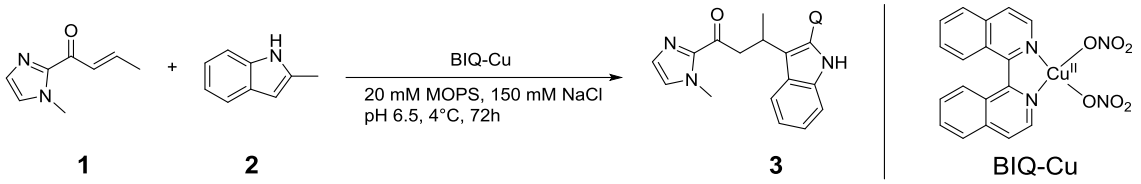

Entry	Catalyst	Yield / %[a]	ee / %[b]
1	BIQ-Cu (5.0%)	6	<5
2	BIQ-Cu (1.0%)	16	<5
3	BIQ-Cu (0.5%)	19	<5
4	BIQ-Cu (0.1%)	6	<5

Typical reaction condition: 1.0 mM of substrate **1** and **2**, 50 μM of mAb (5.0%), 50 μM of BIQ-Cu (5.0%) in 20 mM MOPS buffer (pH 6.5), 150 mM NaCl at 4 °C for 72h. Conditions for HPLC analysis: Daicel ChiralPak AD-H, hexane/2-propanol (90/10), 1.0 mL/min, 40 °C, UV and CD detector at 275 nm and 280 nm. [a]Yields were determined by HPLC using 2-phenylquinoline as an internal standard. [b]ee of (+) isomer. (−) and (+) isomers of **3** are defined based on the HPLC analysis with UV and CD detector.

Table 4-4. Dissociation constants (K_d) of the complexes between mAbs and substrate **1**, **2**, and product **3** of Friedel-Crafts alkylation reaction.

mAb	K_d / M		
	1	**2**	**3**
R44E1	ND[a]	4.8×10^{-3}	4.8×10^{-5}
S1E11	ND[a]	6.5×10^{-3}	ND[a]
34H12	ND[a]	1.8×10^{-3}	1.6×10^{-4}
9H3	ND[a]	ND[a]	ND[a]

[a]Interaction is not detected in competitive ELISA.

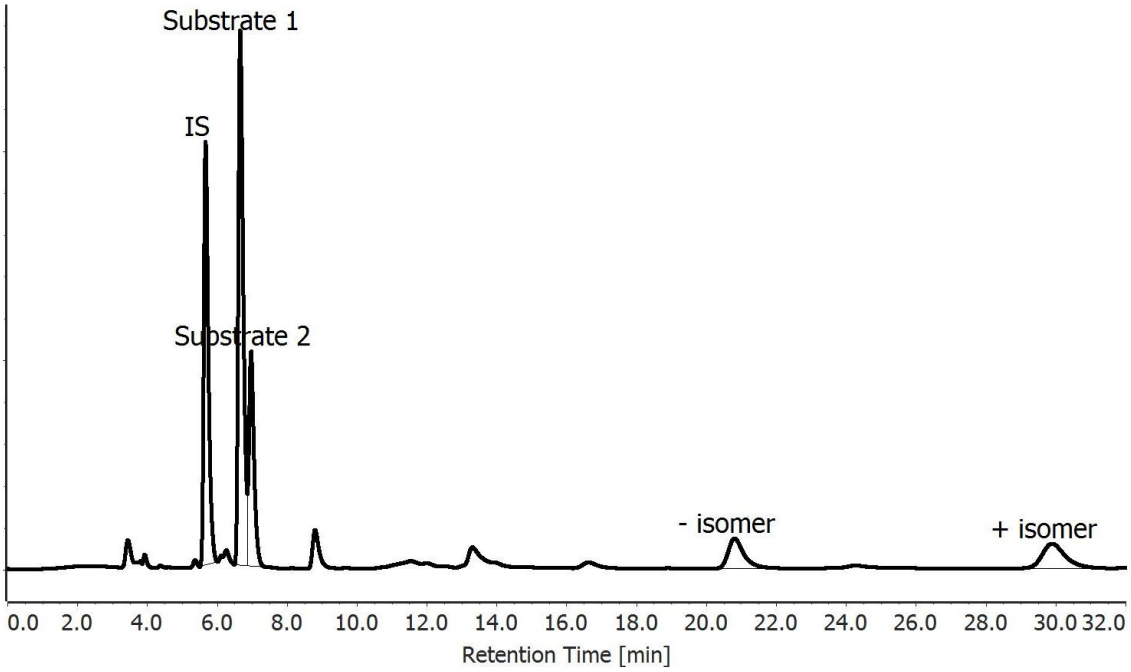

Figure 4-31. Chiral HPLC trace of the Friedel-Crafts alkylation reaction with BIQ-Cu.

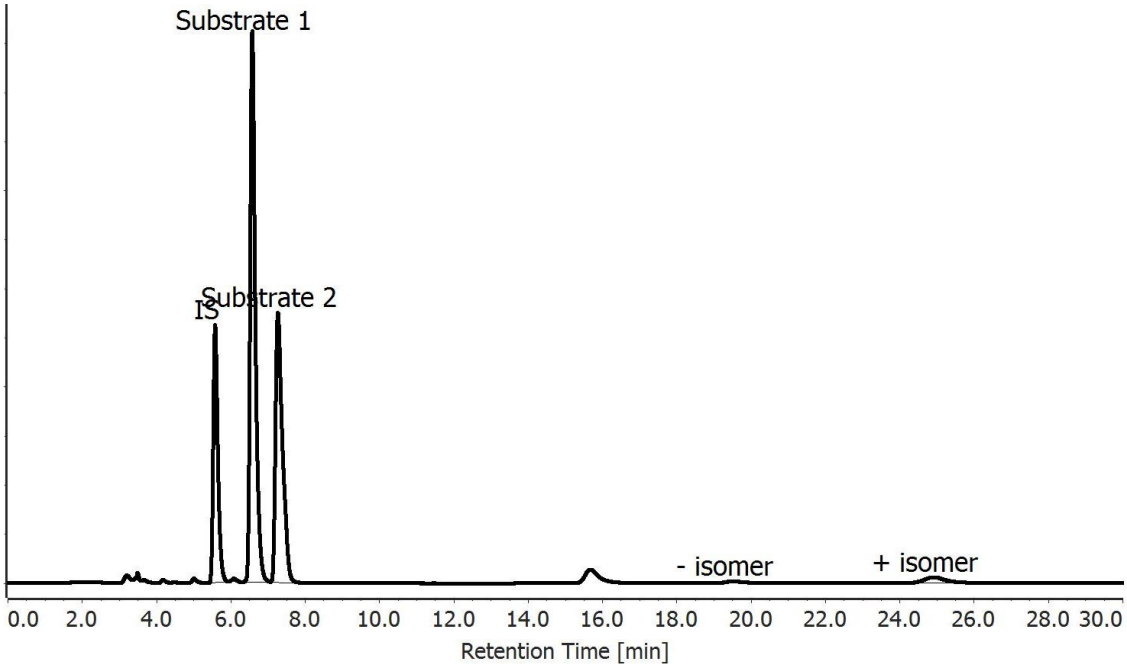

Figure 4-32. Chiral HPLC trace of the Friedel-Crafts alkylation reaction with S1E11+BIQ-Cu.

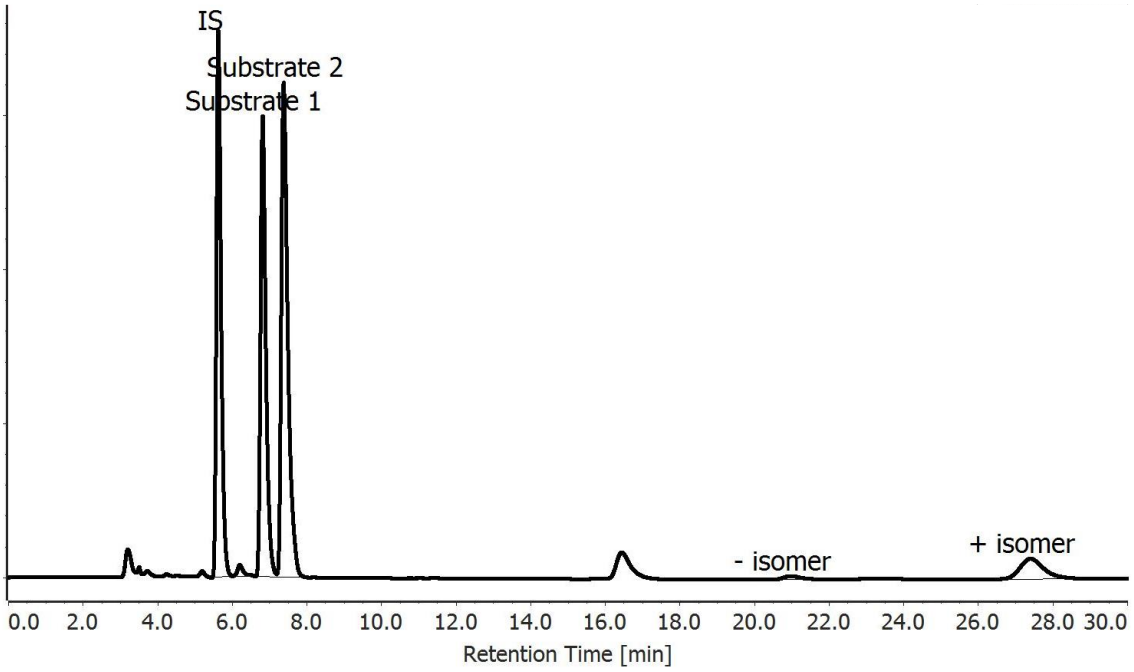

Figure 4-33. Chiral HPLC trace of the Friedel-Crafts alkylation reaction with R44E1+BIQ-Cu.

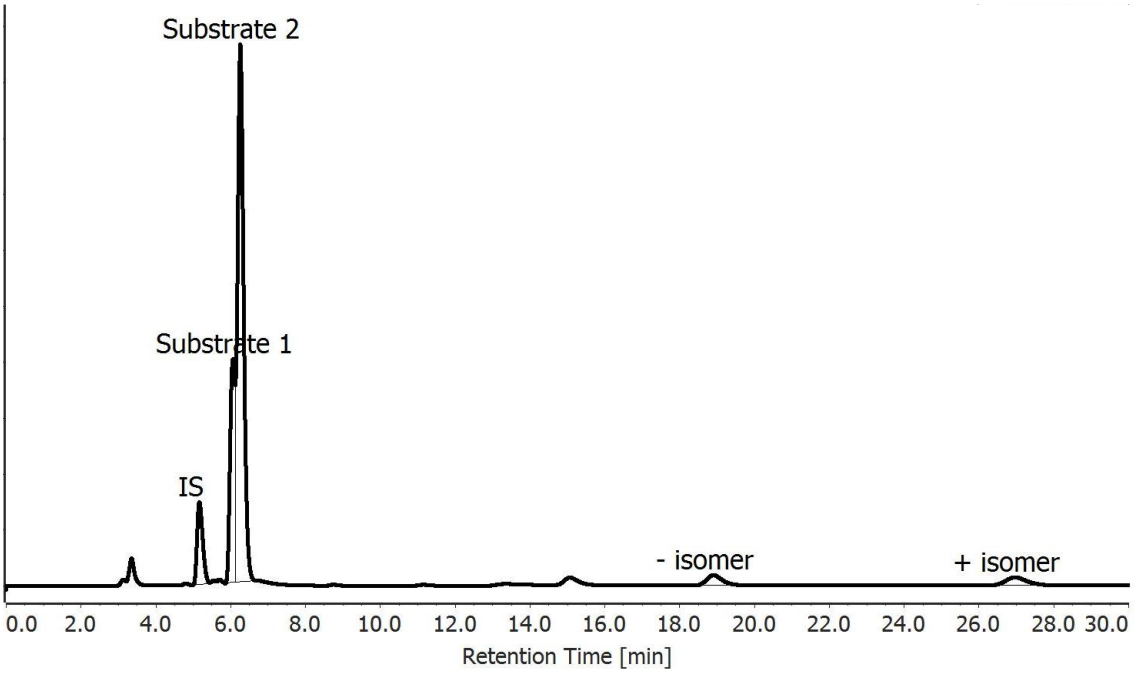

Figure 4-34. Chiral HPLC trace of the Friedel-Crafts alkylation reaction with 34H12+BIQ-Cu.

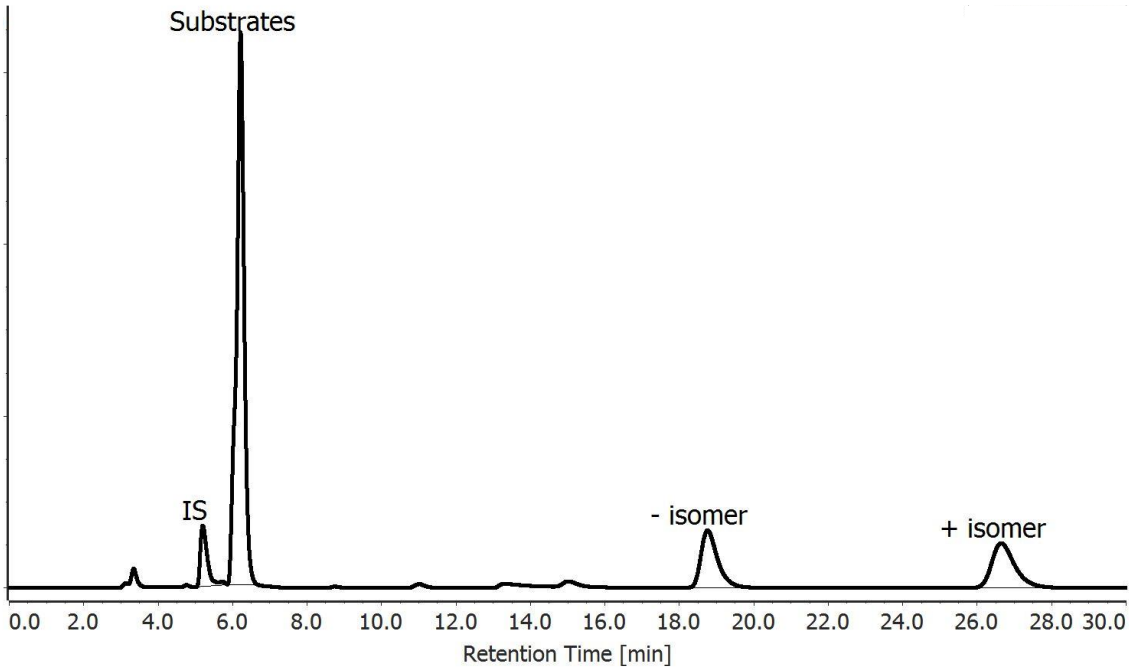

Figure 4-35. Chiral HPLC trace of the Friedel-Crafts alkylation reaction with 9H3+BIQ-Cu.

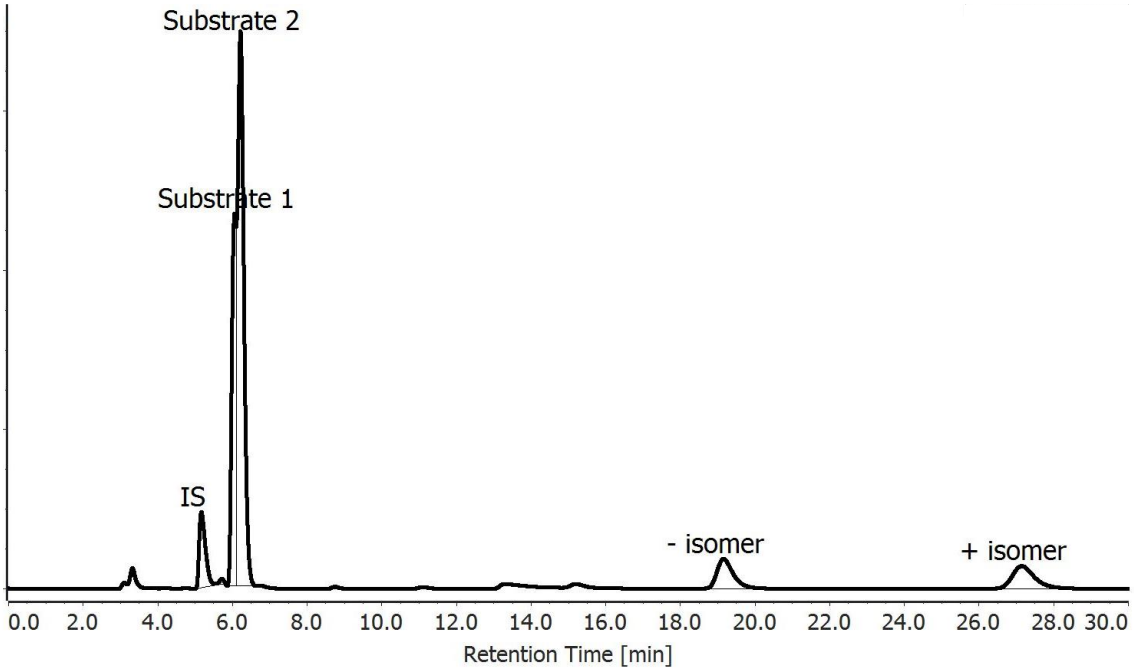

Figure 4-36. Chiral HPLC trace of the Friedel-Crafts alkylation reaction with 2B6+BIQ-Cu.

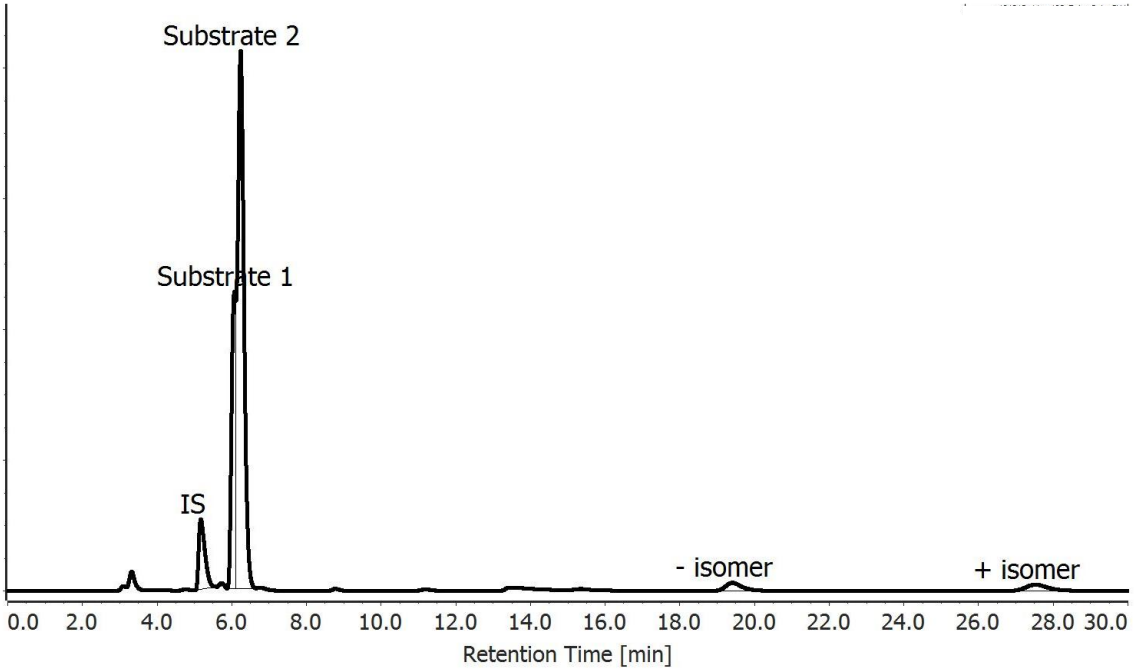

Figure 4-37. Chiral HPLC trace of the Friedel-Crafts alkylation reaction with BSA+BIQ-Cu.

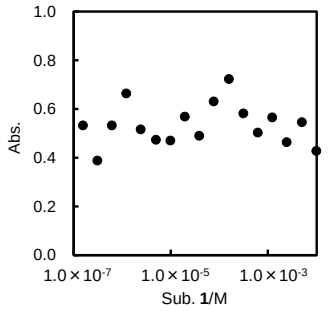

Figure 4-38. Competitive ELISA of mAb R44E1 for substrate **1**.

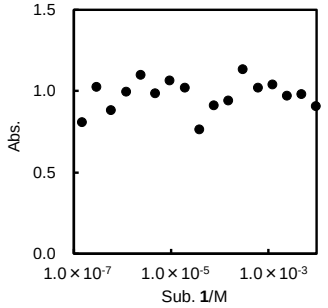

Figure 4-39. Competitive ELISA of mAb S1E11 for substrate **1**.

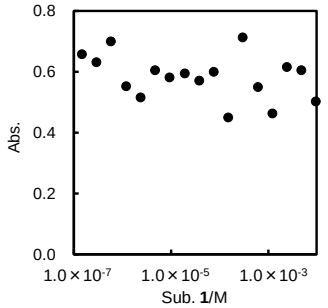

Figure 4-40. Competitive ELISA of mAb 34H12 for substrate **1**.

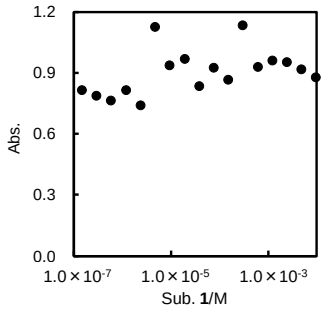

Figure 4-41. Competitive ELISA of mAb 9H3 for substrate **1**.

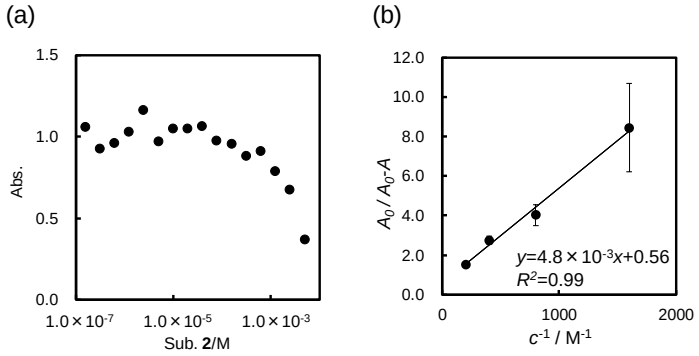

Figure 4-42. Competitive ELISA of mAb R44E1 for substrate **2** (a) and corresponding Klotz plot (b).

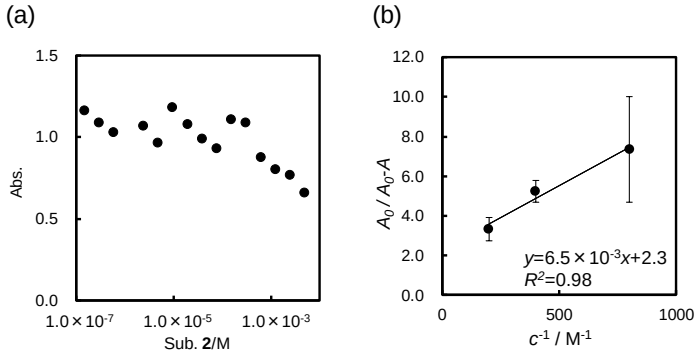

Figure 4-43. Competitive ELISA of mAb S1E11 for substrate **2** (a) and corresponding Klotz plot (b).

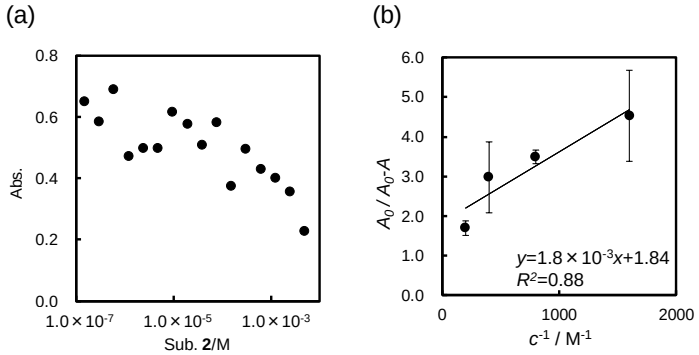

Figure 4-44. Competitive ELISA of mAb 34H12 for substrate **2** (a) and corresponding Klotz plot (b).

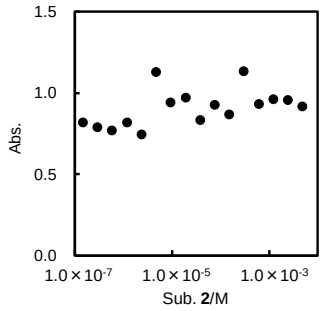

Figure 4-45. Competitive ELISA of mAb 9H3 for substrate **2** (a) and corresponding Klotz plot (b).

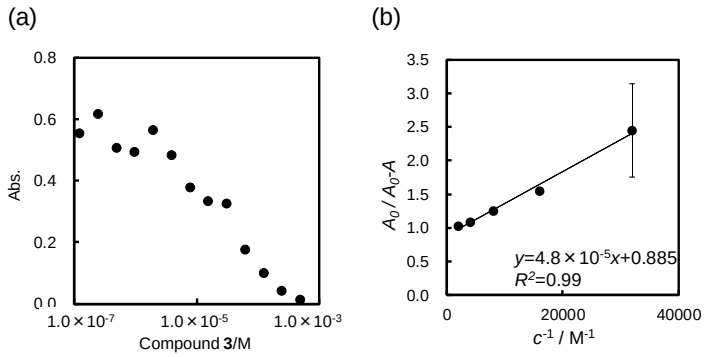

Figure 4-46. Competitive ELISA of mAb R44E1 for compound **3** (a) and corresponding Klotz plot (b).

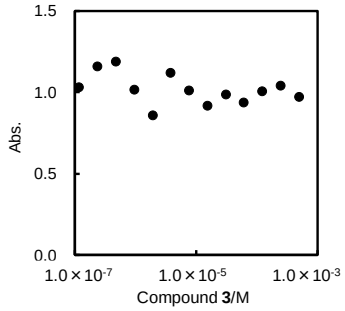

Figure 4-47. Competitive ELISA of mAb S1E11 for compound **3**.

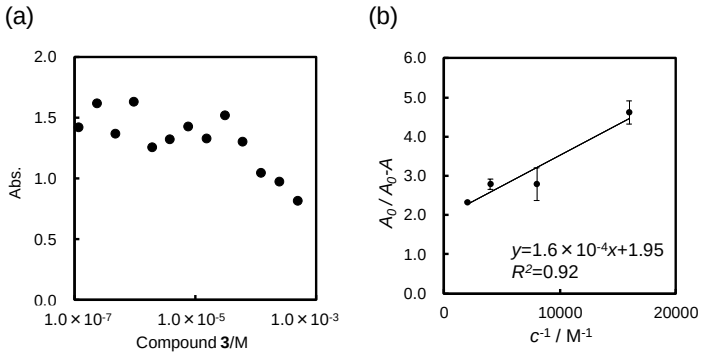

Figure 4-48. Competitive ELISA of mAb 34H12 for compound **3**.

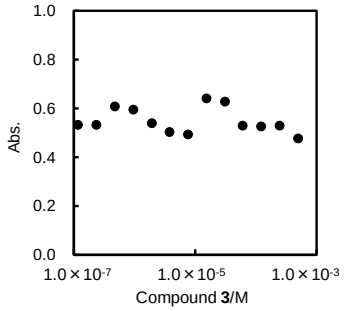

Figure 4-49. Competitive ELISA of mAb 9H3 for compound **3**.

4-4. Conclusion

In this chapter, a novel design strategy for artificial metalloenzymes is developed by introducing BIQ-based metal catalysts into the binding sites of atroposelective antibodies. The atroposelective antibodies for BN bind to four kinds of BIQ-based metal catalysts. These results suggest that the use of structurally simple BN as a hapten is effective to generate binding sites that accommodate variety of BIQ-based metal catalysts. Artificial metalloenzymes bearing BIQ-Cu as a cofactor catalyze Friedel-Crafts alkylation of **1** with **2** with a high ee. As the ratio of supramolecular complexation of mAb R44E1 with BIQ-Cu in the reaction mixture increases, the enantioselectivity dramatically increases. This observation along with the control experiments indicates that the enantioselective reaction occurs inside the binding pockets of mAbs. The catalysis results and affinity for **1**, **2**, and **3** depend on the mAbs used. This is a unique feature of mAbs as a protein scaffold for artificial metalloenzymes. Notably, a BIQ-based hydrophobic catalyst is used as an asymmetric catalyst for the first time in an environmentally benign media. The design strategy accepts various binaphthyl-based metal catalysts, which may allow more precise control of stereochemistry or a range of catalytic reaction, including abiological reactions.

References

(1) Schwizer, F.; Okamoto, Y.; Heinisch, T.; Gu, Y.; Pellizzoni, M. M.; Lebrun, V.; Reuter, R.; Köhler, V.; Lewis, J. C.; Ward, T. R. *Chem. Rev.* **2018**, *118*, 142–231.

(2) Zeymer, C.; Hilvert, D. *Annu. Rev. Biochem.* **2018**, *87*, 131–157.

(3) Sauer, D. F.; Schiffels, J.; Hayashi, T.; Schwaneberg, U.; Okuda, J. *Beilstein J. Org. Chem.* **2018**, *14*, 2861–2871.

(4) Shoji, O.; Watanabe, Y. *Chem. Lett.* **2017**, *46*, 278–288.

(5) Fujieda, N.; Itoh, S. *Bull. Chem. Soc. Jpn.* **2016**, *89*, 733–742.

(6) Renata, H.; Wang, Z. J.; Arnold, F. H. *Angew. Chem. Int. Ed.* **2015**, *54*, 3351–3367.

(7) Ilie, A.; Reetz, M. T. *Isr. J. Chem.* **2015**, *55*, 51–60.

(8) Fukuzumi, S. *Curr. Opin. Chem. Biol.* **2015**, *25*, 18–26.

(9) Hayashi, T.; Sano, Y.; Onoda, A. *Isr. J. Chem.* **2015**, *55*, 76–84.

(10) Drienovská, I.; Roelfes, G. *Isr. J. Chem.* **2015**, *55*, 21–31.

(11) Matsuo, T.; Hirota, S. *Bioorg. Med. Chem.* **2014**, *22*, 5638–5656.

(12) Deuss, P. J.; den Heeten, R.; Laan, W.; Kamer, P. C. J. *Chem. Eur. J.* **2011**, *17*, 4680–4698.

(13) Yamaguchi, H.; Harada, A. *Chem. Lett.* **2008**, *37*, 1184–1189.

(14) Ueno, T.; Abe, S.; Yokoi, N.; Watanabe, Y. *Coord. Chem. Rev.* **2007**, *251*, 2717–2731.

(15) Yamamura, K.; Kaiser, E. T. *J. Chem. Soc. Chem. Commun.* **1976**, 830–831.

(16) Bertucci, C.; Botteghi, C.; Giunta, D.; Marchetti, M.; Paganelli, S. *Adv. Synth. Catal.* **2002**, *344*, 556–562.

(17) Okrasa, K.; Kazlauskas, R. J. *Chem. Eur. J.* **2006**, *12*, 1587–1596.

(18) Xie, J.; Liu, W.; Schultz, P. G. *Angew. Chem. Int. Ed.* **2007**, *46*, 9239–9242.

(19) Abe, S.; Niemeyer, J.; Abe, M.; Takezawa, Y.; Ueno, T.; Hikage, T.; Erker, G.; Watanabe, Y. *J. Am. Chem. Soc.* **2008**, *130*, 10512–10514.

(20) Köhler, V.; Mao, J.; Heinisch, T.; Pordea, A.; Sardo, A.; Wilson, Y. M.; Knörr, L.; Creus, M.; Prost, J.-C.; Schirmer, T.; et al. *Angew. Chem. Int. Ed.* **2011**, *50*, 10863–10866.

(21) Fujieda, N.; Hasegawa, A.; Ishihama, K.; Itoh, S. *Chem. - An Asian J.* **2012**, *7*, 1203–1207.

(22) Coelho, P. S.; Brustad, E. M.; Kannan, A.; Arnold, F. H. *Science* **2013**, *339*, 307–310.

(23) Key, H. M.; Clark, D. S.; Hartwig, J. F. *J. Am. Chem. Soc.* **2015**, *137*, 8261–8268.

(24) Dydio, P.; Key, H. M.; Nazarenko, A.; Rha, J. Y.-E.; Seyedkazemi, V.; Clark, D. S.; Hartwig, J. F. *Science* **2016**, *354*, 102–106.

(25) Key, H. M.; Dydio, P.; Clark, D. S.; Hartwig, J. F. *Nature* **2016**, *534*, 534–537.
(26) Kan, S. B. J.; Lewis, R. D.; Chen, K.; Arnold, F. H. *Science* **2016**, *354*, 1048–1051.
(27) Kan, S. B. J.; Huang, X.; Gumulya, Y.; Chen, K.; Arnold, F. H. *Nature* **2017**, *552*, 132–136.
(28) Levine, H. L.; Nakagawa, Y.; Kaiser, E. T. *Biochem. Biophys. Res. Commun.* **1977**, *76*, 64–70.
(29) Chen, C.; Sigman, D. *Science* **1987**, *237*, 1197–1201.
(30) Roelfes, G.; Feringa, B. L. *Angew. Chem. Int. Ed.* **2005**, *44*, 3230–3232.
(31) Reetz, M. T.; Jiao, N. *Angew. Chem. Int. Ed.* **2006**, *45*, 2416–2419.
(32) Talbi, B.; Haquette, P.; Martel, A.; De Montigny, F.; Fosse, C.; Cordier, S.; Roisnel, T.; Jaouen, G.; Salmain, M. *Dalt. Trans.* **2010**, *39*, 5605–5607.
(33) Onoda, A.; Fukumoto, K.; Arlt, M.; Bocola, M.; Schwaneberg, U.; Hayashi, T. *Chem. Commun.* **2012**, *48*, 9756–9758.
(34) Matsuo, T.; Imai, C.; Yoshida, T.; Saito, T.; Hayashi, T.; Hirota, S. *Chem. Commun.* **2012**, *48*, 1662–1664.
(35) Bos, J.; Fusetti, F.; Driessen, A. J. M.; Roelfes, G. *Angew. Chem. Int. Ed.* **2012**, *51*, 7472–7475.
(36) Philippart, F.; Arlt, M.; Gotzen, S.; Tenne, S.-J. J.; Bocola, M.; Chen, H.-H. H.; Zhu, L.; Schwaneberg, U.; Okuda, J. *Chem. Eur. J.* **2013**, *19*, 13865–13871.
(37) Basauri-Molina, M.; Verhoeven, D. G. A.; Van Schaik, A. J.; Kleijn, H.; Klein Gebbink, R. J. M. *Chem. Eur. J.* **2015**, *21*, 15676–15685.
(38) Zhao, J.; Kajetanowicz, A.; Ward, T. R. *Org. Biomol. Chem.* **2015**, *13*, 5652–5655.
(39) Basauri-Molina, M.; Verhoeven, D. G. A.; van Schaik, A. J.; Kleijn, H.; Klein Gebbink, R. J. M. *Chem. Eur. J.* **2015**, *21*, 15676–15685.
(40) Filice, M.; Romero, O.; Aires, A.; Guisan, J. M.; Rumbero, A.; Palomo, J. M. *Adv. Synth. Catal.* **2015**, *357*, 2687–2696.
(41) Pordea, A.; Creusa, M.; Panek, J.; Duboc, C.; Mathis, D.; Novic, M.; Ward, T. R. *J. Am. Chem. Soc.* **2008**, *130*, 8085–8088.
(42) Podtetenieff, J.; Taglieber, A.; Bill, E.; Reijerse, E. J.; Reetz, M. T. *Angew. Chem. Int. Ed.* **2010**, *49*, 5151–5155.
(43) Der, B. S.; Edwards, D. R.; Kuhlman, B. *Biochemistry* **2012**, *51*, 3933–3940.
(44) Fujieda, N.; Schätti, J.; Stuttfeld, E.; Ohkubo, K.; Maier, T.; Fukuzumi, S.; Ward, T. R. *Chem. Sci.* **2015**, *6*, 4060–4065.
(45) Barik, C. K.; Ganguly, R.; Li, Y.; Przybylski, C.; Salmain, M.; Leong, W. K. *Inorg. Chem.* **2018**, *57*, 12206–12212.
(46) de Jesús Cázares-Marinero, J.; Przybylski, C.; Salmain, M. *Eur. J. Inorg. Chem.*

2018, *2018*, 1383–1393.
(47) Wilson, M. E.; Whitesides, G. M. *J. Am. Chem. Soc.* **1978**, *100*, 306–307.
(48) Schwabacher, A. W.; Weinhouse, M. I.; Auditor, M. T. M.; Lerner, R. A. *J. Am. Chem. Soc.* **1989**, *111*, 2344–2346.
(49) Harada, A.; Okamoto, K.; Kamachi, M.; Honda, T.; Miwatani, T. *Chem. Lett.* **1990**, *19*, 917–918.
(50) Yamaguchi, H.; Hirano, T.; Kiminami, H.; Taura, D.; Harada, A. *Org. Biomol. Chem.* **2006**, *4*, 3571–3573.
(51) Hayashi, T.; Dejima, H.; Matsuo, T.; Sato, H.; Murata, D.; Hisaeda, Y. *J. Am. Chem. Soc.* **2002**, *124*, 11226–11227.
(52) Ohashi, M.; Koshiyama, T.; Ueno, T.; Yanase, M.; Fujii, H.; Watanabe, Y. *Angew. Chem. Int. Ed.* **2003**, *42*, 1005–1008.
(53) Skander, M.; Humbert, N.; Collot, J.; Gradinaru, J.; Klein, G.; Loosli, A.; Sauser, J.; Zocchi, A.; Gilardoni, F.; Ward, T. R. *J. Am. Chem. Soc.* **2004**, *126*, 14411–14418.
(54) Boersma, A. J.; Feringa, B. L.; Roelfes, G. *Org. Lett.* **2007**, *9*, 3647–3650.
(55) Monnard, F. W.; Heinisch, T.; Nogueira, E. S.; Schirmer, T.; Ward, T. R. *Chem. Commun.* **2011**, *47*, 8238–8240.
(56) Watanabe, K.; Ishikawa, N.; Komatsu, T. *Chem. - An Asian J.* **2012**, *7*, 2534–2537.
(57) Bos, J.; Browne, W. R.; Driessen, A. J. M. M.; Roelfes, G. *J. Am. Chem. Soc.* **2015**, *137*, 9796–9799.
(58) Köhler, G.; Milstein, C. *Nature* **1975**, *256*, 495–497.
(59) Iverson, B.; Lerner, R. *Science* **1989**, *243*, 1184–1188.
(60) Cochran, A.; Schultz, P. *Science* **1990**, *249*, 781–783.
(61) Cochran, A. G.; Schultz, P. G. *J. Am. Chem. Soc.* **1990**, *112*, 9414–9415.
(62) Keinan, E.; Sinha, S. C.; Sinha-Bagchi, A.; Benory, E.; Ghozi, M. C.; Eshhar, Z.; Green, B. S. *Pure Appl. Chem.* **1990**, *62*, 2013–2019.
(63) Ghosh, P.; Shabat, D.; Kumar, S.; Sinha, S. C.; Grynszpan, F.; Li, J.; Noodleman, L.; Keinan, E. *Nature* **1996**, *382*, 339–341.
(64) Nimri, S.; Keinan, E. *J. Am. Chem. Soc.* **1999**, *121*, 8978–8982.
(65) Yli-Kauhaluoma, J. T.; Ashley, J. A.; Lo, C.-H.; Tucker, L.; Wolfe, M. M.; Janda, K. D. *J. Am. Chem. Soc.* **1995**, *117*, 7041–7047.
(66) Raffy, Q.; Ricoux, R.; Mahy, J.-P. *Tetrahedron Lett.* **2008**, *49*, 1865–1869.
(67) Takagi, M.; Kohda, K.; Hamuro, T.; Harada, A.; Yamaguchi, H.; Kamachi, M.; Imanaka, T. *FEBS Lett.* **1995**, *375*, 273–276.
(68) Harada, A.; Fukushima, H.; Shiotsuki, K.; Yamaguchi, H.; Oka, F.; Kamachi, M.

Inorg. Chem. **1997**, *36*, 6099–6102.

(69) Yamaguchi, H.; Tsubouchi, K.; Kawaguchi, K.; Horita, E.; Harada, A. *Chem. Eur. J.* **2004**, *10*, 6179–6186.

(70) Landsteiner, K.; van der Scheer, J. *J. Exp. Med.* **1928**, *48*, 315–320.

(71) Reardan, D. T.; Meares, C. F.; Goodwin, D. A.; McTigue, M.; David, G. S.; Stone, M. R.; Leung, J. P.; Bartholomew, R. M.; Frincke, J. M. *Nature* **1985**, *316*, 265–268.

(72) Shreder, K.; Harriman, A.; Iverson, B. L. *J. Am. Chem. Soc.* **1996**, *118*, 3192–3201.

(73) Rasmussen, B. S.; Pedersen, J. M.; Sørensen, J.; Egebjerg, J.; Schiøtt, B.; Mortensen, K. K.; Skrydstrup, T. *ChemBioChem* **2007**, *8*, 1974–1980.

(74) Adachi, T.; Odaka, T.; Harada, A.; Yamaguchi, H. *ChemistrySelect* **2017**, *2*, 2622–2625.

(75) Odaka, T.; Adachi, T.; Harada, A.; Yamaguchi, H. *Chem. Lett.* **2017**, *46*, 1173–1175.

(76) Yoon, T. P.; Jacobsen, E. N. *Science* **2003**, *299*, 1691–1693.

(77) Berthod, M.; Mignani, G.; Woodward, G.; Lemaire, M. *Chem. Rev.* **2005**, *105*, 1801–1836.

(78) Brunel, J. M. *Chem. Rev.* **2007**, *107*, PR1-PR45.

(79) Miyashita, A.; Yasuda, A.; Takaya, H.; Toriumi, K.; Ito, T.; Souchi, T.; Noyori, R. *J. Am. Chem. Soc.* **1980**, *102*, 7932–7934.

(80) Dai, L.; Zhou, Z.-H.; Zhang, Y.-Z.; Ni, C.; Zhang, Z.; Zhou, Y. *J. Chem. Soc., Chem. Commun.* **1987**, *39*, 1760–1762.

(81) Iyoda, M.; Otsuka, H.; Sato, K.; Nisato, N.; Oda, M. *Bull. Chem. Soc. Jpn.* **1990**, *63*, 80–87.

(82) Khrushcheva, N. S.; Bulygina, L. A.; Starikova, Z. A.; Sokolov, V. I. *Russ. Chem. Bull.* **2014**, *63*, 883–889.

(83) Bulygina, L. A.; Khrushcheva, N. S.; Sokolov, V. I.; Khodak, A. A. *Russ. Chem. Bull.* **2015**, *64*, 429–431.

(84) Cheng, L.-K.; Yeung, K.-S.; Che, C.-M.; Cheng, M.-C.; Wang, Y. *Polyhedron* **1993**, *12*, 1201–1207.

(85) Duchemin, N.; Benedetti, E.; Bethge, L.; Vonhoff, S.; Klussmann, S.; Vasseur, J.; Cossy, J.; Smietana, M.; Arseniyadis, S. *Chem. Commun.* **2016**, *52*, 8604–8607.

(86) Boersma, A. J.; Feringa, B. L.; Roelfes, G. *Angew. Chem. Int. Ed.* **2009**, *48*, 3346–3348.

(87) Boersma, A. J.; de Bruin, B.; Feringa, B. L.; Roelfes, G. *Chem. Commun.* **2012**, *48*, 2394–2396.

(88) Gjonaj, L.; Roelfes, G. *ChemCatChem* **2013**, *5*, 1718–1721.
(89) García-Fernández, A.; Megens, R. P.; Villarino, L.; Roelfes, G. *J. Am. Chem. Soc.* **2016**, *138*, 16308–16314.
(90) Drienovská, I.; Rioz-Martínez, A.; Draksharapu, A.; Roelfes, G. *Chem. Sci.* **2015**, *6*, 770–776.
(91) Bersellini, M.; Roelfes, G. *Dalt. Trans.* **2017**, *46*, 4325–4330.
(92) Bersellini, M.; Roelfes, G. *Org. Biomol. Chem.* **2017**, *15*, 3069–3073.

Chapter 5
Summary

In this thesis the author focuses on the chiral recognition ability of mAbs to develop functionalized supramolecular systems. The mAbs developed against BN precisely recognize the chirality of atropisomeric compounds. Therefore, the author defined the mAbs with chiral recognition ability for binaphthyl derivatives as *atroposelective antibodies*. Supramolecular functions including recognition, separation, and creation of chirality based on chiral recognition of atroposelective antibodies are explored.

In chapter 2, mAbs for axially chiral BN were successfully developed by immunization with enantiomeric pure BN and racemic mixture of BN. Immunization with pure enantiomer of BN yields the mAbs with atroposelectivity toward their hapten. These results indicate that the atroposelectivities of antigen binding sites can be rationally designed by the use of enantiomeric pure BN. Immunization with BN (*rac*) can give atroposelective antibodies for BN (*R*) or BN (*S*) at one time. This finding provides a strategy to rapidly diverse the antigen binding sites for BN enantiomer. The obtained mAbs show high affinity and high atroposelectivity for BN enantiomer. In addition, all four mAbs recognize the chirality of BINOL and BNPA. In contrast, very weak affinity for N and BP was observed, even though N and BP is a partial structure of BN. These results suggest that mAbs bind the crossing moiety of the two naphthyl rings of BN. Chiral supramolecular complexes of mAbs with a chiral organic catalyst with binaphthyl backbone is developed for the first time in this study.

In chapter 3, an operationally-simple and rapid methodology for chiral separation was developed. The solutions of the mixture of BN (*rac*) and atroposelective antibodies were subjected to ultrafiltration to afford purified BN. The difference of molecular weight of mAbs and BN enables the direct use of intact antibodies without any pre-processing or immobilization of mAbs on chromatographic supports. In addition, both enantiomers of BN can be obtained by this procedure where mAbs are prepared for each enantiomer. Although the practical use of this methodology is yet to be achieved, the reusability of mAbs in a direct chiral separation is demonstrated.

In chapter 4, artificial metalloenzymes consisting of C_2 symmetric metal catalysts and atroposelective antibodies were developed. The artificial metalloenzymes

catalyze Friedel-Crafts alkylation reaction with high ee. Notably, a BIQ-based hydrophobic catalyst is used as an asymmetric catalyst for the first time by the help of mAbs.

In conclusion, the author has developed supramolecular functionalized systems including recognition, separation and creation of chirality. The key concept in aforementioned functional systems is chiral recognition of mAbs. The atroposelective antibodies elicited against BN precisely recognize the axial chirality. The tailored binding pockets of atroposelective antibodies were used as a chiral selector to develop operationally-simple chiral separation methodology. The methodology does not require any pre-processing or immobilization of mAbs on chromatographic supports. Intact mAbs can be used directly. The binding sites of atroposelective antibodies provide a customized protein scaffold for binaphthyl compounds. Artificial metalloenzymes consisting of BIQ-based metal catalysts and atroposelective antibodies show high ee in Friedel-Crafts alkylation reaction. Precisely designed second coordination spheres of the binding sites of mAbs control the stereochemistry.

Because antigen binding sites of mAbs can be designed by immunization with precisely designed antigens, the author believes that the potential application of mAbs with chiral recognition ability will be found not only in recognition, separation and creation of chirality but also in the creation of chiral supramolecular structures or induction and amplification of molecular chirality.

List of Publication

1. Adachi, T.; Harada, A; Yamaguchi, H.
   Development of Atroposelective Antibodies by immunization with Racemic Mixture of Binaphthyl Derivatives. *To be submitted.*

2. Adachi, T.; Odaka, T.; Harada, A.; Yamaguchi, H.
   Direct Chiral Separation of Binaphthyl Derivatives Using Atroposelective Antibodies. *ChemistrySelect* **2017**, *2*, 2622–2625.

3. Odaka, T.; Adachi, T.; Harada, A.; Yamaguchi, H.
   Visualization of Chiral Binaphthyl Recognition by Atroposelective Antibodies with Thermoresponsive Polymers. *Chem. Lett.* **2017**, *46*, 1173–1175.

4. Adachi, T.; Harada, A.; Yamaguchi, H.
   Atroposelective Antibodies as a Designed Protein Scaffold for Artificial Metalloenzymes. *Submitted.*